



UNIVERSITÀ DEGLI STUDI DI SIENA  
Dipartimento di Biotecnologie, Chimica e Farmacia

DOTTORATO DI RICERCA IN  
**Chemical and Pharmaceutical Sciences**

CICLO XXXVIII

COORDINATORE Prof. Maurizio Taddei

**Valorization of agrifood systems through geographical traceability,  
by-products recovery and novel fortified foods**

SETTORE SCIENTIFICO-DISCIPLINARE: CHIM/01

DOTTORANDO

Dott. Giacomo Fattori

TUTOR

Prof.ssa Gabriella Tamasi

Firma digitale del candidato

ANNO ACCADEMICO: 2024/2025

Università di Siena  
Dottorato in Chemical and Pharmaceutical sciences  
XXXVIII Ciclo

Data dell'esame finale:

14/04/2026

Commissione giudicatrice:

Lorenzo Cecchi - Ricercatore, Università di Firenze

Giuseppe Capobianco - Professore Associato, Sapienza Università di Roma

Alessandro Donati - Professore Associato, Università di Siena

Supplenti

Lorenzo Cotrozzi – Professore Associato, Università di Pisa

## SUMMARY

CHAPTER 1: General Introduction.....	6
1.1 Food authentication and traceability.....	6
1.2 Biofumigation and circular economy.....	10
1.3 Functional food and fortification.....	12
References.....	20
CHAPTER 2: Food quality and traceability.....	25
2.1 Introduction.....	26
2.2 Experimental section.....	29
2.2.1 Chemicals.....	29
2.2.2 Sampling Procedure.....	30
2.2.3 Sample Treatment—Metabolites Extraction.....	32
2.2.4 Sample Treatment—Acid Digestion.....	32
2.2.5 Spectrophotometric Measurements.....	40
2.2.6 HPLC-DAD Metabolites Analysis.....	40
2.2.7 ICP-MS Metal(loid)s Analysis.....	42
2.2.8 Multivariate Analysis.....	44
2.3 Results.....	44
2.3.1 Soil Analysis.....	44
2.3.2 Secondary Metabolites in Drupes and Leaves.....	45
2.3.3 Mineral Content in Drupes and Leaves.....	50
2.3.4 LDA Models.....	51
2.4 Conclusions.....	55
References.....	56
CHAPTER 3: Delivery systems for sustainable agriculture.....	62
3.1 Introduction.....	63
3.2 Experimental Section.....	65
3.2.1 Chemicals.....	65
3.2.2 Hydrogel Synthesis.....	65
3.2.3 Brassica Oleracea Extract Characterization.....	66
3.2.4 Equilibrium Water Content (EWC).....	67
3.2.5 Differential Scanning Calorimetry (DSC) and Free Water Index (FWI).....	67

3.2.6 Scanning Electron Microscopy (SEM) .....	68
3.2.7 Rheometry on Polymer Solutions and Hydrogels.....	68
3.2.8 Encapsulation Efficiency (EE%) .....	68
3.2.9 Release Kinetics in Water and Release Efficiency (RE%).....	69
3.3 Results.....	70
3.3.1 Brassica Oleracea Extract Characterization.....	70
3.3.2 Physico-Chemical Characterization of CMC Hydrogel.....	71
3.4 Conclusions.....	80
References.....	81
CHAPTER 4: alfalfa ( <i>Medicago sativa</i> L.) as a potential ingredient for food fortification .....	87
4.1 Introduction.....	87
4.1.1 Phenolic compounds in Alfalfa: free and bound fractions.....	88
4.1.2 Antioxidant properties and health benefits.....	88
4.1.3 Factors influencing phytochemical content in plants.....	89
4.1.4 Post-harvest processing.....	90
4.1.5 Heavy metals and food safety .....	90
4.1.6 Alfalfa as a functional food ingredient.....	91
4.1.7 Analytical approaches .....	91
4.1.8 Study objectives .....	92
4.2 Experimental section.....	92
4.2.1 Chemicals.....	92
4.2.2 Samples description and pre-treatment .....	93
4.2.3 Extraction of antioxidants compounds.....	94
4.2.4 Spectrophotometric assays.....	95
4.2.5 HPLC-DAD Metabolites Analysis.....	96
4.2.6 Determination of inorganic compounds through ICP-MS.....	97
4.3 Results.....	99
4.3.1 Inorganic composition of <i>Medicago sativa</i> .....	99
4.3.2 Spectrophotometric Assays (2023) .....	101
4.3.3 Spectrophotometric Assays (2024) .....	104
4.3.4 Spectrophotometric Assays (2025) .....	106
4.3.5 Pooled Three-Year Analysis and Inter-Annual Comparison.....	110
4.3.6 Quantification of Phenolic Acids by HPLC-DAD (2024-2025).....	111

4.4 Conclusions.....	114
References.....	115
CAPTHEM 5: Comprehensive Conclusion.....	120
Acknowledgments.....	123
List of Publication.....	124
Scientific communications.....	125

# *CHAPTER 1: General Introduction*

## *1.1 Food authentication and traceability*

The global food industry has undergone a profound transformation in recent decades, evolving from localized production systems to complex international supply chains that span continents. This globalization of food production and distribution has created unprecedented challenges in ensuring food authenticity, quality control, and traceability. Consumer awareness regarding food origin, production methods, and authenticity has simultaneously increased, driven by concerns about food safety, nutritional value, and the desire to support local economies through the purchase of regionally protected products.<sup>49</sup> The economic impact of food fraud is estimated to cost the global food industry between 10 and 15 billion dollars annually, with certain high-value products such as extra virgin olive oil, honey, and wine being particularly susceptible to adulteration and mislabeling regarding their geographical origin.<sup>50</sup> Geographical origin determination has become a critical aspect of food authentication, as the terroir, the unique combination of soil, climate, and traditional production methods, significantly influences the chemical composition and sensory properties of food products. Protected Designation of Origin (PDO) and Protected Geographical Indication (PGI) certifications in the European Union, along with similar systems worldwide, have established legal frameworks that require robust analytical methods to verify origin claims. These regulatory requirements have driven the development of sophisticated analytical techniques capable of detecting subtle chemical differences that reflect the geographical provenance of food products.<sup>51</sup>

Modern food traceability systems integrate multiple layers of information, from farm-level documentation to sophisticated chemical fingerprinting techniques. The implementation of blockchain technology and digital tracking systems has enhanced the documentary traceability of food products, but these systems remain vulnerable to fraudulent documentation. Chemical authentication provides an independent verification method that cannot be falsified through paperwork manipulation, as it relies on the intrinsic chemical composition of the food product itself.<sup>52</sup> The concept of food authenticity encompasses multiple dimensions, including botanical or species identification, geographical origin verification, production method authentication (organic versus conventional), and the detection of adulteration with cheaper ingredients. Each dimension requires specific analytical approaches, though modern multi-platform strategies often address multiple

authentication questions simultaneously. The chemical markers used for geographical origin determination include stable isotope ratios, mineral element profiles, organic compound patterns, and volatile compound signatures, each reflecting different aspects of the product's origin and production conditions.<sup>53</sup> Quality control in the context of geographical authentication extends beyond simple compliance checking to encompass the preservation of traditional production methods and regional food heritage. Many protected food products are associated with specific production techniques that have been refined over centuries, and their authentication requires not only confirming the geographical origin but also verifying that traditional methods have been followed. This complexity necessitates the use of multiple analytical techniques that can capture different aspects of the product's identity. Stable isotope ratio mass spectrometry (IRMS) represents one of the most powerful tools for geographical origin determination. The ratios of stable isotopes, particularly  $^2\text{H}/^1\text{H}$ ,  $^{13}\text{C}/^{12}\text{C}$ ,  $^{15}\text{N}/^{14}\text{N}$ ,  $^{18}\text{O}/^{16}\text{O}$ , and  $^{34}\text{S}/^{32}\text{S}$ , vary systematically with geographical location due to climatic factors, geological characteristics, and agricultural practices. The hydrogen and oxygen isotope ratios in food products primarily reflect the isotopic composition of local precipitation, which varies with latitude, altitude, and distance from the ocean. Carbon isotope ratios can distinguish between plants using different photosynthetic pathways (C3 versus C4), while nitrogen isotope ratios often reflect fertilization practices and soil characteristics.<sup>54</sup> The application of IRMS has been particularly successful in wine authentication, where the  $^{18}\text{O}/^{16}\text{O}$  ratio in wine water correlates strongly with the geographical origin. Similarly, the  $^2\text{H}/^1\text{H}$  ratio in specific molecular positions, determined by site-specific natural isotope fractionation nuclear magnetic resonance (SNIF-NMR), provides additional discriminatory power. Multi-element isotope analysis, combining several isotope ratios in a single analytical approach, has demonstrated success rates exceeding 90% in correctly classifying wines according to their geographical origin.<sup>55</sup> Inductively coupled plasma mass spectrometry (ICP-MS) and inductively coupled plasma optical emission spectrometry (ICP-OES) enable the determination of major, minor, and trace elements in food products. The elemental composition of foods reflects the geological characteristics of the production area, as plants uptake minerals from the soil in patterns that are influenced by soil type, pH, and mineral availability. Elements such as rare earth elements (REEs) are particularly useful for geographical discrimination as they are less affected by agricultural practices and more strongly linked to geological factors.<sup>56</sup> The multi-element approach typically analyzes 20-60 elements simultaneously, creating a comprehensive elemental fingerprint. Statistical analysis of these fingerprints can differentiate products from different geographical regions with high accuracy. For example, the combination of Sr, Rb, Mn, and REEs has been successfully used to authenticate the origin of rice, tea, and coffee. The development of high-resolution ICP-MS instruments has further enhanced the capability to detect ultra-trace elements, providing additional

markers for origin determination.<sup>57</sup> High-performance liquid chromatography (HPLC) and gas chromatography (GC), often coupled with mass spectrometry (MS), provide detailed profiles of organic compounds that can serve as geographical markers. These techniques are particularly valuable for analyzing secondary metabolites, such as polyphenols, alkaloids, and terpenes, whose production is influenced by environmental stress factors and consequently varies with geographical location. The volatile compound profile, analyzed by GC-MS, reflects both the plant's genetics and its interaction with the environment, making it a powerful tool for origin authentication.<sup>58</sup> Ultra-high-performance liquid chromatography (UHPLC) coupled with high-resolution mass spectrometry (HRMS) has emerged as a particularly powerful platform for non-targeted metabolomics approaches. These systems can detect thousands of compounds in a single analysis, providing comprehensive chemical fingerprints that capture subtle differences between products from different origins. Time-of-flight (TOF) and Orbitrap mass analyzers offer the mass accuracy and resolution necessary to identify unknown compounds and discover new geographical markers.<sup>59</sup> Near-infrared spectroscopy (NIR), mid-infrared spectroscopy (MIR), and Raman spectroscopy offer rapid, non-destructive alternatives to traditional analytical methods. While these techniques generally provide less specific chemical information than chromatographic or mass spectrometric methods, their speed, low cost, and minimal sample preparation requirements make them attractive for routine screening applications. When combined with appropriate chemometric methods, spectroscopic techniques can achieve classification accuracies comparable to more sophisticated analytical approaches.<sup>60</sup> Nuclear magnetic resonance (NMR) spectroscopy occupies a unique position among spectroscopic techniques, providing both structural information about specific compounds and comprehensive metabolite profiles. <sup>1</sup>H-NMR fingerprinting has been successfully applied to authenticate olive oil, honey, and fruit juices, while <sup>13</sup>C-NMR provides complementary information about the carbon skeleton of organic compounds. The quantitative nature of NMR, requiring no compound-specific calibration, makes it particularly valuable for detecting adulteration and verifying authenticity claims.<sup>61</sup> The complexity of modern analytical data, particularly from techniques that generate hundreds or thousands of variables per sample, necessitates the use of sophisticated statistical methods for data interpretation. Chemometrics, the application of mathematical and statistical methods to chemical data, provides the tools necessary to extract meaningful information from complex datasets and build reliable classification models for food authentication.<sup>62</sup> PCA is the most widely used chemometric technique in food authentication studies. This method reduces the dimensionality of complex datasets by identifying the directions (principal components) along which the data varies most. By projecting the original multi-dimensional data onto a smaller number of principal components, PCA enables visualization of sample relationships and identification of

patterns that would be impossible to detect in the raw data. In geographical origin studies, PCA can reveal natural groupings of samples from different regions and identify the chemical variables that contribute most to these separations.<sup>63</sup> The application of PCA has been particularly successful in olive oil authentication, where the combination of fatty acid profiles, phenolic compounds, and volatile components analyzed by PCA can differentiate oils from different Mediterranean regions with accuracy rates exceeding 85%. The loading plots generated by PCA also provide valuable information about which chemical compounds are most important for geographical discrimination, guiding the development of targeted analytical methods.<sup>64</sup> Linear discriminant analysis (LDA) and partial least squares discriminant analysis (PLS-DA) are supervised classification methods that build mathematical models to predict sample categories based on chemical data. Unlike PCA, which is unsupervised and exploratory, discriminant analysis methods use known sample classifications to optimize the separation between groups. These techniques are particularly valuable for building predictive models that can classify unknown samples according to their geographical origin. Cross-validation procedures are essential to assess the reliability of these models and avoid overfitting.<sup>65</sup> The combination of multiple discriminant analysis techniques, known as ensemble learning, has shown improved classification performance compared to single methods. For example, the authentication of honey geographical origin using a combination of LDA and PLS-DA applied to multi-element data achieved classification accuracies above 95%, demonstrating the power of integrated chemometric approaches.<sup>66</sup> Recent advances in machine learning have introduced powerful new tools for food authentication, including support vector machines (SVM), random forests (RF), and artificial neural networks (ANN). These methods can capture non-linear relationships in data and often achieve higher classification accuracies than traditional linear methods. Deep learning approaches, particularly convolutional neural networks applied to spectroscopic data, represent the cutting edge of chemometric applications in food authentication, though their "black box" nature can limit their acceptance in regulatory contexts where model interpretability is important.<sup>67</sup> The application of machine learning to food authentication has been particularly successful when dealing with complex, high-dimensional datasets. For instance, random forest models applied to untargeted metabolomics data from LC-MS analysis have shown remarkable ability to identify subtle patterns that distinguish products from different geographical origins, even when traditional statistical methods fail to find clear separations. These advanced methods are particularly valuable for detecting sophisticated fraud where adulterants have been specifically chosen to mimic the chemical profile of authentic products.<sup>68</sup> The authentication of geographical origin represents a critical challenge in ensuring food authenticity and protecting both consumers and honest producers from fraud. The combination of advanced analytical techniques with sophisticated chemometric methods provides

powerful tools for origin verification, with success rates often exceeding 95% for well-characterized products. However, the dynamic nature of food fraud requires continuous development of new analytical approaches and regular updating of authentication databases to include new production regions and potential adulterants. The future of geographical origin authentication lies in the integration of multiple analytical platforms and the development of portable, field-deployable instruments that can provide rapid screening at various points in the supply chain. The combination of documentary traceability systems with chemical authentication methods offers the most robust approach to ensuring food authenticity. As analytical technologies continue to advance and become more accessible, the vision of comprehensive farm-to-fork traceability based on chemical fingerprinting becomes increasingly achievable.

## *1.2 Biofumigation and circular economy*

Modern agriculture faces a paradoxical challenge: ensuring food security for a growing global population, estimated to reach 9.7 billion by 2050, while simultaneously minimizing the environmental impact of intensive agricultural practices. The systematic use of synthetic pesticides, although effective for immediate pathogen control, has generated a cascade of environmental and health concerns that demand urgent reconsideration of current agricultural paradigms.<sup>39</sup> The accumulation of persistent organic pollutants in soil matrices, contamination of water resources, and documented decline in pollinator populations represent only a fraction of the ecological consequences associated with conventional pest management strategies. Furthermore, the emergence of pesticide-resistant pathogen populations and the bioaccumulation of toxic compounds through trophic chains have raised significant concerns about the long-term sustainability of chemical-intensive agriculture.<sup>40</sup> The transition toward a circular economy model in agriculture represents a fundamental shift from the traditional linear "take-make-dispose" approach to a regenerative system that maximizes resource efficiency and minimizes waste generation. This paradigm shift is particularly relevant in the context of agricultural waste management, where plant residues and processing by-products, traditionally considered as disposal problems, are increasingly recognized as valuable resources for the development of bio-based alternatives to synthetic inputs.<sup>41</sup> The circular economy framework not only addresses waste management challenges but also provides opportunities for creating added value from agricultural biomass, reducing dependency on fossil fuel-derived

chemicals, and enhancing the resilience of agricultural systems through diversification of pest management strategies. Within this context, the Brassicaceae family emerges as a particularly promising source of bioactive compounds for sustainable crop protection. This plant family, comprising approximately 3,700 species including economically important crops such as cabbage (*Brassica oleracea*), rapeseed (*Brassica napus*), and mustard (*Sinapis alba*), is characterized by the presence of glucosinolates (GSLs) – sulfur-containing secondary metabolites that serve as the plant's natural defense system (4).<sup>42</sup> The unique glucosinolate-myrosinase system, often referred to as the "mustard oil bomb," represents one of the most sophisticated chemical defense mechanisms in the plant kingdom. Upon tissue disruption, glucosinolates are enzymatically hydrolyzed by myrosinase to produce a range of bioactive compounds, predominantly isothiocyanates (ITCs), which exhibit broad-spectrum antimicrobial, nematicidal, and herbicidal activities.<sup>43</sup> The exploitation of glucosinolate-containing plant materials for pest management, termed biofumigation, has gained considerable attention as an environmentally sustainable alternative to synthetic soil fumigants, particularly following the phase-out of methyl bromide under the Montreal Protocol. The incorporation of Brassicaceae residues into soil, either as fresh green manure or as processed seed meals from oil extraction industries, releases volatile ITCs that suppress a wide range of soilborne pathogens, including *Fusarium* spp., *Rhizoctonia solani*, and *Verticillium dahliae*, as well as plant-parasitic nematodes such as *Meloidogyne* spp.<sup>44</sup> This approach not only provides effective pest control but also contributes to soil organic matter enhancement, nutrient cycling, and improvement of soil physical properties, thereby addressing multiple aspects of sustainable soil management. The valorization of Brassicaceae processing waste represents a significant opportunity within the circular economy framework. The global production of rapeseed alone exceeds 70 million tonnes annually, generating substantial quantities of seed meal after oil extraction. These meals, containing 1-2% glucosinolates, have traditionally been used as animal feed after detoxification processes. However, their potential as biopesticides offers a higher-value application that aligns with circular economy principles.<sup>45</sup> Similarly, vegetable processing industries generate considerable volumes of Brassicaceae waste, including leaves, stems, and roots that are typically discarded or composted. These materials contain significant concentrations of glucosinolates and other bioactive compounds that could be extracted and formulated into biopesticide products, thereby creating value from waste streams while reducing the environmental burden of waste disposal. The chemical diversity of glucosinolates, with over 130 identified structures, provides opportunities for targeting different pest species and developing integrated pest management strategies. Aliphatic glucosinolates, such as sinigrin and glucoraphanin, produce volatile ITCs with strong fumigant properties, while aromatic and indole glucosinolates yield compounds with specific biological activities against particular

pathogen groups.<sup>46</sup> This structural diversity, combined with the possibility of selecting or breeding Brassicaceae varieties with optimized glucosinolate profiles, offers flexibility in developing tailored biopesticide solutions for different agricultural contexts. Recent advances in extraction technologies and formulation science have enhanced the feasibility of developing commercial biopesticide products from Brassicaceae materials. Supercritical fluid extraction, microwave-assisted extraction, and enzyme-assisted extraction methods have been optimized to maximize the recovery of bioactive compounds while minimizing energy consumption and solvent use.<sup>47</sup> Furthermore, encapsulation technologies and controlled-release formulations have been developed to overcome the limitations associated with the high volatility and reactivity of ITCs, improving their stability, shelf-life, and field efficacy. These technological innovations are critical for translating the laboratory-demonstrated potential of Brassicaceae-derived biopesticides into practical agricultural applications. The integration of Brassicaceae-based pest management strategies into existing agricultural systems requires consideration of multiple factors, including crop rotation sequences, timing of application, environmental conditions affecting ITC release and persistence, and compatibility with other pest management practices. The effectiveness of biofumigation is influenced by soil temperature, moisture content, pH, and organic matter content, all of which affect the hydrolysis of glucosinolates and the fate of resulting ITCs in soil.<sup>48</sup> Understanding these interactions is essential for optimizing the efficacy of Brassicaceae-based interventions and ensuring their reliable performance under field conditions.

### *1.3 Functional food and fortification*

The term "nutraceutical" was coined in 1989 by Stephen DeFelice, combining the words "nutrition" and "pharmaceutical" to describe food-derived products that provide both nutritional value and health benefits beyond basic nutrition.<sup>1</sup> Nutraceuticals represent a rapidly expanding sector at the intersection of food science, nutrition, and pharmacology, encompassing a diverse range of bioactive compounds, functional foods, and dietary supplements.<sup>2</sup> These products have gained significant attention due to their potential role in disease prevention, health promotion, and therapeutic applications.<sup>3</sup> The nutraceutical market's exponential growth over the past three decades tells a story of changing attitudes toward health. As consumers have discovered the powerful connection between diet and wellness, they've increasingly turned to these products as a proactive solution. This shift is fueled by converging forces: an aging population seeking to maintain vitality, healthcare costs that

make prevention more appealing than treatment, and a cultural embrace of natural approaches to wellness. Rather than waiting for illness to strike, today's consumers view nutraceuticals as daily investments in their long-term health, transforming what was once a niche market into a thriving industry that reflects our evolving relationship with preventive care. Nutraceuticals can be categorized into several classes based on their origin, chemical structure, and biological function. These include vitamins, minerals, amino acids, fatty acids, probiotics, prebiotics, phytochemicals, and bioactive peptides.<sup>4</sup> Among these, plant-derived phytochemicals, particularly polyphenolic compounds, have attracted considerable scientific interest due to their potent antioxidant properties and diverse health-promoting effects.<sup>5</sup> The regulatory landscape for nutraceuticals varies significantly across different countries and regions, creating challenges for standardization, quality control, and consumer protection. In the European Union, nutraceuticals fall under food supplement regulations, while in the United States, they are governed by the Dietary Supplement Health and Education Act (DSHEA).<sup>6</sup> This regulatory complexity underscores the importance of rigorous scientific validation, analytical characterization, and authentication methods for nutraceutical products.

Antioxidants are molecules capable of inhibiting or delaying the oxidation of other substrates by scavenging free radicals, chelating metal ions, or modulating cellular antioxidant defence systems.<sup>7</sup> From a chemical perspective, antioxidants function as reducing agents that donate electrons or hydrogen atoms to reactive oxygen species (ROS) and reactive nitrogen species (RNS), thereby neutralizing their harmful effects.<sup>8</sup>

The biological importance of antioxidants stems from the fundamental role of oxidative stress in cellular dysfunction and disease pathogenesis. Under physiological conditions, cells maintain a delicate balance between the production of reactive species and their neutralization by endogenous antioxidant systems, including enzymatic defenses such as superoxide dismutase (SOD), catalase (CAT), and glutathione peroxidase (GPx), as well as non-enzymatic antioxidants like glutathione, vitamins C and E, and carotenoids.<sup>9</sup> When this balance is disrupted, excessive accumulation of ROS can damage cellular macromolecules leading to oxidative stress.<sup>10</sup> This oxidative damage has been implicated in the etiology of numerous chronic diseases, including cardiovascular disorders, neurodegenerative diseases, diabetes, cancer, and inflammatory conditions.<sup>11</sup> Dietary antioxidants, particularly those derived from plant sources, complement endogenous antioxidant defenses and may help restore redox homeostasis.<sup>12</sup> These exogenous antioxidants work through multiple mechanisms: direct scavenging of free radicals, chelation of pro-oxidant metal ions (iron and copper), inhibition of oxidative enzymes such as NADPH oxidase and xanthine oxidase, and upregulation of endogenous

antioxidant enzyme expression through activation of transcription factors like Nuclear factor erythroid 2-related factor 2 (Nrf2).<sup>13</sup> The effectiveness of antioxidant molecules depends fundamentally on their chemical architecture, which determines how they interact with and neutralize free radicals. Critical structural features enable these compounds to donate electrons while remaining stable themselves. Hydroxyl groups attached to aromatic rings are particularly important, as they readily donate hydrogen atoms to reactive species. The resulting radicals are then stabilized through resonance delocalization across the aromatic system, preventing further chain reactions. Conjugated double bond systems represent another essential feature, creating networks that allow electron delocalization across multiple bonds. This arrangement enables antioxidants to absorb and dissipate energy from reactive species effectively. The ability to stabilize unpaired electrons through resonance is what truly distinguishes effective antioxidants from other molecules, preventing them from propagating the oxidative damage they're meant to stop.<sup>14</sup> Phenolic compounds exemplify these structural principles and constitute the largest class of dietary antioxidants. Their aromatic rings with hydroxyl groups create an optimal framework for radical scavenging activity. Research has shown that even subtle variations in molecular structure, such as the positioning of hydroxyl groups or the extent of conjugation, can significantly impact antioxidant potency.<sup>14</sup>

Polyphenols constitute the most abundant class of secondary metabolites in the plant kingdom, with over 8,000 different structures identified.<sup>15</sup> These compounds are characterized by the presence of multiple phenolic hydroxyl groups attached to one or more aromatic rings, conferring potent antioxidant properties and diverse biological activities.<sup>16</sup> The classification of polyphenols is based on the number of phenolic rings and the structural elements that bind these rings together. The major classes include phenolic acids, flavonoids, stilbenes, and lignans, with flavonoids representing the largest and most studied subgroup.<sup>17</sup> Phenolic acids represent a fundamental class of polyphenolic compounds characterized by their relatively simple molecular architecture, consisting of a single benzene ring that carries both a carboxylic acid functional group and one or more hydroxyl groups. This structural simplicity, however, belies their significant biological activity and widespread distribution in plant-based foods. These compounds are traditionally classified into two major categories based on their carbon skeleton structure: the hydroxybenzoic acids, which possess a C6-C1 configuration where the carboxylic acid group is directly attached to the benzene ring, and the hydroxycinnamic acids, featuring a C6-C3 structure that includes a three-carbon side chain between the benzene ring and the carboxylic acid group.<sup>18</sup> The hydroxybenzoic acid family encompasses several important compounds that play crucial roles in plant metabolism and human nutrition, including gallic acid with its three hydroxyl groups that confer potent antioxidant properties,

protocatechuic acid which serves as a precursor to more complex polyphenols, the simpler p-hydroxybenzoic acid with a single hydroxyl group in the para position, vanillic acid bearing both hydroxyl and methoxy substituents, and syringic acid with its distinctive pattern of methoxylation. These compounds rarely exist as free acids in plant tissues but are instead predominantly found in bound forms, covalently linked to cell wall components such as cellulose, lignin, and structural proteins through ester and ether bonds. This structural integration into the plant cell wall matrix not only contributes to the mechanical properties and defense mechanisms of plants but also influences the bioavailability and release of these beneficial compounds during food processing and digestion, requiring specific conditions or enzymatic action to liberate them from their bound state and make them accessible for absorption in the human digestive system.<sup>18</sup> Hydroxycinnamic acids represent the more abundant branch of phenolic acids in plants, distinguished by their three-carbon side chain that provides greater structural versatility than hydroxybenzoic acids. This group includes nutritionally significant compounds such as caffeic acid, which serves as a building block for complex phenolic structures, ferulic acid that cross-links plant cell walls, p-coumaric acid that acts as a precursor for various plant metabolites, and sinapic acid with its distinctive dimethoxy groups that influence both antioxidant capacity and lignification processes. These acids rarely exist as free compounds but instead occur in conjugated forms throughout plant tissues, most notably esterified with quinic acid to form chlorogenic acids, abundant in coffee and associated with potential benefits for glucose metabolism and cardiovascular health. Additionally, hydroxycinnamic acids are extensively bound to cell wall polysaccharides through ester linkages, particularly with arabinoxylans in cereals and pectins in fruits, where they contribute to structural integrity while serving as a reservoir of bioactive compounds.<sup>19</sup> This dual existence in both soluble and bound forms means the dietary intake of hydroxycinnamic acids is substantially higher than analyses of free acids suggest, with their bioavailability depending on food matrix characteristics, processing methods, and intestinal esterase activity capable of releasing them from their conjugated state.<sup>19</sup> Flavonoids constitute one of the most diverse and abundant classes of plant polyphenols, unified by their distinctive C6-C3-C6 carbon skeleton architecture that consists of two aromatic rings, designated as A and B rings, connected through a three-carbon bridge that typically cyclizes to form a heterocyclic C ring.<sup>20</sup> This fundamental structural framework serves as a molecular scaffold that nature has modified through countless evolutionary iterations, resulting in thousands of distinct compounds that differ in their oxidation states, hydroxylation patterns, methylation, glycosylation, and other structural modifications. The remarkable diversity within this class necessitates further subdivision based primarily on the oxidation state and substitution pattern of the central C ring, yielding the major subclasses of

flavonols, flavones, flavanones, flavanonols, flavanols, anthocyanidins, and isoflavones, each with distinct chemical properties and biological activities.

Among these subclasses, flavonols such as quercetin, kaempferol, and myricetin stand out as perhaps the most ubiquitous flavonoids in the human diet, characterized by their 3-hydroxyflavone backbone that confers both structural stability and potent antioxidant activity. These compounds rarely exist as free aglycones in nature but instead occur predominantly as glycosides, with various sugar moieties attached most commonly at the 3-position of the C ring, though glycosylation can also occur at multiple positions on the A or B rings, creating a vast array of naturally occurring derivatives that influence both their solubility and bioavailability.<sup>21</sup> In contrast, flavones like apigenin and luteolin, which lack the characteristic 3-hydroxyl group of flavonols, show a more restricted distribution in common fruits and vegetables but are particularly abundant in herbs such as parsley and chamomile, as well as in certain cereals, where they contribute to both flavor profiles and potential health benefits. The flavanone subclass, exemplified by compounds such as naringenin in grapefruit and hesperidin in oranges, represents a structurally unique group characterized by a fully saturated C ring lacking the C2-C3 double bond found in flavones and flavonols, a feature that significantly influences their three-dimensional structure and consequently their biological activities.<sup>22</sup> These compounds are particularly concentrated in citrus fruits where they occur primarily in the white spongy portion of the peel, contributing to both the bitter taste and the documented cardiovascular benefits associated with citrus consumption. Meanwhile, the flavanol category, which includes the monomeric catechins and epicatechins as well as their oligomeric and polymeric derivatives known as proanthocyanidins or condensed tannins, represents some of the most studied flavonoids due to their abundance in widely consumed beverages like tea and wine, as well as in cocoa products.<sup>23</sup> These compounds exhibit remarkable structural complexity, ranging from simple monomers to massive polymers with degrees of polymerization exceeding 50 units, creating molecules with diverse physical properties and biological activities that depend heavily on their chain length and interflavanol linkage patterns. Finally, the anthocyanidins and their glycosylated forms, the anthocyanins, represent the most visually striking members of the flavonoid family, responsible for the vibrant red, purple, and blue hues that paint the surfaces of countless fruits, vegetables, and flowers. The six common anthocyanidins found in foods – cyanidin, delphinidin, pelargonidin, peonidin, petunidin, and malvidin – differ only in their hydroxylation and methylation patterns on the B ring, yet these subtle structural variations produce dramatic differences in colour that range from the orange-red of pelargonidin in strawberries to the deep purple of delphinidin in blueberries.<sup>24</sup> In nature, these compounds exist almost exclusively as glycosides, with sugar attachments that stabilize the flavylum

cation and modulate both colour expression and stability under different pH conditions, creating a natural pH indicator system that has fascinated chemists and nutritionists alike for its dual role in plant physiology and human health. Beyond the well-characterized flavonoids and phenolic acids, the plant kingdom produces a diverse array of other polyphenolic compounds that contribute significantly to both plant physiology and human nutrition, including stilbenes, lignans, curcuminoids, and tannins, each with unique structural features and biological properties. Stilbenes, which are characterized by their distinctive C6-C2-C6 structure consisting of two phenyl rings connected by an ethylene bridge, have garnered exceptional scientific interest, particularly resveratrol, the most studied member of this class found notably in grape skins, red wine, and peanuts. The trans-resveratrol isomer, which predominates in nature, has been extensively investigated for its cardioprotective effects, including its ability to modulate lipid metabolism, reduce platelet aggregation, and improve endothelial function, while its potential anti-aging properties have sparked interest due to its activation of sirtuins, a family of proteins associated with longevity and metabolic regulation.<sup>25</sup> Lignans represent another fascinating class of diphenolic compounds formed through the oxidative dimerization of two cinnamic acid residues, creating structures that often exhibit potent biological activities including phytoestrogenic effects. Secoisolariciresinol and matairesinol, the primary dietary lignans, are particularly abundant in flaxseed, which contains concentrations hundreds of times higher than other food sources, though they are also found in meaningful amounts in whole grains, legumes, and various vegetables. These compounds undergo transformation by intestinal bacteria to produce enterolignans, specifically enterodiols and enterolactone, which are the bioactive metabolites absorbed and circulated in human plasma, contributing to the observed associations between lignan consumption and reduced risks of hormone-dependent cancers and cardiovascular disease. The tannin family, traditionally divided into condensed and hydrolyzable tannins, represents some of the most complex polyphenolic structures in nature, with hydrolyzable tannins consisting of gallic acid or its dimeric form, ellagic acid, esterified to a central polyol core, most commonly glucose.<sup>26</sup> Gallotannins, which contain multiple gallic acid units, and ellagitannins, featuring the more complex ellagic acid moieties, are abundant in foods such as pomegranates, walnuts, and oak-aged wines, where they contribute not only to astringency and colour stability but also to significant antioxidant and anti-inflammatory activities that have been linked to various health benefits including improved cardiovascular health and potential anticancer effects.<sup>26</sup> The biological effects of polyphenols extend far beyond their antioxidant properties, encompassing anti-inflammatory, antimicrobial, anticarcinogenic, cardioprotective, neuroprotective, and metabolic regulatory activities.<sup>27</sup> Epidemiological studies have consistently demonstrated inverse associations between polyphenol-rich diet consumption and the risk of chronic diseases. Cardiovascular benefits of polyphenols include

improvement of endothelial function, reduction of blood pressure, inhibition of platelet aggregation, modulation of lipid metabolism, and protection against LDL oxidation. These effects contribute to reduced atherosclerotic plaque formation and decreased cardiovascular event risk.<sup>28</sup> In the context of metabolic health, polyphenols have been shown to improve insulin sensitivity, regulate glucose homeostasis, modulate adipocyte differentiation and function, and influence gut microbiota composition. These mechanisms may contribute to the prevention and management of obesity, type 2 diabetes, and metabolic syndrome.<sup>29</sup> The neuroprotective effects of polyphenols are mediated through multiple mechanisms, including protection against oxidative stress-induced neuronal damage, modulation of neuroinflammation, enhancement of neuroplasticity, and potential effects on amyloid-beta aggregation and tau phosphorylation in neurodegenerative diseases.<sup>30</sup> Emerging evidence suggests that polyphenols may also influence epigenetic mechanisms, including DNA methylation, histone modifications, and microRNA expression, potentially affecting gene expression patterns related to disease susceptibility and aging processes.<sup>31</sup>

Functional foods are defined as foods that provide health benefits beyond basic nutrition due to the presence of physiologically active components.<sup>32</sup> This concept encompasses naturally functional foods (such as fruits, vegetables, whole grains, and fish) and modified or fortified foods where specific bioactive compounds have been added, increased, or removed to enhance health benefits. The functional food market has grown substantially in response to consumer demand for foods that support health and prevent disease. Categories of functional foods include probiotic and prebiotic foods, fortified foods enriched with vitamins, minerals, or phytochemicals, foods with added omega-3 fatty acids, and products containing plant sterols or stanols.<sup>33</sup> The development of functional foods requires careful consideration of several factors: the bioavailability and stability of added bioactive compounds, potential interactions with food matrix components, sensory properties and consumer acceptability, regulatory compliance, and scientific substantiation of health claims.<sup>34</sup> Fortification strategies have been successfully applied to various food categories to address nutritional deficiencies or enhance health benefits. Common examples include cereals fortified with vitamins and minerals, dairy products enriched with vitamin D and calcium, margarines containing plant sterols, beverages fortified with antioxidants or vitamins, and bakery products enriched with dietary fiber or omega-3 fatty acids. Recent innovations in food fortification have focused on the incorporation of plant-derived bioactive compounds, including polyphenols, carotenoids, and glucosinolates, into conventional food matrices. These developments require advanced encapsulation technologies to protect sensitive bioactives from degradation during processing and storage while ensuring their release and bioavailability upon consumption.<sup>35</sup> The fortification of foods with polyphenol-rich

extracts represents a promising strategy for enhancing the nutritional and functional properties of food products, yet it presents considerable technical challenges that must be carefully addressed. The inherent reactivity of polyphenolic compounds, combined with their pronounced effects on sensory characteristics such as bitterness, astringency, and color modification, can significantly impact consumer acceptability of fortified products. Furthermore, these bioactive compounds exhibit marked susceptibility to degradation when exposed to environmental factors including light, oxygen, elevated temperatures, and various processing conditions, potentially compromising their stability and biological activity. To overcome these limitations, food technologists have developed sophisticated delivery systems, including microencapsulation and nanoencapsulation technologies, as well as complexation strategies with proteins or polysaccharides, which can protect polyphenols from degradation while masking their undesirable sensory attributes.<sup>36</sup>

In this context, the exploration of medicinal herbs as novel sources for food fortification has gained considerable momentum, driven by their cost-effectiveness, widespread availability, and rich nutritive qualities. *Medicago sativa* L., commonly known as alfalfa or lucerne, exemplifies this trend as a particularly promising candidate for functional food development. Originally cultivated as a perennial legume forage crop valued for its nitrogen-fixing capacity and exceptional nutritional profile, alfalfa contains an impressive 15-25% protein on a dry weight basis, surpassing many conventional plant protein sources. This protein richness is complemented by significant concentrations of essential vitamins, particularly vitamin K, vitamin C, and B-complex vitamins, along with important minerals including calcium, potassium, phosphorus, and iron, as well as substantial amounts of dietary fiber.<sup>37</sup> What makes alfalfa particularly intriguing for food fortification applications extends beyond its macronutrient composition to its remarkable array of bioactive phytochemicals that confer various health-promoting effects. The plant serves as a natural repository of diverse secondary metabolites, including triterpene saponins that contribute to its hypocholesterolemic properties, flavonoids and phenolic acids that provide potent antioxidant activity, and phytoestrogens such as coumestrol and formononetin that may offer protective effects against hormone-dependent conditions. Additionally, alfalfa contains alkaloids, tannins, polysaccharides, and chlorophyll derivatives, collectively contributing to a spectrum of biological activities encompassing antioxidant, anti-inflammatory, immunostimulatory, and potentially anticarcinogenic properties.<sup>38</sup> This unique combination of nutritional density and bioactive compound diversity positions alfalfa as an attractive multifunctional ingredient for developing fortified foods that can deliver both essential nutrients and health-promoting phytochemicals, though careful consideration must be given to processing methods and formulation strategies to maintain bioactivity

while ensuring acceptable sensory properties in the final food products. Alfalfa sprouts and young leaves have been consumed as vegetables and used in traditional medicine systems for centuries. Modern research has validated some traditional uses and revealed additional potential applications in functional foods, nutraceuticals, and pharmaceutical formulations.<sup>38</sup>

## *References*

1. DeFelice SL. The nutraceutical revolution: its impact on food industry R&D. *Trends Food Sci Technol.* 1995;6(2):59-61.
2. Santini A, Novellino E. Nutraceuticals in hypercholesterolaemia: an overview. *Br J Pharmacol.* 2017;174(11):1450-1463.
3. Daliu P, Santini A, Novellino E. From pharmaceuticals to nutraceuticals: bridging disease prevention and management. *Expert Rev Clin Pharmacol.* 2019;12(1):1-7.
4. Pandey M, Verma RK, Saraf SA. Nutraceuticals: new era of medicine and health. *Asian J Pharm Clin Res.* 2010;3(1):11-15.
5. Das L, Bhaumik E, Raychaudhuri U, Chakraborty R. Role of nutraceuticals in human health. *J Food Sci Technol.* 2012;49(2):173-183.
6. Kris-Etherton PM, Hecker KD, Bonanome A, et al. Bioactive compounds in foods: their role in the prevention of cardiovascular disease and cancer. *Am J Med.* 2002;113(9B):71S-88S.
7. Halliwell B, Rafter J, Jenner A. Health promotion by flavonoids, tocopherols, tocotrienols, and other phenols: direct or indirect effects? Antioxidant or not? *Am J Clin Nutr.* 2005;81(1):268S-276S.
8. Lobo V, Patil A, Phatak A, Chandra N. Free radicals, antioxidants and functional foods: Impact on human health. *Pharmacogn Rev.* 2010;4(8):118-126.
9. Pisoschi AM, Pop A. The role of antioxidants in the chemistry of oxidative stress: A review. *Eur J Med Chem.* 2015;97:55-74.
10. Sies H, Jones DP. Reactive oxygen species (ROS) as pleiotropic physiological signalling agents. *Nat Rev Mol Cell Biol.* 2020;21(7):363-383.
11. Pham-Huy LA, He H, Pham-Huy C. Free radicals, antioxidants in disease and health. *Int J Biomed Sci.* 2008;4(2):89-96.
12. Forman HJ, Zhang H. Targeting oxidative stress in disease: promise and limitations of antioxidant therapy. *Nat Rev Drug Discov.* 2021;20(9):689-709.
13. Zhang YJ, Gan RY, Li S, et al. Antioxidant phytochemicals for the prevention and treatment of chronic diseases. *Molecules.* 2015;20(12):21138-21156.

14. Rice-Evans CA, Miller NJ, Paganga G. Structure-antioxidant activity relationships of flavonoids and phenolic acids. *Free Radic Biol Med.* 1996;20(7):933-956.
15. Tsao R. Chemistry and biochemistry of dietary polyphenols. *Nutrients.* 2010;2(12):1231-1246.
16. Manach C, Scalbert A, Morand C, Rémésy C, Jiménez L. Polyphenols: food sources and bioavailability. *Am J Clin Nutr.* 2004;79(5):727-747.
17. Del Rio D, Rodriguez-Mateos A, Spencer JP, Tognolini M, Borges G, Crozier A. Dietary (poly)phenolics in human health: structures, bioavailability, and evidence of protective effects against chronic diseases. *Antioxid Redox Signal.* 2013;18(14):1818-1892.
18. Shahidi F, Ambigaipalan P. Phenolics and polyphenolics in foods, beverages and spices: Antioxidant activity and health effects – A review. *J Funct Foods.* 2015;18:820-897.
19. Tomás-Barberán FA, Clifford MN. Dietary hydroxybenzoic acid derivatives – nature, occurrence and dietary burden. *J Sci Food Agric.* 2000;80(7):1024-1032.
20. Pérez-Jiménez J, Neveu V, Vos F, Scalbert A. Identification of the 100 richest dietary sources of polyphenols: an application of the Phenol-Explorer database. *Eur J Clin Nutr.* 2010;64(S3):S112-S120.
21. Erlund I. Review of the flavonoids quercetin, hesperetin, and naringenin. Dietary sources, bioactivities, bioavailability, and epidemiology. *Nutr Res.* 2004;24(10):851-874.
22. Panche AN, Diwan AD, Chandra SR. Flavonoids: an overview. *J Nutr Sci.* 2016;5:e47.
23. Gu L, Kelm MA, Hammerstone JF, et al. Concentrations of proanthocyanidins in common foods and estimations of normal consumption. *J Nutr.* 2004;134(3):613-617.
24. Khoo HE, Azlan A, Tang ST, Lim SM. Anthocyanidins and anthocyanins: colored pigments as food, pharmaceutical ingredients, and the potential health benefits. *Food Nutr Res.* 2017;61(1):1361779.
25. Baur JA, Sinclair DA. Therapeutic potential of resveratrol: the in vivo evidence. *Nat Rev Drug Discov.* 2006;5(6):493-506.
26. Khanbabaee K, van Ree T. Tannins: classification and definition. *Nat Prod Rep.* 2001;18(6):641-649.
27. Pandey KB, Rizvi SI. Plant polyphenols as dietary antioxidants in human health and disease. *Oxid Med Cell Longev.* 2009;2(5):270-278.
28. Tresserra-Rimbau, Anna, et al. "Polyphenol intake and mortality risk: a re-analysis of the PREDIMED trial." *BMC medicine* 12.1 (2014): 77.
29. Williamson, G1. "The role of polyphenols in modern nutrition." *Nutrition bulletin* 42.3 (2017): 226-235.

30. Spencer, Jeremy PE. "The impact of fruit flavonoids on memory and cognition." *British Journal of Nutrition* 104.S3 (2010): S40-S47.
31. Meeran, Syed M., Amiya Ahmed, and Trygve O. Tollefsbol. "Epigenetic targets of bioactive dietary components for cancer prevention and therapy." *Clinical epigenetics* 1.3 (2010): 101-116.
32. Bigliardi, Barbara, and Francesco Galati. "Innovation trends in the food industry: The case of functional foods." *Trends in Food Science & Technology* 31.2 (2013): 118-129.
33. Roberfroid, Marcel. "Functional food concept and its application to prebiotics." *Digestive and liver Disease* 34 (2002): S105-S110.
34. Siró, István, et al. "Functional food. Product development, marketing and consumer acceptance—A review." *Appetite* 51.3 (2008): 456-467.
35. Fang Z, Bhandari B. Encapsulation of polyphenols – a review. *Trends Food Sci Technol.* 2010;21(10):510-523.
36. Ezhilarasi, Perumal Natarajan, et al. "Microencapsulation of Garcinia fruit extract by spray drying and its effect on bread quality." *Journal of the Science of Food and Agriculture* 94.6 (2014): 1116-1123.
37. Bora, Kundan Singh, and Anupam Sharma. "The genus Artemisia: a comprehensive review." *Pharmaceutical biology* 49.1 (2011): 101-109.
38. Mielmann, Annchen. "The utilisation of lucerne (*Medicago sativa*): a review." *British Food Journal* 115.4 (2013): 590-600.
39. Carvalho, Fernando P. "Pesticides, environment, and food safety." *Food and energy security* 6.2 (2017): 48-60.
40. Aktar, Md Wasim, Dwaipayan Sengupta, and Ashim Chowdhury. "Impact of pesticides use in agriculture: their benefits and hazards." *Interdisciplinary toxicology* 2.1 (2009): 1.
41. Geissdoerfer, Martin, et al. "The Circular Economy—A new sustainability paradigm?." *Journal of cleaner production* 143 (2017): 757-768.
42. Blažević, Ivica, et al. "Glucosinolate structural diversity, identification, chemical synthesis and metabolism in plants." *Phytochemistry* 169 (2020): 112100.
43. Hanschen, Franziska S., et al. "Degradation of biofumigant isothiocyanates and allyl glucosinolate in soil and their effects on the microbial community composition." *PloS one* 10.7 (2015): e0132931.
44. Matthiessen, John N., and John A. Kirkegaard. "Biofumigation and enhanced biodegradation: opportunity and challenge in soilborne pest and disease management." *Critical reviews in plant sciences* 25.3 (2006): 235-265.

45. Doheny-Adams, Timothy, et al. "Development of an efficient glucosinolate extraction method." *Plant methods* 13.1 (2017): 17.
46. Ishida, Masahiko, et al. "Glucosinolate metabolism, functionality and breeding for the improvement of Brassicaceae vegetables." *Breeding science* 64.1 (2014): 48-59.
47. Wang, Lijun, et al. "Supercritical CO<sub>2</sub> extraction of lipids from grain sorghum dried distillers grains with solubles." *Bioresource technology* 99.5 (2008): 1373-1382.
48. Gimsing, Anne Louise, and John A. Kirkegaard. "Glucosinolates and biofumigation: fate of glucosinolates and their hydrolysis products in soil." *Phytochemistry Reviews* 8.1 (2009): 299-310.
49. Danezis, Georgios P., et al. "Food authentication: Techniques, trends & emerging approaches." *TrAC Trends in Analytical Chemistry* 85 (2016): 123-132.
50. Spink, John, and Douglas C. Moyer. "Defining the public health threat of food fraud." *Journal of food science* 76.9 (2011): R157-R163..
51. Luykx, Dion MAM, and Saskia M. Van Ruth. "An overview of analytical methods for determining the geographical origin of food products." *Food chemistry* 107.2 (2008): 897-911
- Kelly, Simon, Karl Heaton, and Jurian Hoogewerff. "Tracing the geographical origin of food: The application of multi-element and multi-isotope analysis." *Trends in Food Science & Technology* 16.12 (2005): 555-567.
52. Kelly, Simon, Karl Heaton, and Jurian Hoogewerff. "Tracing the geographical origin of food: The application of multi-element and multi-isotope analysis." *Trends in Food Science & Technology* 16.12 (2005): 555-567.
53. Gonzalvez, A., S. Armenta, and M. De La Guardia. "Trace-element composition and stable-isotope ratio for discrimination of foods with Protected Designation of Origin." *TrAC Trends in Analytical Chemistry* 28.11 (2009): 1295-1311.
54. Camin, Federica, et al. "Stable isotope ratio analysis for assessing the authenticity of food of animal origin." *Comprehensive Reviews in Food Science and Food Safety* 15.5 (2016): 868-877.
55. Versari, Andrea, et al. "Progress in authentication, typification and traceability of grapes and wines by chemometric approaches." *Food Research International* 60 (2014): 2-18.
56. Drivelos, Spiros A., and Constantinos A. Georgiou. "Multi-element and multi-isotope-ratio analysis to determine the geographical origin of foods in the European Union." *TrAC Trends in Analytical Chemistry* 40 (2012): 38-51.
57. Zhao, Haiyan, et al. "Multi-element composition of wheat grain and provenance soil and their potentialities as fingerprints of geographical origin." *Journal of Cereal Science* 57.3 (2013): 391-397.

58. Cubero-Leon, Elena, Rosa Peñalver, and Alain Maquet. "Review on metabolomics for food authentication." *Food Research International* 60 (2014): 95-107.
59. Castro-Puyana, María, and Miguel Herrero. "Metabolomics approaches based on mass spectrometry for food safety, quality and traceability." *TrAC Trends in Analytical Chemistry* 52 (2013): 74-87.
60. Oliveri, Paolo, and Gerard Downey. "Multivariate class modeling for the verification of food-authenticity claims." *TrAC Trends in Analytical Chemistry* 35 (2012): 74-86.
61. Mannina, Luisa, Anatoly P. Sobolev, and Stéphane Viel. "Liquid state <sup>1</sup>H high field NMR in food analysis." *Progress in Nuclear Magnetic Resonance Spectroscopy* 66 (2012): 1-39.
62. Berrueta, Luis A., Rosa M. Alonso-Salces, and Károly Héberger. "Supervised pattern recognition in food analysis." *Journal of chromatography A* 1158.1-2 (2007): 196-214.
63. Granato, Daniel, et al. "Use of principal component analysis (PCA) and hierarchical cluster analysis (HCA) for multivariate association between bioactive compounds and functional properties in foods: A critical perspective." *Trends in Food Science & Technology* 72 (2018): 83-90.
64. Bajoub, Aadil, et al. "Olive oil authentication: A comparative analysis of regulatory frameworks with especial emphasis on quality and authenticity indices, and recent analytical techniques developed for their assessment. A review." *Critical Reviews in Food Science and Nutrition* 58.5 (2018): 832-857.
65. Callao, M. Pilar, and Itziar Ruisánchez. "An overview of multivariate qualitative methods for food fraud detection." *Food Control* 86 (2018): 283-293.
66. Karabagias, Ioannis K., et al. "Characterization and classification of *Thymus capitatus* (L.) honey according to geographical origin based on volatile compounds, physicochemical parameters and chemometrics." *Food Research International* 55 (2014): 363-372.
67. Jiménez-Carvelo, Ana M., et al. "Alternative data mining/machine learning methods for the analytical evaluation of food quality and authenticity—A review." *Food research international* 122 (2019): 25-39.
68. Riedl, Janet, Susanne Esslinger, and Carsten Fauhl-Hassek. "Review of validation and reporting of non-targeted fingerprinting approaches for food authentication." *Analytica Chimica Acta* 885 (2015): 17-32.

## *CHAPTER 2: Food quality and traceability*

The valorisation of agricultural products, particularly those linked to specific regions of origin, has become increasingly important in recent years. This emphasis on geographical provenance serves to protect product quality and authenticity for both producers and consumers alike.

In response to the growing threat of counterfeiting and the need to safeguard consumer interests, there has been considerable interest in developing robust methods for certifying the origin of agricultural goods. To enhance the accuracy of geographical traceability models, it is essential to integrate multiple analytical techniques through a multivariate approach.

This chapter presents a study focused on the development of such a model. During the sampling campaign, leaves and fruits (olives or drupes) were collected from multiple orchards and farms across different geographical locations. Metabolite profiles were determined using HPLC-DAD, while trace and ultra-trace metal/metalloid concentrations were quantified by ICP-MS (QqQ). These complementary datasets were then combined to construct a comprehensive model for geographical traceability.

Furthermore, the mineral content of the soil, evaluated by ICP-MS, was correlated with both the mineral composition of leaves and drupes and their metabolomic profiles. This multi-level analysis enabled a deeper investigation of the relationship between orchard location and the distinctive characteristics of the final products.

The study is part of the Italian PNRR-founded Agritech center (Centro Nazionale per le Tecnologie dell'Agricoltura).

The results reported in this chapter are published in the following article:

- Nardin, R., Tamasi, G., Baglioni, M., Fattori, G., Boldrini, A., Esposito, R., & Rossi, C. (2024). Combining Metal(loid) and Secondary Metabolite Levels in *Olea europaea* L. Samples for Geographical Identification. *Foods*, 13(24), 4017.

## 2.1 Introduction

Olive cultivation (*Olea europaea* L.) represents one of the most ancient agricultural practices in human civilization, with archaeological evidence documenting systematic cultivation throughout the Mediterranean basin dating back over 6,000 years.<sup>1</sup> This evergreen species, belonging to the Oleaceae family, has been traditionally cultivated for its drupes, from which olive oil is extracted through mechanical pressing processes that preserve the unique organoleptic and nutritional characteristics of the final product.<sup>2</sup> As a cornerstone of the Mediterranean dietary pattern, olive oil has garnered unprecedented scientific attention due to its well-documented health-promoting properties.<sup>3</sup> Extensive epidemiological and clinical research has demonstrated significant cardioprotective, anti-inflammatory, and neuroprotective effects,<sup>4-5</sup> benefits primarily attributed to the synergistic action of monounsaturated fatty acids and the rich polyphenolic fraction.<sup>6</sup> These bioactive compounds, including hydroxytyrosol, oleuropein, and oleocanthal, represent crucial quality markers of the product, with concentrations varying substantially based on cultivar genetics, geographical provenance, pedoclimatic conditions, and fruit maturation indices.<sup>7</sup> Beyond their physiological benefits, polyphenols contribute fundamentally to the characteristic sensory profile of olive oil, determining critical organoleptic parameters including bitterness intensity, pungency, and overall gustatory complexity.<sup>8</sup>

Among the various commercial categories, Extra Virgin Olive Oil (EVOO) represents the highest quality grade, obtained exclusively through cold mechanical extraction processes ( $\leq 27^{\circ}\text{C}$ ) that preserve the full spectrum of natural antioxidants, vitamins, and bioactive compounds.<sup>9</sup> The stringent definition of EVOO is regulated at both European and international levels through comprehensive frameworks, with rigorous chemical-physical and organoleptic standards that guarantee superior quality.<sup>10-11</sup> However, the premium market value and exponentially growing consumer demand for authentic EVOO have made it increasingly vulnerable to sophisticated adulteration schemes, mislabeling practices, and fraudulent origin claims that threaten both legitimate producers and consumer confidence.<sup>12-13</sup> The growing complexity of global food supply chains, coupled with significant economic incentives associated with premium products, has intensified the urgent need for robust, scientifically validated authentication methodologies capable of protecting geographical denominations and verifying varietal claims.<sup>14</sup>

The European Union's Database of Origin and Registration (DOOR) currently recognizes over forty Protected Designations of Origin (PDO) and Protected Geographical Indications (PGI) for olive oil, with this number continuing to expand as regional producers seek to protect and valorize their

traditional products through formal recognition of unique territorial characteristics.<sup>15</sup> This proliferation of geographical appellations, while celebrating the rich biodiversity of European olive oil production and acknowledging the inseparable link between product quality and territorial specificity, has simultaneously complicated authentication efforts and potentially increased opportunities for fraudulent origin claims.<sup>16</sup> The analytical challenge becomes particularly complex when discriminating oils from geographically contiguous regions, where pedoclimatic conditions may present substantial similarities and traditional varieties frequently overlap across administrative boundaries.<sup>17</sup>

Within the strategic framework of the Italian National Agritech Center, funded through the Piano Nazionale di Ripresa e Resilienza (PNRR), significant research efforts are currently underway to enhance the precision and reliability of existing authentication methodologies while reducing the geographical identification range for premium agricultural products.<sup>18</sup> The ambitious objective involves advancing from discrimination at national or regional scales toward finer characterization capable of identifying origin at sub-regional, provincial, or even individual production district levels. The rapidly expanding market for premium monocultivar EVOO, characterized by oils produced from single olive varieties often associated with specific terroirs, demands the development of sophisticated analytical approaches capable not only of verifying geographical provenance but also of simultaneously confirming cultivar identity and overall compositional authenticity.<sup>19</sup> This dual authentication requirement presents unique analytical challenges, as both genetic factors (cultivar-specific metabolism) and environmental factors (terroir expression) contribute synergistically to the final chemical composition of olive products.<sup>20</sup>

To address these multifaceted authentication challenges, the scientific community has developed various complementary analytical strategies that exploit different dimensions of olive oil chemical complexity and the plant materials from which it derives.<sup>21</sup> These approaches can be broadly categorized into several methodological streams: metabolomic profiling focusing on plant secondary metabolites,<sup>22</sup> elemental analysis characterizing the inorganic composition derived from soil-plant mineral transfer,<sup>23</sup> isotopic ratio analysis examining stable isotope patterns,<sup>24</sup> and genomic approaches targeting DNA markers.<sup>25</sup> Each methodology is founded on the fundamental principle that geographical origin and cultivar identity leave distinctive molecular signatures in plant tissues and derived products, resulting from complex interactions among genetic factors, environmental conditions, and agronomic practices.<sup>26</sup>

The metabolomic approach exploits natural variability in secondary metabolite profiles, particularly phenolic compounds known to vary significantly with both geographical origin and cultivar genetics.<sup>27</sup> These specialized metabolites, produced through complex biosynthetic pathways, perform crucial ecological functions including defense against biotic and abiotic stresses, pollinator attraction, and allelopathic interactions.<sup>28</sup> In olive tissues, the secondary metabolites of greatest authentication interest belong primarily to phenolic compound classes, encompassing simple phenols, phenolic acids, flavonoids, secoiridoids, and lignans.<sup>29</sup> High-performance liquid chromatography (HPLC) coupled with diode array detection (DAD) represents a well-established methodology for quantification of these compounds, offering reliable quantitative data for major phenolic constituents.<sup>30</sup> Recent technological advances have expanded the metabolomic toolbox to include ultra-high-performance liquid chromatography coupled to high-resolution mass spectrometry (UHPLC-HRMS), enabling simultaneous detection and putative identification of hundreds of compounds, thereby providing comprehensive chemical fingerprints with unprecedented resolution.<sup>31</sup>

Complementary to metabolomic profiling, multi-elemental analysis provides a powerful orthogonal approach for geographical authentication based on characterization of the inorganic fraction.<sup>32</sup> This strategy exploits the well-established principle that plants naturally accumulate mineral elements from soil through complex root uptake mechanisms, and that elemental composition of agricultural soils presents considerable spatial heterogeneity reflecting underlying geological substrates, pedogenic processes, atmospheric deposition, and anthropogenic inputs.<sup>33-34</sup> Inductively coupled plasma mass spectrometry (ICP-MS), particularly in triple quadrupole (QQQ) configuration, has emerged as the analytical technique of choice for simultaneous determination of trace and ultra-trace elements in complex food matrices.<sup>35</sup>

The integration of multiple analytical techniques with advanced chemometric approaches has demonstrated superior discrimination capabilities compared to single-technique approaches, particularly when distinguishing samples from geographically proximate regions where compositional differences may be subtle.<sup>36</sup> Data fusion strategies, implemented at various levels from low-level raw data concatenation to high-level decision integration, offer promising approaches for enhancing authentication accuracy and model robustness.<sup>37</sup>

Despite the proliferation of authentication studies, significant knowledge gaps persist regarding the mechanistic relationships linking soil composition to plant metabolite profiles and the spatial variability of both mineral and phytochemical content within geographically defined areas.<sup>38</sup> A particularly promising research direction involves systematic investigation of the entire soil-plant-

product continuum, examining how geological and pedological characteristics influence chemical composition throughout the production chain.<sup>39</sup> Tuscany, with its extraordinary geological heterogeneity spanning metamorphic formations, ophiolitic complexes, marine sedimentary deposits, and volcanic covers, provides an ideal natural laboratory for investigating these relationships.<sup>40</sup> The region hosts several important olive oil PDOs and represents a major production area for premium monocultivar EVOO, making it an exemplary case study for developing and validating integrated authentication approaches.

The present study addresses these research needs by systematically investigating the relationships between soil mineral composition, plant tissue chemistry (leaves and drupes), and secondary metabolite profiles in olive samples from Tuscan production areas, specifically targeting farms in the Siena and Grosseto provinces during the 2022 harvest season. Through integrated analysis using ICP-MS (QqQ configuration) for comprehensive elemental profiling and HPLC-DAD for phenolic metabolite quantification, combined with spectrophotometric assessment of total phenolic content (TPC) and trolox equivalent antioxidant capacity (TEAC), this work aims to: characterize the variability of ultra-trace element composition and secondary metabolite profiles across Tuscan production areas; examine relationships between soil characteristics and secondary metabolite profiles; evaluate the discriminatory power of elemental and metabolomic data for both geographical and cultivar identification; and assess the potential of multivariate data fusion approaches to enhance discrimination capabilities at sub-regional scale. By examining the entire soil-plant-fruit system using complementary analytical platforms and applying rigorous chemometric validation strategies, this study seeks to establish a comprehensive understanding of how geological, environmental, and genetic factors interact to determine the chemical fingerprint of olive products, with broader implications for authentication of high-value agricultural products.

## *2.2 Experimental section*

### *2.2.1 Chemicals*

Nitric acid (HNO<sub>3</sub>, 70%, re-distilled, >99.999% trace metal basis) and hydrogen peroxide (H<sub>2</sub>O<sub>2</sub>, 30%, Suprapur<sup>®</sup>) were both acquired from Merck KGaA (Darmstadt, Germany). Diluted (1% v/v) nitric acid was used for all dilutions and standard preparation and was obtained using ultra-pure (UP) water (18.2 MΩ cm, Direct-Pure, RephiLe Bioscience, filtered with a 0.2 μm PES filter).

Multielement REEs standard (16 elements, 50 mg/L each: Sc, Y, La, Ce, Pr, Nd, Sm, Eu, Gd, Tb, Dy, Ho, Er, Tm, Yb and Lu in 2% nitric acid) and multielement “Periodic Mix” standard (33 elements, 10 mg/L each: Al, As, Ba, Be, Bi, B, Ca, Cd, Cs, Cr, Co, Cu, Ga, In, Fe, Pb, Li, Mg, Mn, Ni, P, K, Rb, Se, Si, Ag, Na, Sr, S, Te, Tl, V e Zn in 10% nitric acid—Tr. HF) were acquired from Merck KGaA (Darmstadt, Germany). Internal standard and single element (Ge, Ti, Zr, Hf, Rh, Sn, Sb) solutions were obtained by dilution of the stock solution of each metal (1000 mg/L in 2% HNO<sub>3</sub>) acquired from Merck KGaA (Darmstadt, Germany). Au standard (1000 mg/L in HCl) was acquired from Fluka, HClO<sub>4</sub> (70%, 99.999% trace metal basis) and HCl (36%, Suprapur<sup>®</sup>) was acquired from Merck KGaA (Darmstadt, Germany).

Gradient grade methanol (MeOH), n-hexane and formic acid were acquired from Merck KGaA (Darmstadt, Germany); tyrosol (>99%), verbascoside (>98%), nuzhenide (>95%), oleuropein (>98%), luteolin (>99%) and spigenin (>99%) standards were acquired from Extrasynthese (Genay, France); whilst hydroxytyrosol (> 98%), caffeic acid (>98%), p-coumaric acid (>98%), ferrulic acid (99%), oleacin (>90%), oleocanthal (>90%) and Ligstroside (>95%) standards were acquired from Merck KGaA (Darmstadt, Germany). Folin–Ciocalteu, Na<sub>2</sub>CO<sub>3</sub> anhydrous and gallic acid (GA) were acquired from Merck KGaA (Darmstadt, Germany). Gradient grade ethanol (EtOH), K<sub>2</sub>S<sub>2</sub>O<sub>8</sub>, ABTS and Trolox<sup>®</sup> were acquired from Merck KGaA (Darmstadt, Germany).

### 2.2.2 Sampling Procedure

A total of 14 orchards belonging to 9 farms were sampled in the present work during the harvest of 2022. Most of these farms grow multiple cultivars of *Olea europea* L., and the three cultivars interest of this work (Leccino, Frantoio and Moraiolo) were all sampled when available. The location of each sampling site is reported in **Figure 1**. Samples were divided into four regions (A, Colli Senesi; B, Val d’Arbia; C Val d’Orcia; D, Grosseto), roughly following PDOs’ geographical regions and prior knowledge on the chemical composition of the soil from previous studies. To avoid conflicts of interests, neither the PDO geographical trade name nor the name of the farms is reported as shown in **Figure 1**.

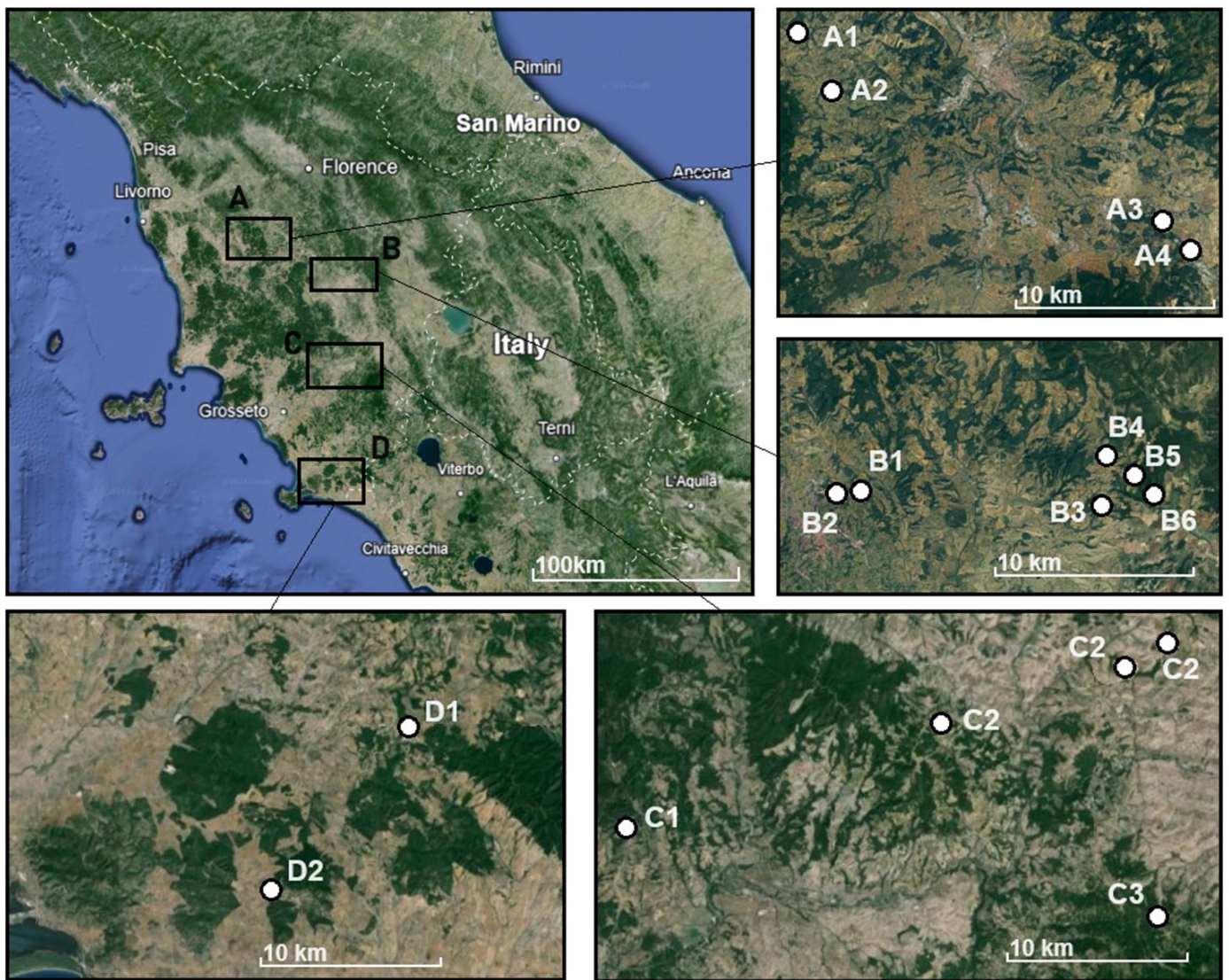


**Figure 1.** Position of the farms/orchards from where samples were collected. Zone A roughly corresponds to the Colli Senesi Region, Zone B Val d'Arbia, Zone C Val D'Orcia and Zone D Grosseto.

Soil samples (three replicates per orchard and per variety) were collected using a stainless-steel corer: the uppermost layer of dirt (approx. 10 cm) was discarded and then a 20 cm core was retrieved to collect a portion of soil where the roots are at the densest.<sup>41-42</sup>

Of this, the top and bottom 5 cm were also discarded to remove possible contaminants from the handling of the sample and coring. Samples were sealed in pre-cleaned PE plastic bags to avoid dust contamination.

Leaves and fruits (drupes) samples (three replicates per orchard and per variety) were collected by hand from different plants (at least three different trees to ensure a good representation of the internal variability of the orchards) and from branches that were not displaying any signs of disease or

damage. At least 250 g of olives and 100 g of leaves per tree were collected. Samples were sealed in pre-cleaned PE plastic bags and then treated within the following 24 h to avoid damages.

Leaves and drupes samples were therefore washed with UP water to remove possible traces of pesticides and or dust layers, then freeze dried ( $-45\text{ }^{\circ}\text{C}$ ,  $360\text{ }\mu\text{bar}$ ) and pulverized in a blade mill (Pulverisette 11, Fritsch, Idar-Oberstein, Germany) in a liquid nitrogen ( $-196\text{ }^{\circ}\text{C}$ ) bath to avoid degradation of the samples due to the heat of the blades and motor. The pulverization occurred in 4 cycles of 5 s each at a speed of 10,000 rpm (3 s rest in between each cycle). Leaf samples were then sieved ( $500\text{ }\mu\text{m}$ ) to remove debris and unprocessed leaf stems. Powdered samples were stored at  $-20\text{ }^{\circ}\text{C}$  in the dark in pre-cleaned PE containers until analysis.

Soil samples were left air-drying under a flow hood in the same bag used for the collection (up to two weeks) and then grounded using an agate mortar. The resulting powder was sieved ( $125\text{ }\mu\text{m}$ ) and stored in pre-cleaned PE containers until further processes.

### *2.2.3 Sample Treatment—Metabolites Extraction*

Samples were analytically weighted (approx. 500 mg), and the hydrophilic components were extracted using a mixture of MeOH and UP water (80:20% v/v). Each sample was extracted with three portions of solvent (10 mL each) using an ultrasound bath (Bandelin Sonorex) followed by centrifuge to separate the samples from the solution (3 min, 4000 rpm). Some of the lipophilic compounds were also extracted during this process when treating olive samples (most likely short chain fatty acids) and they were removed with a quick clean up with 5 mL of n-hexane that was separated by centrifugation (3 min, 4000 rpm).

### *2.2.4 Sample Treatment—Acid Digestion*

Samples were digested using an Ethos Easy microwave assisted digester equipped with Teflon tubes. Multiple acids combinations were considered for the digestion of soil samples. Indeed, some of the elements considered such as Si and Ti, are poorly soluble in  $\text{HNO}_3$ , with HF the most effective mineral acid for breaking the Si-O bonds in the bulk of the soil and Ti oxides needing a strong oxidant acid such as perchloric acid to fully solubilize the material. A quick experimental design (two level, full factorial) was therefore set in place before the analysis of the soil samples using CRM NIST 2710a Montana Soil, using  $\text{HNO}_3$  as the main acid used for the digestion and a combination of  $\text{H}_2\text{O}_2$ , HCl and  $\text{HClO}_4$  added to the digestion tube (1 mL each). The quantity of sample to be digested was also

varied to gauge whether solubility was a limiting factor and a contribution to the poor recovery of some of the metals. The list of levels used in the experimental design is reported in **Table 1**. Each experiment was replicated three times. Due to the nature of the digestion, no true randomization of the experiment run was needed as each sample was prepared into the same digestion run. Still, each experiment run was randomly assigned to a Teflon tube to avoid any possible bias. Experimental Design (ED) analysis was performed using Design Expert Software (ver. 13.0.5.0, StatEase®)

**Table 1.** Levels used in the ED to maximize recovery of the mineralization of soils.

	Level -1	Level +1
HNO <sub>3</sub>	5 mL	5 mL
H <sub>2</sub> O <sub>2</sub>	0 mL	1 mL
HCl	0 mL	1 mL
HClO <sub>4</sub>	0 mL	1 mL
Smpl. mass	50 mg	100 mg

For all runs, the same temperature run was used and is reported in **Table 2**. After each cycle of microwave assisted digestion, samples were diluted with HNO<sub>3</sub> 1%, and the tubes cleaned using HNO<sub>3</sub> 1% and the temperature run reported in **Table 2**.

**Table 2.** Temperature ramp used for the microwave-assisted digestion of soils and leaves samples. The asterisk (\*) indicates a cooling step; samples were removed from the digester once reached a temperature of 50 °C or below. The temperature ramp used for the clean-up process of the Teflon tubes is also reported.

Step	Time(min)	Power(W)	Temperature (°C)
Soil samples			
1	10	1800	160
2	15	1800	210
3	10	1800	210
4	20	0—VENT *	50 *
Leaf samples			
1	10	1800	150
2	10	1800	180
3	10	1800	180
4	20	0—VENT *	50 *
Teflon tube clean-up process			
1	10	1800	150
2	10	1800	180
3	10	1800	180
4	20	0—VENT *	50 *

Recovery results are reported in **Table 3**; the analytical merits of the methods are reported in **Table 4**. Despite the optimization of the digestion process, some elements were found to display a rather low recovery (in some cases below 50%). This is most likely due to the exclusion of HF from the digestion process, which was performed in an effort to reduce the toxicity of the process. Indeed, every sample's insoluble matter was left on the bottom of the digestion vessels, contributing to the overall poor recovery of some elements in the Si-rich powder.

**Table 3.** Elemental mass fraction, uncertainty (95% confidence interval) and recovery percentage as found from the ICP-MS analysis of the SRM 2710a (Apple Leaves). Elements are classified according to NIST certification level: elements without asterisks have certified values with the highest metrological traceability. Reference Values are indicated with an asterisk (\*). Non-certified elements and their respective recovery are marked with two asterisks (\*\*). No uncertainty is provided by NIST

for the non-certified mass fraction, but it's reported for completeness for the one calculated in this work.

<b>Element</b>	<b>Mass</b>	<b>m fraction NIST (%)</b>	<b>m fraction (%)</b>	<b>Recovery (%)</b>
<b>Magnesium (Mg)</b>	24	0.734 ± 0.038	0.354 ± 0.010	48.30
<b>Aluminum (Al)</b>	27	5.95 ± 0.05	1.88 ± 0.08	31.60
<b>Phosphorus (P)</b>	31	0.105 ± 0.004	0.0824 ± 0.0034	75.42
<b>Potassium (K)</b>	39	2.17 ± 0.13	0.745 ± 0.035	34.32
<b>Titanium (Ti)</b>	47	0.311 ± 0.007	0.108 ± 0.002	33.41
<b>Manganese (Mn)</b>	55	0.214 ± 0.006	0.153 ± 0.0019	68.68
<b>Iron (Fe)</b>	56	4.32 ± 0.08	3.52 ± 0.8	81.62
<b>Copper (Cu)</b>	63	0.342 ± 0.005	0.298 ± 0.0048	83.50
<b>Zinc (Zn)</b>	66	0.418 ± 0.015	0.354 ± 0.0039	81.26
<b>Arsenic (As)</b>	75	0.154 ± 0.010	0.143 ± 0.0019	89.15
<b>Lead (Pb)</b>	208	0.552 ± 0.003	0.479 ± 0.0084	86.73
<b>Element</b>	<b>Mass</b>	<b>m fraction NIST (mg/kg)</b>	<b>m fraction (mg/kg)</b>	<b>Recovery (%)</b>
<b>Boron (B)**</b>	11	20	8	40.00
<b>Scandium (Sc)*</b>	45	9.9 ± 0.1	4.1 ± 0.1	41.41
<b>Vanadium (V)*</b>	51	82 ± 9	57 ± 2	66.74
<b>Chromium (Cr)*</b>	52	23 ± 6	15.4 ± 0.4	67.16
<b>Cobalt (Co)</b>	59	5.99 ± 0.14	4.10 ± 0.06	68.47
<b>Nickel (Ni)*</b>	60	8 ± 1	6.8 ± 0.3	85.19
<b>Rubidium (Rb)*</b>	85	117 ± 3	52 ± 2	44.98

<b>Strontium (Sr)</b>	88	255 ± 7	61.4 ± 1.4	24.10
<b>Silver (Ag)**</b>	107	40	41	102.5
<b>Cadmium (Cd)</b>	111	12.3 ± 0.3	10.2 ± 0.1	79.83
<b>Antimony (Sb)</b>	121	52.5 ± 1.6	20.4 ± 4.8	38.88
<b>Cesium (Cs)*</b>	133	8.25 ± 0.11	6.08 ± 0.08	73.74
<b>Barium (Ba)</b>	137	792 ± 36	482 ± 6	58.34
<b>Lanthanum (La)</b>	139	30.6 ± 1.2	19.6 ± 0.7	61.64
<b>Cerium (Ce)**</b>	140	60	38	63.30
<b>Neodymium (Nd)*</b>	146	22 ± 2	14.5 ± 0.5	63.19
<b>Samarium (Sm)*</b>	147	4.0 ± 0.2	2.64 ± 0.1	63.37
<b>Europium (Eu)*</b>	153	0.82 ± 0.01	0.45 ± 0.01	55.73
<b>Gadolinium (Gd)*</b>	157	3.0 ± 0.1	2.20 ± 0.06	73.38
<b>Terbium (Tb)**</b>	159	0.5	0.3	75.00
<b>Dysprosium (Dy)**</b>	163	3	1.8	60.00
<b>Ytterbium (Yb)**</b>	172	2	1	50.00
<b>Lutetium (Lu)*</b>	175	0.31 ± 0.01	0.134 ± 0.006	41.31
<b>Thallium (Tl) *</b>	205	1.52 ± 0.02	0.99 ± 0.03	61.98

**Table 4.** Limit of Detection and Limit of Quantification for each Element measured in this work as calculated as reported in the main text. Element Mass number (A) is reported in parenthesis.

<b>Element (A)</b>	<b>LoD (ppb)</b>	<b>LoQ (ppb)</b>	<b>Element(A)</b>	<b>LoD(ppb)</b>	<b>LoQ(ppb)</b>
<b>Li (7)</b>	0.18	0.60	<b>Mo (95)</b>	2.53	8.45
<b>B (11)</b>	1.24	4.14	<b>Ag (107)</b>	0.026	0.086
<b>Na (23)</b>	2.54	8.47	<b>Cd (111)</b>	0.0022	0.0072
<b>Mg (24)</b>	1.03	3.09	<b>Sb (121)</b>	0.052	0.172
<b>Al (27)</b>	2.15	7.18	<b>Te (125)</b>	0.047	0.156
<b>Si (28)</b>	-	-	<b>Cs (133)</b>	0.061	0.203
<b>P (31)</b>	10.3	34.2	<b>Ba (137)</b>	0.055	0.183
<b>K (39)</b>	-	-	<b>La (139)</b>	0.013	0.040
<b>Ca (42)</b>	18.9	62.8	<b>Ce (140)</b>	0.042	0.12
<b>Sc (45)</b>	0.31	0.93	<b>Pr (141)</b>	0.0023	0.0078
<b>Ti (47)</b>	0.11	0.37	<b>Nd (146)</b>	0.024	0.072
<b>V (51)</b>	0.023	0.069	<b>Sm (147)</b>	0.0023	0.0078
<b>Cr (52)</b>	0.030	0.099	<b>Eu (153)</b>	0.0071	0.021
<b>Mn (55)</b>	0.13	0.39	<b>Gd (157)</b>	0.014	0.042
<b>Fe (56)</b>	0.42	1.39	<b>Tb (159)</b>	0.0023	0.0077
<b>Co (59)</b>	0.049	0.15	<b>Dy (163)</b>	0.0012	0.0036
<b>Ni (60)</b>	0.035	0.114	<b>Ho (165)</b>	0.0080	0.024
<b>Cu (63)</b>	0.11	0.33	<b>Er (166)</b>	0.00040	0.0012

<b>Zn (66)</b>	0.19	0.57	<b>Tm (169)</b>	0.0090	0.027
<b>As (75)</b>	0.24	0.79	<b>Yb (172)</b>	0.00040	0.0012
<b>Se (78)</b>	5.6	16.8	<b>Lu (175)</b>	0.0018	0.0054
<b>Rb (85)</b>	0.122	0.407	<b>Tl (205)</b>	0.045	0.151
<b>Sr (88)</b>	0.073	0.21	<b>Pb (208)</b>	0.084	0.281
<b>Y (89)</b>	0.081	0.24	<b>Bi (209)</b>	0.086	0.187

For leaves and fruit samples, a simple acidic digestion<sup>43-44</sup> using HNO<sub>3</sub> and H<sub>2</sub>O<sub>2</sub> (4:1 ratio) and the temperature run reported in **Table 2** have been proven to be an effective method to fully digest the majority of the elements of interest for zoning purposes with a recovery > 95% (97% on average). The efficacy of the digestion method was tested using CRM NIST 1515 (Apple Leaves) and recovery is reported in **Table 5**.

**Table 5.** Elemental mass fraction, uncertainty (95% confidence interval) and recovery percentage as found from the ICP-MS analysis of the SRM 1515 (Apple Leaves). Non-certified elements and their respective recovery are marked with an asterisk (\*). No uncertainty is provided by NIST for the non-certified mass fraction, but it's reported for completeness for the one calculated in this work.

<b>Element</b>	<b>Mass</b>	<b>m fraction NIST (mg/kg)</b>	<b>m fraction (mg/kg)</b>	<b>Recovery (%)</b>
<b>Boron (B)</b>	11	27.6 ± 2.8	29.7 ± 2.2	107.6
<b>Magnesium (Mg)</b>	24	2710 ± 120	2585 ± 75	95.4
<b>Aluminum (Al)</b>	27	284.5 ± 5.8	257 ± 13	90.3
<b>Phosphorous (P)</b>	31	1593 ± 68	1585 ± 50	99.5
<b>Potassium (K)</b>	39	16080 ± 210	15660 ± 590	97.4
<b>Calcium (Ca)</b>	42	15250 ± 100	13750 ± 450	90.1

<b>Vanadium (V)</b>	51	0.254 ± 0.027	0.261 ± 0.025	102.8
<b>Chromium (Cr)*</b>	52	0.3	0.34 ± 0.034	113*
<b>Manganese (Mn)</b>	55	54.1 ± 1.1	50.3 ± 3.7	93.0
<b>Iron (Fe)</b>	56	82.7 ± 2.6	82.4 ± 4.9	99.6
<b>Cobalt (Co)*</b>	59	0.09	0.081 ± 0.003	90*
<b>Nickel (Ni)</b>	60	0.936 ± 0.094	1.035 ± 0.09	110.6
<b>Copper (Cu)</b>	63	5.69 ± 0.13	5.52 ± 0.16	97.0
<b>Zinc (Zn)</b>	66	12.45 ± 0.43	15.36 ± 2.54	123.4
<b>Rubidium (Rb)</b>	85	10.2 ± 1.6	8.4 ± 0.2	82.4
<b>Strontium (Sr)</b>	88	25.1 ± 1.1	22.9 ± 0.3	91.2
<b>Molybdenum (Mo)</b>	95	0.095 ± 0.011	0.068 ± 0.02	71.6
<b>Cadmium (Cd)</b>	111	0.0132 ± 0.0015	0.0119 ± 0.0092	90.2
<b>Antimony (Sb)*</b>	121	0.013	0.010 ± 0.001	77*
<b>Barium (Ba)</b>	137	48.8 ± 2.3	46.26 ± 2.19	94.8
<b>Lanthanum (La)*</b>	139	20	20.8 ± 1.3	104*
<b>Cerium (Ce)*</b>	140	3	3.1 ± 0.1	103*
<b>Neodymium (Nd)*</b>	146	17	17.1 ± 0.8	101*
<b>Samarium (Sm)*</b>	147	3	2.95 ± 0.1	98*
<b>Europium (Eu)*</b>	153	0.2	0.25 ± 0.02	125*
<b>Gadolinium (Gd)*</b>	156	3	3.1 ± 0.2	103*
<b>Terbium (Tb)*</b>	159	0.4	0.38 ± 0.02	95*

<b>Ytterbium (Yb)*</b>	172	0.3	0.20 ± 0.05	66*
<b>Lead (Pb)</b>	208	0.470 ± 0.024	0.475 ± 0.045	101.1

### 2.2.5 Spectrophotometric Measurements

In-depth details of the method used to estimate the total content of polyphenolic compounds (TPC) and the total equivalent antioxidant capacity (TEAC) of the samples are reported in other works.<sup>45</sup> Briefly, for TPC, 100  $\mu$ L of sample were added to 1000  $\mu$ L of UP water and 100  $\mu$ L of Folin–Ciocalteu reactive. After 5 min, 300  $\mu$ L of Na<sub>2</sub>CO<sub>3</sub> 20% *m/v* were added and further diluted with 500  $\mu$ L of UP water. Measurements of absorbance were registered at 765 nm after 30 min incubation time. A 5-point external calibration curve using gallic acid was used to estimate TPC, expressed in mg of GA equivalent per g of dry sample. For TEAC, briefly, 30  $\mu$ L of samples were diluted in 70  $\mu$ L of EtOH and added to 1000  $\mu$ L of ABTS\*<sup>+</sup>. Radical removal percentage was evaluated by absorbance measurements at 734 nm after 30 min of incubation time of the samples. A 5-point calibration curve using Trolox<sup>®</sup> was built to extrapolate TEAC, expressed as  $\mu$ mol of Trolox<sup>®</sup> per g of dry samples.

### 2.2.6 HPLC-DAD Metabolites Analysis

Samples were analyzed using a Dionex UltiMate 3000 HPLC-DAD equipped with a Kinetex 5  $\mu$ m Biphenyl 100A Phenomenex (100  $\times$  2.1 mm). DAD operated in 3D field mode (min. wavelength: 190 nm, max. wavelength: 500 nm, bunch width: 1 nm) and quantification of the metabolites was done by integrating the peak at a wavelength of 220 nm.

MeOH/H<sub>2</sub>O acidified with formic acid (0.1% *v/v*) gradient run was used to separate the compounds of interest in the extracts as reported in **Table 6**.

**Table 6.** Gradient run used in the separation of metabolites via HPLC-DAD. The asterisk (\*) indicates a linear gradient

Time (min)	% MeOH
0.0	5.0
1.0	5.0
30.0	60.0 *
31.0	95.0 *
35.0	95.0
36.0	5.0 *
48.0	5.0

Eluent flow was set at 0.4 mL/min and kept constant for the separation. Examples of chromatographic separations of leaves and drupes phytochemicals are reported in **Figures 2** and **3**, respectively.

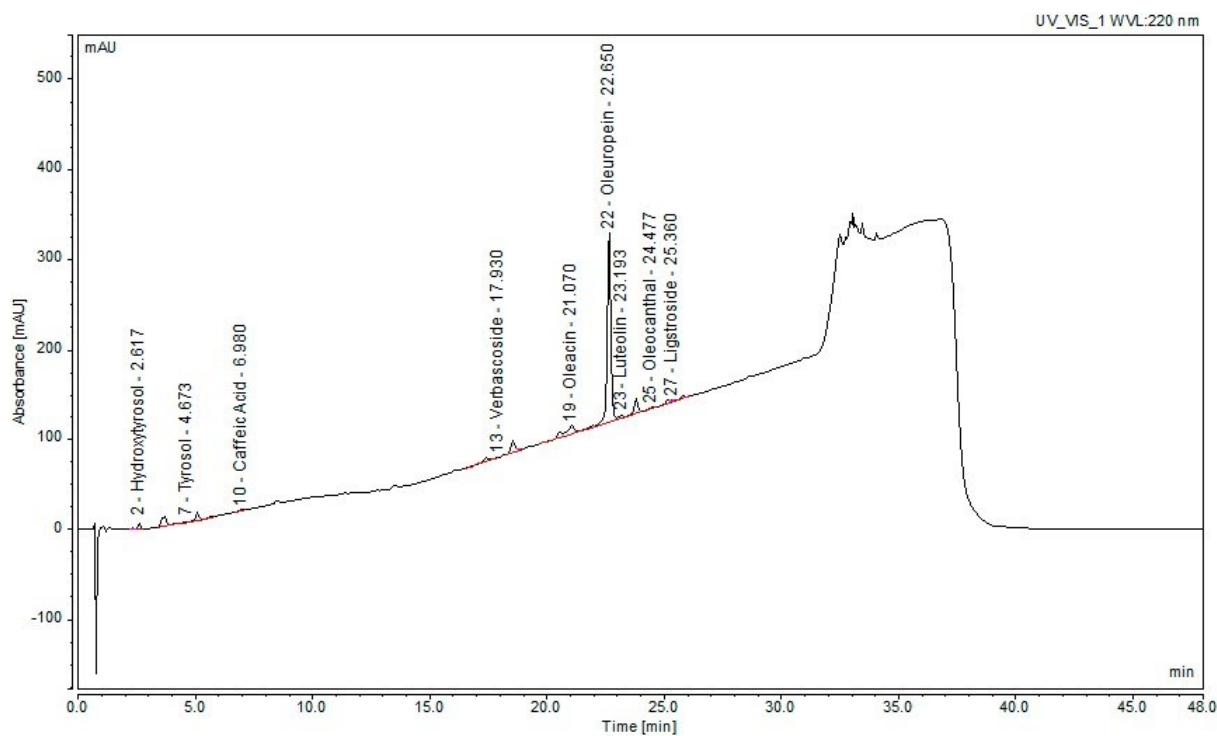


**Figure 2.** Example of chromatographic separation of phytochemicals found in leaves of *Olea europaea* L.

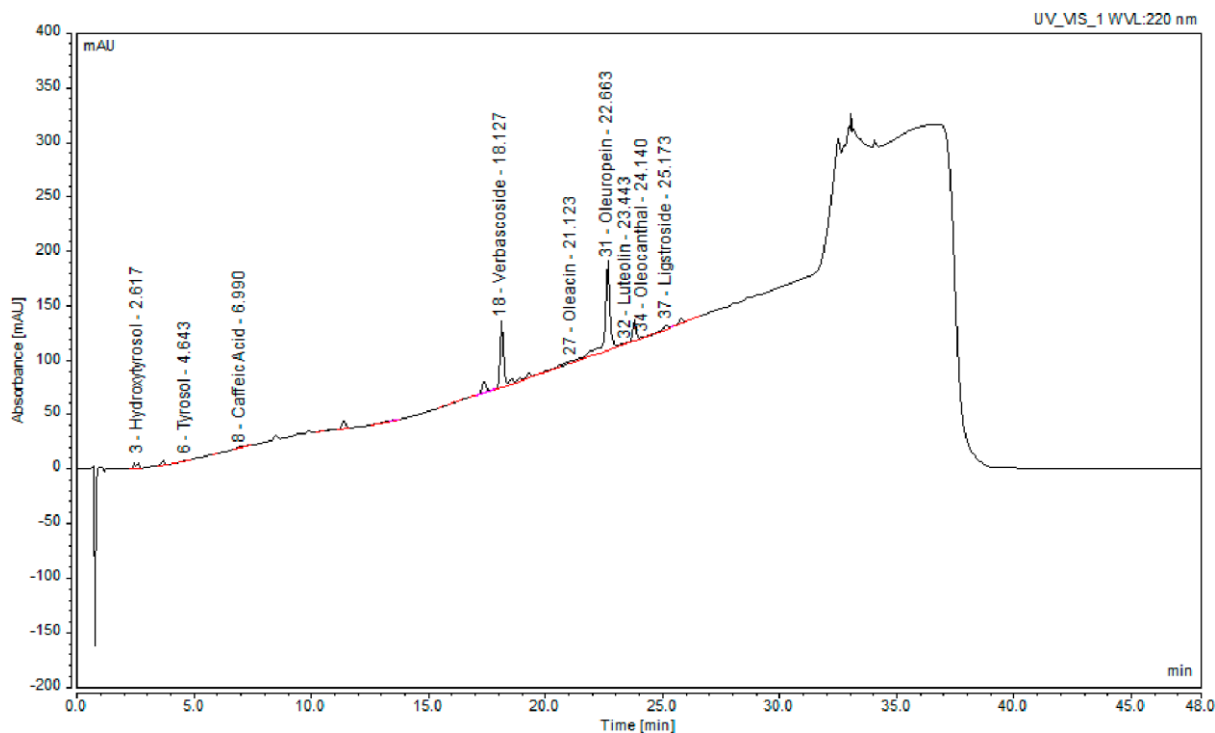


**Figure 3.** Example of chromatographic separation of phytochemicals found in drupes of *Olea europaea* L.

External 8-point external calibration curves were used for the quantitative determination of each metabolite; standard solutions were prepared by diluting concentrated (approx. 500–1000 mg/L) MeOH solutions of each compound in UP water.

### 2.2.7 ICP-MS Metal(loid)s Analysis

Samples were analyzed using an Agilent 8900 ICP-MS QQQ (Agilent Technologies, Santa Clara, CA, USA) equipped with Ni-Cu interfaces cones and a quartz shielded torch with a 2.5mm injector. Samples were introduced using an Agilent SPS 4 Autosampler connected to a MicroMist glass concentric nebulizer, a quartz Scott spray chamber cooled by a Peltier thermoelectric module (2 °C) to reduce water vapors in each sample. Twelve-point external calibration curves were used for the quantitative determination of each element; standard solutions were prepared by diluting concentrated (10 mg/L) standard just before analysis to avoid possible contamination. Internal standard (Ge) solution was added to both standards and samples to a concentration of approx. 20 µg/L. Most elements were analyzed in He mode, except for Li, B, Si, P and S which were also analyzed in No-Gas mode. Characteristics of plasma and sample uptake are reported in **Tables 7** and **8**, respectively.

**Table 7.** Plasma characteristics and argon flow used in the analysis.

<b>Plasma</b>	
Plasma Mode	HMI
RF Power	1600 W
RF Matching	1.80 V
Nebulizer Gas	0.68 L/min
Makeup/Dilution Gas	0.27 L/min
Plasma Gas	15.0 L/min
Auxiliary Gas	0.9 L/min

**Table 8.** Sample uptake speed and cleanup procedure. RPS (Round per seconds) refers to the speed of the peristaltic pump.

<b>Pre Run</b>	
Uptake speed (Nebulizer Pump)	0.3 RPS
Uptake time	30 s
Stabilize	40 s
<b>Post Run</b>	
Rinse speed (Nebulizer Pump)	0.3 RPS
Rinse time (2% HNO <sub>3</sub> , 0.5% HCl)	10 s
Rinse time (1% HNO <sub>3</sub> )	30 s
Uptake speed (Nebulizer Pump)	0.3 RPS
Uptake time	30 s
Stabilize	40 s

## 2.2.8 Multivariate Analysis

Multivariate analysis was performed through R Statistical Software ver. 4.3.1<sup>46</sup> using the FactoMineR package.<sup>47</sup> For PCA and caret package<sup>48</sup> for LDA. All figures were plotted using R's package ggplot2.<sup>49</sup> The tidyverse package<sup>50</sup> was used in data handling and statistical analysis.

## 2.3 Results

### 2.3.1 Soil Analysis

Chemical variability, here interpreted as different mineral composition of the soil, was investigated by means of PCA. Major elements such as boron<sup>51-52</sup>, nitrogen<sup>53-54</sup> and phosphorous<sup>53-55</sup> are known to affect plant growth but can also modulate secondary metabolite levels in plants. This is also true for non-essential metal(loid)s such as REEs<sup>56</sup> and heavy metals<sup>57-58</sup>, with effects on the production of antioxidants due to the metalinduced stress<sup>58-59</sup>. Here, metal(loid) variability throughout the sampling area was investigated. **Figure 4** reports the PCA data of all the sampling sites considered.

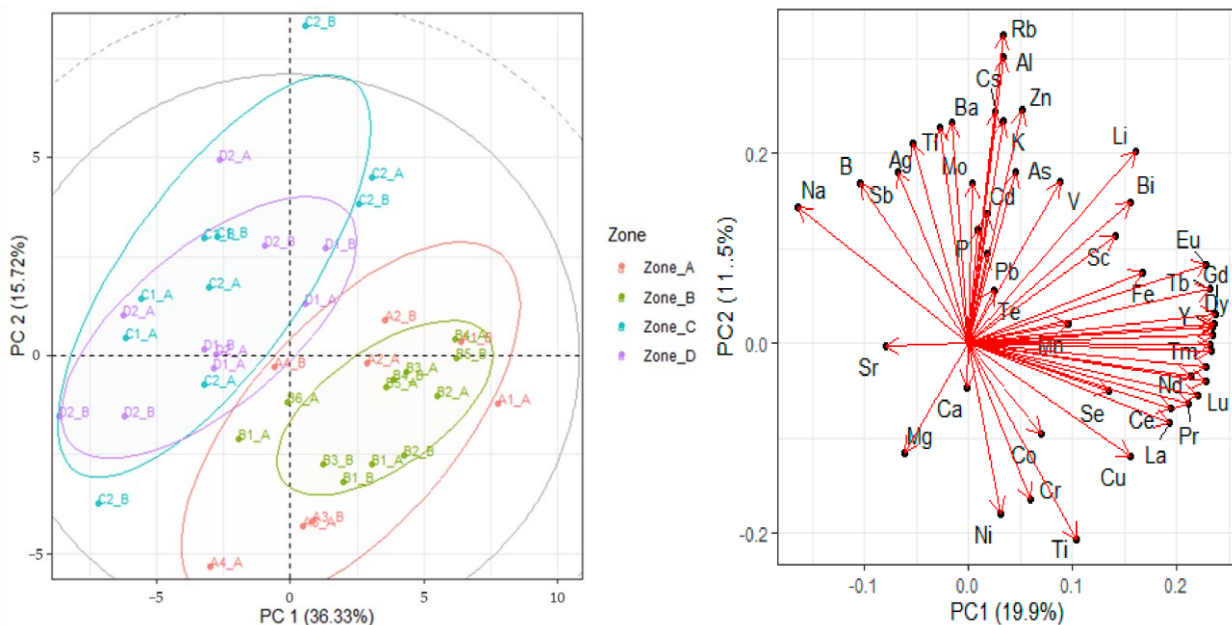


**Figure 4.** PC1 vs PC2 scores and loadings plot of the soil mineral composition in the four zones considered. Ellipses are built at a critical  $T^2$  value at  $p = 0.05, 0.01$  and  $0.001$ .

It is worth noting that whenever multiple varieties were grown in the same orchard, samples from nearby each tree were collected and analyzed separately. This is the case for samples from the C2

(where Frantoio, Moraiolo and Leccino olive trees are grown), D2 (Leccino and Moraiolo) and D1 (Leccino and Frantoio) farms. A clear pattern emerges when considering the PC1 vs PC2 plot, with samples coming from the southern region of Tuscany (Zone C and D) clearly separated from the ones in the nearby Siena (Zone A and B), a statistically significant difference (Wilks' =  $1.8 \times 10^{-7}$ ;  $F(105, 6.9) = 11.5$ ;  $p = 0.0012$ ) that could be kept in the plant mineral content and therefore exploited in the zoning efforts. This finding seems to be in agreement with the geological composition of Tuscan soil,<sup>40</sup> even if its complex variability sometimes makes the assignment of a single geological profile to a given sampling area quite tricky.

### 2.3.2 Secondary Metabolites in Drupes and Leaves

Metabolite levels found in both the pulp of the drupes and the leaves of olive trees considered in this work are reported in **Figures 5** and **6**, respectively. The analytical merits of the method are reported elsewhere<sup>45</sup> but it is worth noting that below-LoD metabolites (apigenin, 0.19 mg/L; ferrulic acid, 0.13 mg/L; acid p-coumaric, 0.75 mg/L and nuzhenide 0.21 mg/L, each estimated as  $3.3 \sigma/S$  where  $\sigma$  is the standard deviation of the response and S the slope of the calibration curve) were not reported and were not considered in the following analysis. Statistically significant differences (see **Table 9**) were found when considering most of the secondary metabolites analyzed, with only oleacin, oleocanthal and tyrosol levels not being tied to the cultivar of *Olea europaea* L. (ANOVA,  $\alpha = 0.05$ ) despite the fact that these compounds share metabolic pathways.<sup>53</sup>

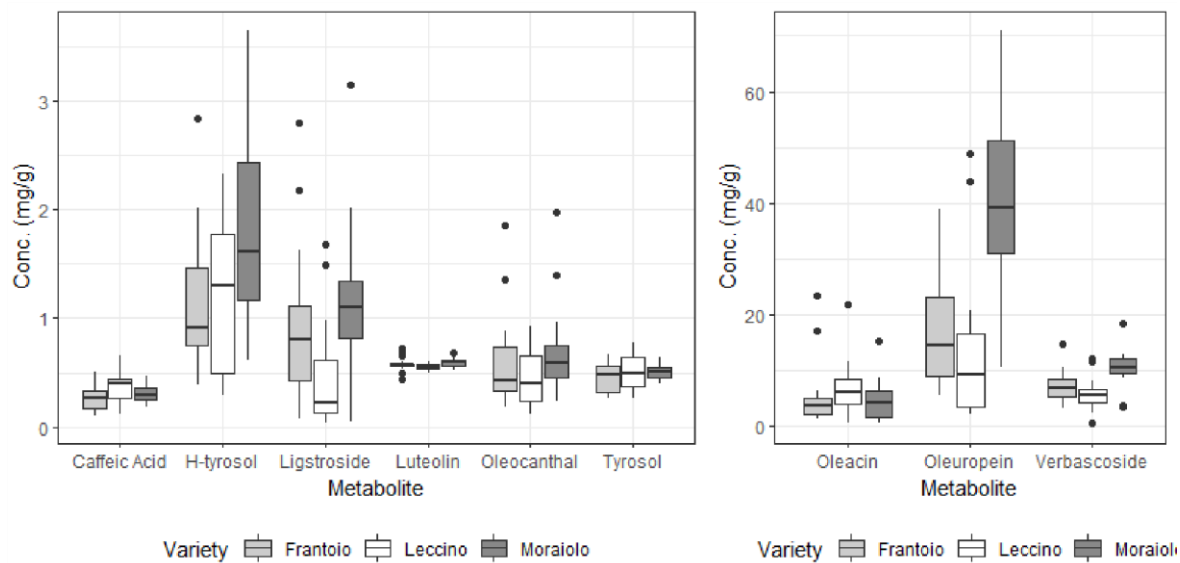


**Figure 5.** Metabolite levels (in mg/g of dried sample) found in the drupe pulps of each cultivar of *Olea europaea* L. considered.

**Table 9.** ANOVA results highlighting the differences in secondary metabolite levels between drupe samples coming from different cultivar of *Olea europaea* L. and different geographical zones.

	Variety			Zone		
	F	F Crit	p-Value	F	F Crit	p-Value
Hydroxytyrosol	4.88	3.18	0.0114	2.10	2.78	0.112
Tyrosol	0.67	3.18	0.512	1.27	2.78	0.331
Caffeic Acid	5.51	3.18	0.0067	4.18	2.78	0.0101
Verbascoside	10.08	3.18	0.0002	1.78	2.78	0.161
Oleacin	0.92	3.18	0.404	2.81	2.78	0.0485
Oleuropein	20.68	3.18	$2.46 \times 10^{-7}$	1.04	2.78	0.350
Luteolin	3.66	3.18	0.0325	1.99	2.78	0.125
Oleocanthal	2.02	3.18	0.142	2.52	2.78	0.0682
Ligstroside	5.35	3.18	0.00767	4.04	2.78	0.0118
TPC	10.22	3.18	0.00018	1.70	2.78	0.178
TEAC	17.72	3.18	$1.35 \times 10^{-6}$	0.187	2.78	0.905

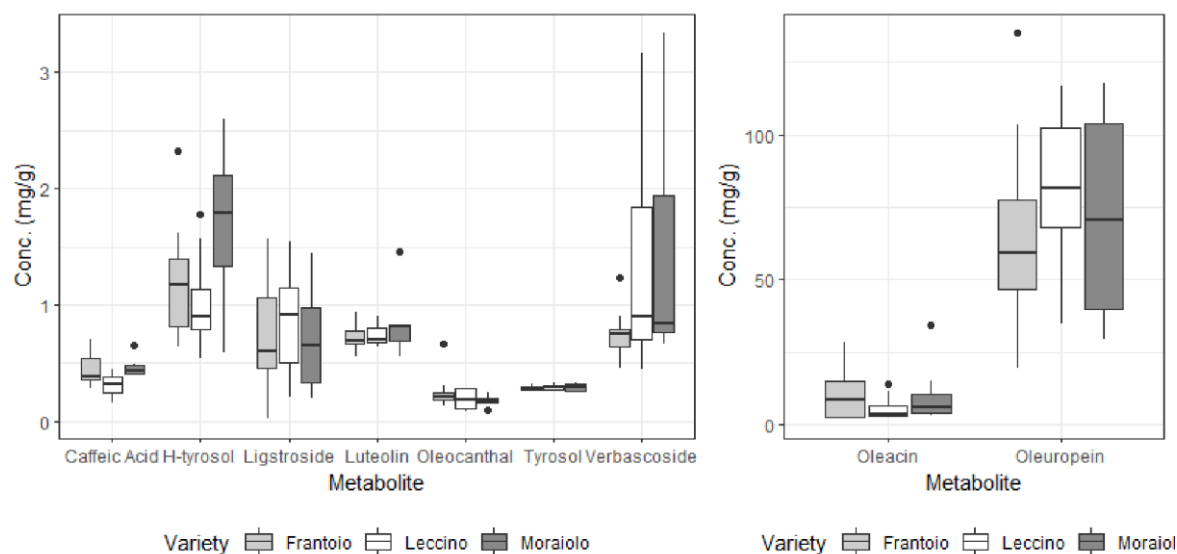


**Figure 6.** Metabolite levels (in mg/g of dried sample) found in the leaves of *Olea europaea* L. for each cultivar considered.

On the other hand, when considering the different sampling areas (see **Table 9**), only ligstroside, caffeic acid and oleacin (even though with a borderline statistical significance) levels show a correlation with the location of the orchards. Samples were collected in a relatively short period (less than two weeks), which leads to excluding possible variation in the ripening of the drupes influencing the results. Furthermore, despite differences in polyphenols being tied to abiotic factors and therefore geographical location<sup>60</sup> it must be stressed that all sites are extremely close together (approx. 30 km from one another), making zonation efforts particularly complex.

Similar considerations can be made for TPC and TEAC, whose levels are reported in **Figure 7**. Due to oleuropein and hydroxytyrosol being two of the strongest antioxidant compounds found in EVOOs and therefore in the drupes<sup>61-63</sup>, and their concentrations being amongst the highest between the compounds considered, a trend emerges, similar to what was observed for single metabolites. Indeed, both TPC and TEAC are strongly related to the cultivar, but differences in climate and abiotic factors between the four considered regions are most likely not stark enough to force a different response in plants, so that no statistically significant differences are observed when looking at the four selected zones.

The same analysis was performed on the data collected for olive leaves (see **Table 10**), and contrarily to what was observed for the drupe samples of all the investigated metabolites, only hydroxytyrosol and caffeic acid seem to be relevant distinguishing between the three varieties, and, when considering

the geographical origin of samples, only olacein is close to the significance value (even if slightly higher, with  $p = 0.051$ ).

Multivariate analysis confirms the ANOVA results. The first two components of PCA, reported in **Figure 8**, explaining more than 50% of the total variance of the dataset, highlighting the similitudes between samples of the Leccino and Frantoio varieties and the differences between these two and the Moraiolo ones, most likely due to the similitudes in the two cultivars when compared to the latter.<sup>64-65</sup> These findings were in perfect agreement with previous results obtained through a discriminant analysis of HPLC-HRMS data on the polyphenolic profile of olive leaves of the same three varieties considered in the present work.<sup>66</sup> In the case of drupe samples, this difference is significant when considering the different varieties of olive tree (Wilk's = 0.201;  $F(22, 84) = 4.71$ ;  $p < 0.01$ ) but the significance drops when investigating the differences between zones ( $p = 0.209$ ) and MANOVA tests confirmed that for leaves, the apparent differences found are not significant when considering both geographical origin and variety ( $p = 0.248$  and  $p = 0.374$ , respectively).

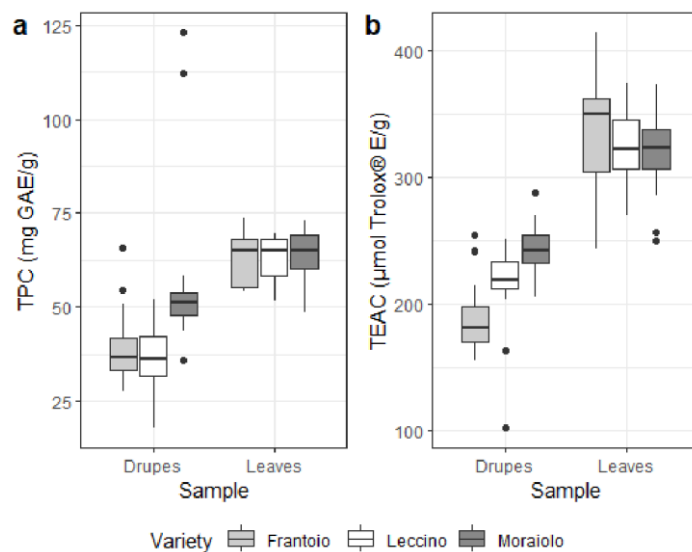


**Figure 7.** Spectrophotometric assays evaluating the TPC (a) and TEAC (b) results in samples of leaves and drupes of *Olea europaea* L. for each cultivar considered.

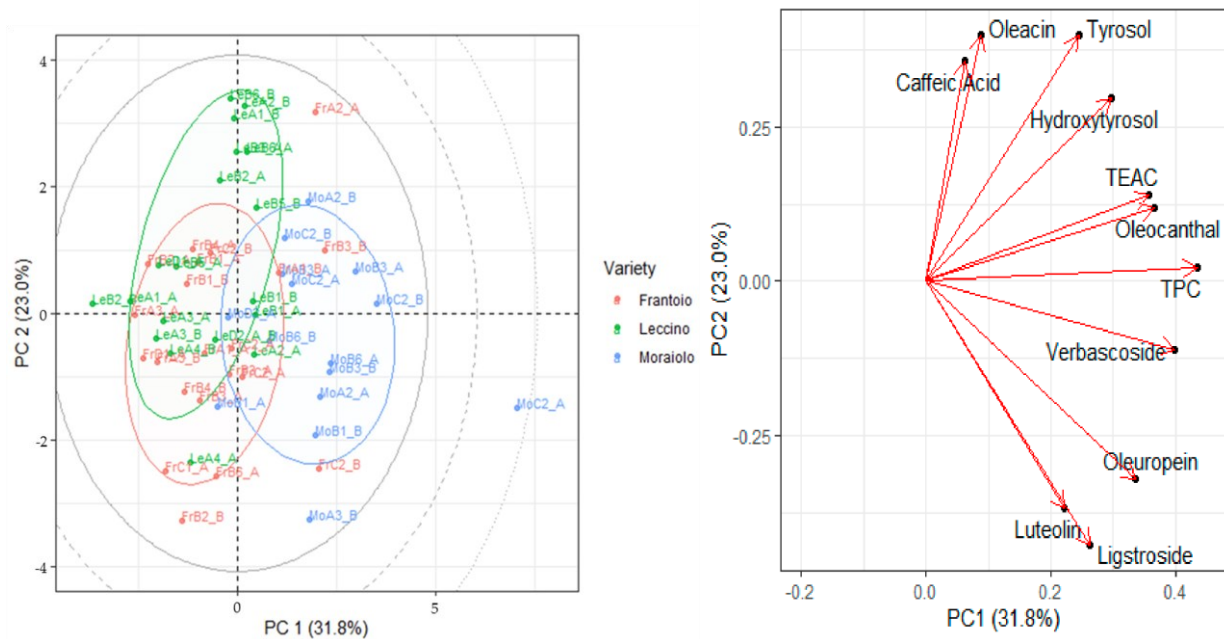


**Figure 8.** PC1 vs PC2 scores and loadings plot of the secondary metabolite levels in the drupes of the three cultivars considered. Grey ellipses: critical T<sup>2</sup> value at  $p = 0.05, 0.01$  and  $0.001$ .

**Table 10.** ANOVA results highlighting the differences in secondary metabolite levels between leaves samples coming from different cultivars of *Olea europaea* L. and different geographical zones.

	Variety			Zone		
	F	F Crit	p-Value	F	F Crit	p-Value
H-Tyr	3.68	3.42	0.041	2.47	3.05	0.0897
Tyrosol	0.355	3.42	0.704	2.21	3.05	0.116
Caffeic acid	5.10	3.42	0.015	0.344	3.05	0.793
Verbascoside	1.72	3.42	0.200	2.04	3.05	0.137
Oleacin	1.03	3.42	0.372	3.02	3.05	0.051
Oleuropein	0.394	3.42	0.679	2.19	3.05	0.118
Luteolin	0.973	3.42	0.393	1.58	3.05	0.223
Oleocanthal	1.28	3.42	0.297	0.898	3.05	0.458
Ligstroside	0.278	3.42	0.760	1.51	3.05	0.239
TPC	0.182	3.42	0.835	2.89	3.05	0.058
TEAC	0.451	3.42	0.643	0.473	3.05	0.704

### 2.3.3 Mineral Content in Drupes and Leaves

**Figure 9** reports the PC1 vs PC2 scores plot for the mineral levels inside the samples of drupes analyzed. Indeed, the clear cut difference between samples coming from southern regions of Tuscany and the one from the Siena region displayed in the soils samples is here absent, despite the MANOVA test seeming to indicate statistical differences between samples coming from different regions (Wilks = 0.0022;  $F(108, 54.8) = 3.35$ ;  $p < 0.01$ ) and trees of different variety (Wilks = 0.016;  $F(27, 38) = 3.67$ ;  $p < 0.01$ ) when considering the 36 elements selected for the analysis (elements whose concentration was below LoD in more than half of the samples were discarded). When considering the leaves samples, the number of these coming from Zone D makes it difficult to investigate the variability throughout all Tuscany, but unlike with drupes, a clearer path seems to emerge from PCA as reported in **Figure 10**, with PC1 separating the samples based on sea-distance. Also, this finding is in agreement with what was observed for olive leaves' geographical origin assessed by the quantification of the polyphenolic profiles through HPLC-HRMS analyses, where the distance from the sea was identified as a key parameter influencing plants' secondary metabolites amounts.<sup>66</sup> Removing samples from Zone D in the drupe's dataset did not improve separation.

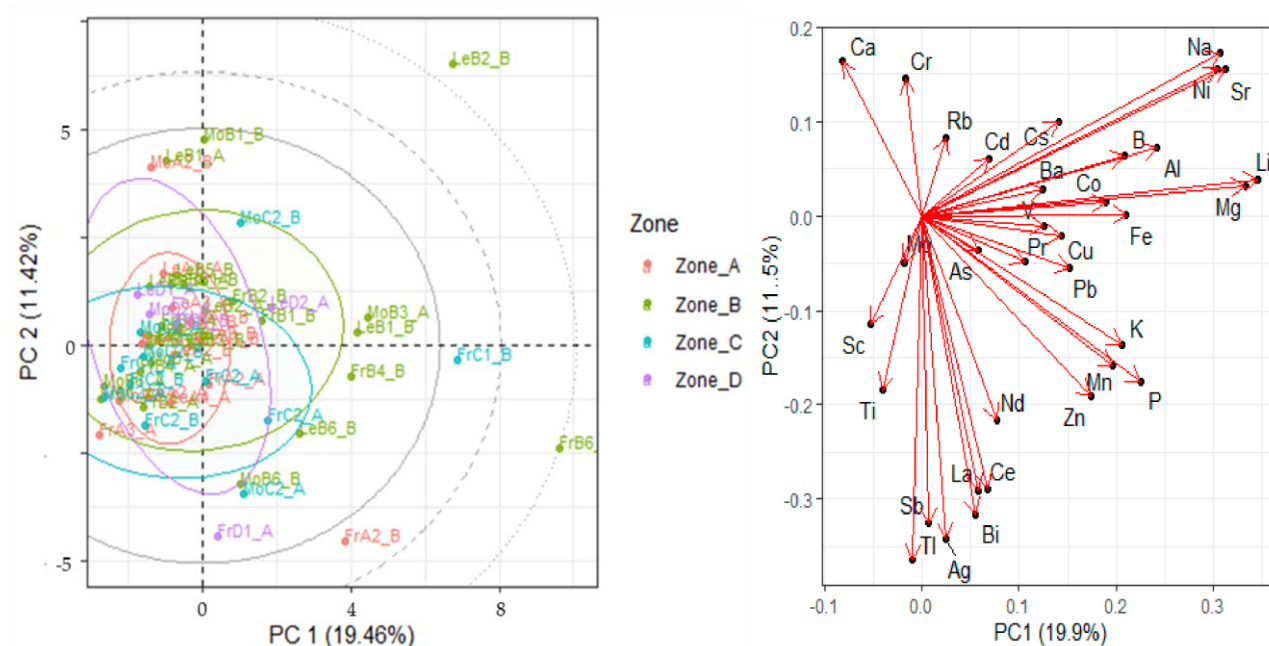


**Figure 9.** PC1 vs PC2 scores and loadings plot of mineral levels in the drupe samples in the four areas. Ellipses: critical  $T^2$  value at  $p = 0.05, 0.01$  and  $0.001$ .

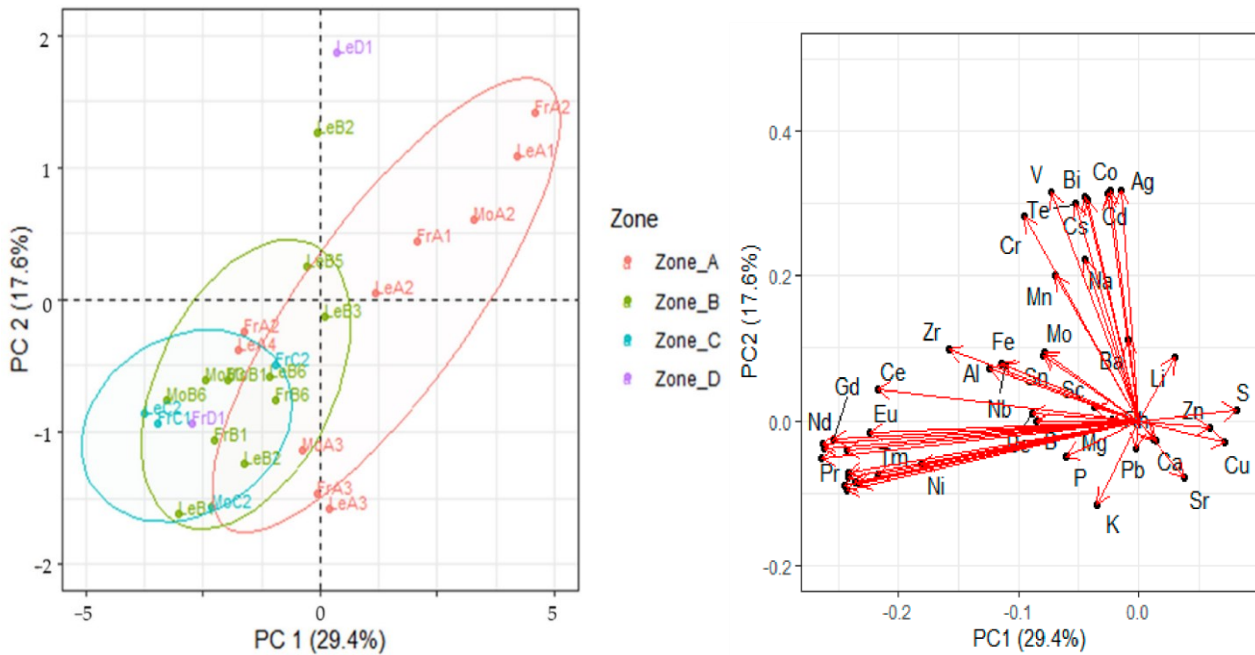


**Figure 10.** PC1 vs PC2 scores and loadings plot of the mineral levels in the leaf samples in the four areas. Ellipses: critical T<sup>2</sup> value at  $p = 0.05, 0.01$  and  $0.001$ .

Indeed, plants naturally adsorb metal(loid)s from the soil, both essentials<sup>67-68</sup> and non-essentials<sup>68-69</sup>, but this process is dependent on the form in which these elements are in the soil and the substrate characteristic such as pH and humidity.<sup>70</sup> Furthermore, the distribution of the adsorbed metals in the plant is not uniform, with leaves usually collecting a higher concentration of metals.<sup>71-72</sup> This makes it so that a one-to-one correlation between minerals in the soil and plants is rarely present.

Indeed, when considering the metal(loid) levels in the orchards subject to study in this work, only Cs seems to display a somewhat linear correlation between the concentration in soil and the one found in the drupes, but despite this being statistically significant ( $p < 0.01$ ), correlation is negligible albeit positive ( $r^2 = 0.388$ ). Even when considering non-essentials minerals such as REEs, correlation is lacking with the highest degree of correlation being Pr ( $r^2 = 0.0225, p < 0.01$ ) and the lowest being Ce ( $r^2 = 0.000352, p < 0.01$ ).

### 2.3.4 LDA Models

Since leaves commonly only contribute to a small fraction of the material used in EVOO production (and usually they are introduced in the milling process by mistake rather than as a pondered addition) building a model able to discriminate their origin is less useful. Moreover, leaves' mineral levels alone already provide a quite clear separation, observed in the PCA score plot (**Figure 10**) computed

assessing their geographical origin, while in the case of drupes their metal(loid) levels were not enough to do so.

Hence, here a major interest was devoted to combining the information obtained from the two used techniques, i.e., exploiting both the metabolite and mineral content of drupes. Models were then created merging metabolite levels and mineral content as is and using the combined dataset to gauge the effectiveness of every option. The obtained models were tested both in test validation and cross validation using a randomized partition (20% of the dataset was used in validation, each class was split separately between train and test). TPC and TEAC were discarded from the LDA model due to the linearity with phenolic compound concentration<sup>73</sup>.

To gauge the effectiveness of the models, both the cross validation and test validation of the models were repeated in multiple cycles (1500).

Metabolite levels in drupes were used directly in the creation of the model due to their limited number, but when it came to using metals levels, the number of levels compared to the number of samples made it so that some level of data manipulation on the dataset was needed. Two possible options were considered: i) removing some of the metals from the dataset until the number of levels was acceptable or ii) performing PCA on the data first to reduce dimensionality and only use the loadings in the first  $n$  PC in the making on the model. The former was discarded, as the PCA loadings plot did not show any metal that contributed to the variance. Furthermore, by applying PCA first and then LDA, it should also reduce overfitting tendencies.<sup>74</sup> The appropriate number of PC to use in the models using the PCA-LDA approach was selected as a compromise between highest mean prediction of the model and tendencies of overfitting.

Cross validation does, of course, pose the risk of overfitting the data, although it must be noted that this does not seem to be the case in any of the instances here presented. It is worth noting that combining the two datasets proved to improve the mean prediction of the model used especially when considering variety as a discriminant factor. Focusing on these LDAs, it is clear from **Figure 11** how the model improves when considering the combined dataset of metal(loid)s and metabolites, both in cross- and test validation.

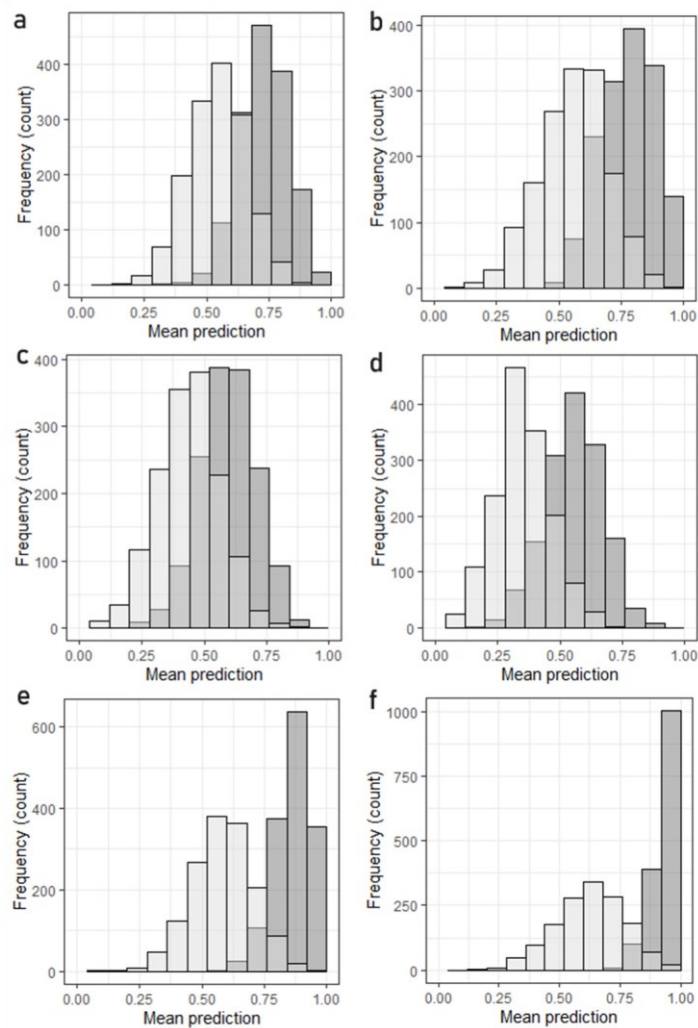


**Figure 11.** (a,c,e), LDA discriminating the variety of drupes; (b,d,f) the geographical zone. (a,b) PCA-LDA using mineral content, (c,d) HPLC metabolites, (e,f) PCA-LDA approach on both datasets. White histograms report the results of the repeated test validation, dark grey report cross validation.

In particular, considering the models distinguishing geographical areas, it is clear how the use of secondary metabolites alone poses a challenge when discriminating zones very close to one another, with the model displaying a low percentage of correct predictions both in test (min. 7%, avg. 34% max. 69%) and in cross validation (min. 16%, avg. 54%, max 84%). Due to the possible direct link between minerals in the soil and plant tissue, the mineral content in drupes can be used in creating a more effective model in the discrimination of geographical origin, but a modest increase in percentage of correct predictions was found when combining the two datasets both in test (from avg. 58% to avg. 62%) and cross validation (from avg. 81% to avg. 92%). **Table 11** summarizes the performances of the LDA tests.

**Table 11.** Correct predictions in test and cross-validation for the LDA models discriminating variety and geographical zone of origin of the drupes based on the metal(loid) content, secondary metabolites or a combined approach.

		Variety			Zone		
Test Validation	min	avg	max	min	Avg	max	
Metal(loid)s	0.16	0.56	0.91	0.08	0.58	1.00	
Metabolites	0.00	0.45	0.91	0.07	0.34	0.69	
Combined PCA	0.08	0.60	1.00	0.16	0.62	1.00	
		Variety			Zone		
Cross Validation	min	avg	max	min	Avg	max	
Metal(loid)s	0.33	0.76	1.00	0.50	0.81	1.00	
Metabolites	0.25	0.61	0.91	0.16	0.54	0.84	
Combined PCA	0.58	0.91	1.00	0.69	0.92	1.00	

More interesting are the results of the LDA model applied to the discrimination of the variety of the different samples. As it was already noted, genetic similarities between two of the species<sup>64-65</sup> make it difficult to use secondary metabolites in the creation of an effective model, and, indeed, the poor performances of the model both in test (min 0% avg. 45% max 91%) and cross validation (min 25% avg. 61% max 91%) are explained by the overlapping of Leccino and Frantioio samples in the LDA space. What is interesting to note is that the combined approach improves the effectiveness of the models. The tendency of mixing the two very similar varieties of olives is still somewhat present, but especially in cross validation (min 58% avg. 91% max 100%) it is clear how the combination of multiple techniques and data fusion can provide a more robust dataset and base for a discriminant model to use in the validation of origin and variety of agrifood products.

The limited dataset also provides limitations on the number of models that can be used in the discrimination of the different samples' class. LDA is a classification technique focusing on separating samples by identifying linear functions on the dimensionally reduced dataset. A consequence of this is that samples external to the initial dataset (e.g., different varieties of drupes)

will still be classified into the existing classes. Conversely, by expanding the dataset with future studies focusing not only on Tuscany orchards, but on samples coming from all throughout Italy, it may be possible to create a model capable of clustering and identifying outliers and/or samples associated with different classes.

## 2.4 Conclusions

Tuscany's diverse geological terrain leads to significant variability in soil element concentrations, which can affect the elemental composition of crops grown in the region. This variability is helpful in product traceability, enhancing marketability and protecting against fraud. Using ICP-MS, trace and ultra-trace metal(loid) levels in *Olea europaea* L. leaves and drupes were analyzed and compared with orchard soil levels. Furthermore, the specific geographical area in which trees are cultivated has been proven to affect the levels of certain secondary metabolites, further providing a tool to accurately discriminate the geographical origin of certain foods and derivatives. Secondary metabolites were quantified by means of HPLC-DAD and their levels used alongside the inorganic profile to identify the olive's cultivar, helpful due to the growing interest mono-varietal, luxury EVOOs.

It was found that soils from northern Tuscany significantly differ from those from southern Tuscany for what concerns their metal(loid) content, and this is in agreement with geological maps of this region. On the other hand, among investigated metabolites, oleacin was found as the most interesting marker to assess both for the varietal and geographical origin of drupes and leaves. This provides a new strategy to further protect consumer choice and producers of olive oil and especially EVOO which is characterized by a higher market price due to the restrictive quality parameters and the presence of specific PDOs. Rather than focusing on a single technique, multiple approaches to combine the two datasets were tested, with a combined PCA-LDA chemometric analysis on the data being the most reliable of the approaches both in the varietal and the geographical assessment, with an increase of the average correct prediction of the model of up to 30%. The use of multiple techniques not only has been proved to improve accuracy of the classification method used, but it must be noted that it also provides an additional benefit for the consumer as the product is tested on multiple levels. Indeed, not only can metabolomic profile provide important information to help discriminate adulteration in the EVOO production chain, as specific levels of polyphenols are associated with specific genus of *Olea europaea* L., but also monitoring metal(loid) levels is an integral part of one of the goals of the Agritech project, which strives for quality control. Indeed, several of the

metal(loid)s used in the multivariate approach here presented are known to be toxic and their levels must be closely monitored in the finished product to ensure consumers' safety.

Despite the limitation of the dataset, the results of this paper confirm that the study of raw matter along the whole agrifood chain can contribute greatly to traceability and quality assessment of the final product (i.e., EVOO in this case), besides deepening our knowledge on the correlation between plants' chemistry and their geographical location. Most importantly, then, this study shows the potential of multi-analytical approaches, still quite unexplored in this context, especially when combined with multivariate statistical models. Such an integrated and synergistic approach surely represents the future of traceability and quality assessment in the agrifood field.

## References

1. Liphshitz, N., Gophna, R., Hartman, M. & Biger, G. The Beginning of Olive (*Olea europaea*) Cultivation in the Old World: A Reassessment. *J. Archaeol. Sci.* **18**, 441–453 (1991).
2. Servili, M., Selvaggini, R., Esposito, S., Taticchi, A., Montedoro, G. & Morozzi, G. Health and Sensory Properties of Virgin Olive Oil Hydrophilic Phenols: Agronomic and Technological Aspects of Production that Affect Their Occurrence in the Oil. *J. Chromatogr. A* **1054**, 113–127 (2004).
3. Trichopoulou, A. Mediterranean Diet as Intangible Heritage of Humanity: 10 Years On. *Nutr. Metab. Cardiovasc. Dis.* **31**, 1943–1948 (2021).
4. Covas, M. I., Nyyssönen, K., Poulsen, H. E. *et al.* The Effect of Polyphenols in Olive Oil on Heart Disease Risk Factors: A Randomized Trial. *Ann. Intern. Med.* **145**, 333–341 (2006).
5. Angeloni, C., Malaguti, M., Barbalace, M. C. & Hrelia, S. Bioactivity of Olive Oil Phenols in Neuroprotection. *Int. J. Mol. Sci.* **18**, 2230 (2017).
6. Gorzynik-Debicka, M., Przychodzen, P., Cappello, F. *et al.* Potential Health Benefits of Olive Oil and Plant Polyphenols. *Int. J. Mol. Sci.* **19**, 686 (2018).
7. Bendini, A., Cerretani, L., Carrasco-Pancorbo, A. *et al.* Phenolic Molecules in Virgin Olive Oils: A Survey of Their Sensory Properties, Health Effects, Antioxidant Activity and Analytical Methods. *Molecules* **12**, 1679–1719 (2007).
8. Andrewes, P., Busch, J. L., de Joode, T., Groenewegen, A. & Alexandre, H. Sensory Properties of Virgin Olive Oil Polyphenols: Identification of Deacetoxy-ligstroside Aglycon as a Key Contributor to Pungency. *J. Agric. Food Chem.* **51**, 1415–1420 (2003).

9. Boskou, D., Blekas, G. & Tsimidou, M. Olive Oil Composition. In: Boskou, D., ed. *Olive Oil: Chemistry and Technology*. 2nd ed. AOCS Press; 2006:41–72.
10. European Commission. Commission Delegated Regulation (EU) 2022/2104. *Off. J. Eur. Union* **L284**, 1–22 (2022).
11. International Olive Council. Trade Standard Applying to Olive Oils and Olive Pomace Oils. COI/T.15/NC No 3/Rev. 19. Madrid: IOC; 2022.
12. Casadei, E., Valli, E., Panni, F. *et al.* Emerging Trends in Olive Oil Fraud and Possible Countermeasures. *Food Control* **124**, 107902 (2021).
13. Conte, L., Bendini, A., Valli, E. *et al.* Olive Oil Quality and Authenticity: A Review of Current EU Legislation, Standards, Relevant Methods of Analyses, Their Drawbacks and Recommendations for the Future. *Trends Food Sci. Technol.* **105**, 483–493 (2020).
14. Bajoub, A., Bendini, A., Fernández-Gutiérrez, A. & Carrasco-Pancorbo, A. Olive Oil Authentication: A Comparative Analysis of Regulatory Frameworks with Especial Emphasis on Quality and Authenticity Indices, and Recent Analytical Techniques Developed for Their Assessment. *Crit. Rev. Food Sci. Nutr.* **58**, 832–857 (2018).
15. European Commission. eAmbrosia – The EU Geographical Indications Register. Brussels: European Commission; 2023.
16. Mailer, R. J., Ayton, J. & Graham, K. The Influence of Growing Region, Cultivar and Harvest Timing on the Diversity of Australian Olive Oil. *J. Am. Oil Chem. Soc.* **87**, 877–884 (2010).
17. Longobardi, F., Ventrella, A., Napoli, C. *et al.* Classification of Olive Oils According to Geographical Origin by Using <sup>1</sup>H NMR Fingerprinting Combined with Multivariate Analysis. *Food Chem.* **130**, 177–183 (2012).
18. Italian Ministry of University and Research. National Recovery and Resilience Plan - National Research Centre for Agricultural Technologies. Rome: MUR; 2022.
19. Ghisoni, S., Lucini, L., Angilletta, F. *et al.* Discrimination of Extra-Virgin-Olive Oils from Different Cultivars and Geographical Origins by Untargeted Metabolomics. *Food Res. Int.* **121**, 746–753 (2019).
20. Tura, D., Gigliotti, C., Pedò, S., Failla, O., Bassi, D. & Serraiocco, A. Influence of Cultivar and Site of Cultivation on Levels of Lipophilic and Hydrophilic Antioxidants in Virgin Olive Oils (*Olea europaea* L.) and Correlations with Oxidative Stability. *Sci. Hort.* **112**, 108–119 (2007).
21. Medina, S., Perestrelo, R., Silva, P., Pereira, J. A. & Câmara, J. S. Current Trends and Recent Advances on Food Authenticity Technologies and Chemometric Approaches. *Trends Food Sci. Technol.* **85**, 163–176 (2019).

22. Gil-Solsona, R., Raro, M., Sales, C. *et al.* Metabolomic Approach for Extra Virgin Olive Oil Origin Discrimination Making Use of Ultra-High Performance Liquid Chromatography-Quadrupole Time-of-Flight Mass Spectrometry. *Food Control* **70**, 350–359 (2016).
23. Benincasa, C., Lewis, J., Perri, E., Sindona, G. & Tagarelli, A. Determination of Trace Element in Italian Virgin Olive Oils and Their Characterization According to Geographical Origin by Statistical Analysis. *Anal. Chim. Acta* **585**, 366–370 (2007).
24. Camin, F., Larcher, R., Perini, M. *et al.* Characterisation of Authentic Italian Extra-Virgin Olive Oils by Stable Isotope Ratios of C, O and H and Mineral Composition. *Food Chem.* **118**, 901–909 (2010).
25. Pasqualone, A., Montemurro, C., Summo, C., Sabetta, W., Caponio, F. & Blanco, A. Effectiveness of Microsatellite DNA Markers in Checking the Identity of Protected Designation of Origin Extra Virgin Olive Oil. *J. Agric. Food Chem.* **55**, 3857–3862 (2007).
26. Hannachi, H., Breton, C., Msallem, M., Ben El Hadj, S., El Gazzah, M. & Bervillé, A. Differences Between Native and Introduced Olive Cultivars as Revealed by Morphology of Drupes, Oil Composition and SSR Polymorphisms. *Sci. Hortic.* **116**, 280–290 (2008).
27. Talhaoui, N., Taamalli, A., Gómez-Caravaca, A. M., Fernández-Gutiérrez, A. & Segura-Carretero, A. Phenolic Compounds in Olive Leaves: Analytical Determination, Biotic and Abiotic Influence, and Health Benefits. *Food Res. Int.* **77**, 92–108 (2015).
28. Lattanzio, V. Phenolic Compounds: Introduction. In: Ramawat, K. & Mérillon, J. M., eds. *Natural Products*. Springer; 2013:1543–1580.
29. Obied, H. K., Prenzler, P. D., Omar, S. H. *et al.* Pharmacology of Olive Biophenols. *Adv. Mol. Toxicol.* **6**, 195–242 (2012).
30. Carrasco-Pancorbo, A., Cerretani, L., Bendini, A., Segura-Carretero, A., Gallina-Toschi, T. & Fernández-Gutiérrez, A. Analytical Determination of Polyphenols in Olive Oils. *J. Sep. Sci.* **28**, 837–858 (2005).
31. Angeloni, S., Navarini, L., Zagotto, G. *et al.* Development of an Untargeted Ultrahigh-Performance Liquid Chromatography-High-Resolution Mass Spectrometry Method for the Characterization of the Phenolic Composition of Virgin Olive Oils. *J. Agric. Food Chem.* **68**, 5881–5889 (2020).
32. Kelly, S., Heaton, K. & Hoogewerff, J. Tracing the Geographical Origin of Food: The Application of Multi-Element and Multi-Isotope Analysis. *Trends Food Sci. Technol.* **16**, 555–567 (2005).
33. Kabata-Pendias, A. *Trace Elements in Soils and Plants*. 4th ed. CRC Press; 2010.

34. Pereira, L., Gomes, S., Barrias, S., Fernandes, J. R. & Martins-Lopes, P. Applying High-Resolution Melting (HRM) Technology to Olive Oil and Wine Authenticity. *Food Res. Int.* **103**, 170–181 (2018).
35. Balcaen, L., Bolea-Fernandez, E., Resano, M. & Vanhaecke, F. Inductively Coupled Plasma-Tandem Mass Spectrometry (ICP-MS/MS): A Powerful and Universal Tool for the Interference-Free Determination of (Ultra)trace Elements. *Anal. Chim. Acta* **894**, 7–19 (2015).
36. Borràs, E., Ferré, J., Boqué, R., Mestres, M., Aceña, L. & Busto, O. Data Fusion Methodologies for Food and Beverage Authentication and Quality Assessment. *Anal. Chim. Acta* **891**, 1–14 (2015).
37. Callao, M. P. & Ruisánchez, I. An Overview of Multivariate Qualitative Methods for Food Fraud Detection. *Food Control* **86**, 283–293 (2018).
38. Aceto, M., Calà, E., Musso, D. *et al.* A Preliminary Study on the Authentication and Traceability of Extra Virgin Olive Oil Made from Taggiasca Olives by Means of Trace and Ultra-Trace Elements Distribution. *Food Chem.* **298**, 125047 (2019).
39. Mercurio, M., Grilli, E., Odierna, P. *et al.* A Geo-Pedological and Geochemical Study for Wine Characterization and Traceability. *Catena* **121**, 86–98 (2014).
40. Carmignani, L., Conti, P., Cornamusini, G. & Pirro, A. Geological Map of Tuscany (Italy). *J. Maps* **9**, 487–497 (2013).
41. Deng, Shixin, *et al.* "Drip irrigation affects the morphology and distribution of olive roots." *HortScience* **52.9** (2017): 1298-1306.
42. Masmoudi-Charfi, C., M. Masmoudi, and N. Ben Mechlia. "Root distribution in young Chétoui olive trees (*Olea europaea* L.) and agronomic applications." (2011): 112-122.
43. Nardin, Raffaello, *et al.* "Determination of Elemental Content in Vineyard Soil, Leaves, and Grapes of Sangiovese Grapes from the Chianti Region Using ICP-MS for Geographical Identification." *ACS Food Science & Technology* **4.11** (2024): 2585-2599.
44. Pequerul, A., *et al.* "A rapid wet digestion method for plant analysis." *Optimization of plant nutrition: refereed papers from the eighth international colloquium for the optimization of plant nutrition, 31 august–8 September 1992, Lisbon, Portugal*. Dordrecht: Springer Netherlands, 1993.
45. Tamasi, Gabriella, *et al.* "Chemical characterization and antioxidant properties of products and by-products from *Olea europaea* L." *Food Science & Nutrition* **7.9** (2019): 2907-2920.
46. R Core Team. "R: A language and environment for statistical computing." *R foundation for statistical computing, Vienna, Austria* (2021).
47. Le, S.; Josse, J.; Husson, F. FactoMineR: An R Package for Multivariate Analysis. *J. Stat. Softw.* **2008**, **25**, 1–18.

48. Kuhn, Max. "Building predictive models in R using the caret package." *Journal of statistical software* 28 (2008): 1-26.
49. Wickham, Hadley. "Data analysis." *ggplot2: elegant graphics for data analysis*. Cham: Springer international publishing, 2016. 189-201.
50. Wickham, Hadley, et al. "Welcome to the Tidyverse." *Journal of open source software* 4.43 (2019): 1686.
51. Liakopoulos, Georgios, and George Karabourniotis. "Boron deficiency and concentrations and composition of phenolic compounds in *Olea europaea* leaves: a combined growth chamber and field study." *Tree physiology* 25.3 (2005): 307-315.
52. Toker, Cem, and Namik Yavuz. "The effect of boron application on chemical characterization and volatile compounds of virgin olive oil of Ayvalik olive cultivar." *Journal of the American Oil Chemists' Society* 92.10 (2015): 1421-1428.
53. Arbonés Florensa, Amadeo, et al. "The influence of olive tree fertilization on the phenols in virgin olive oils. A review." *Grasas y aceites*.
54. Zayed, Omar, et al. "Nitrogen journey in plants: From uptake to metabolism, stress response, and microbe interaction." *Biomolecules* 13.10 (2023): 1443.
55. Poirier, Yves, Aime Jaskolowski, and Joaquín Clúa. "Phosphate acquisition and metabolism in plants." *Current Biology* 32.12 (2022): R623-R629.
56. Tyler, G. Rare Earth Elements in Soil and Plant Systems—A Review. *Plant Soil* **2004**, 267, 191–206.
57. Asare, Michael O., Jiřina Száková, and Pavel Tlustoš. "The fate of secondary metabolites in plants growing on Cd-, As-, and Pb-contaminated soils—a comprehensive review." *Environmental science and pollution research* 30.5 (2023): 11378-11398.
58. Asiminicesei, Dana-Mihaela, Daniela Ionela Fertu, and Maria Gavrilesu. "Impact of heavy metal pollution in the environment on the metabolic profile of medicinal plants and their therapeutic potential." *Plants* 13.6 (2024): 913.
59. Anjitha, K. S., P. P. Sameena, and Jos T. Puthur. "Functional aspects of plant secondary metabolites in metal stress tolerance and their importance in pharmacology." *Plant Stress* 2 (2021): 100038.
60. Cavaca, Lídia AS, et al. "The olive-tree leaves as a source of high-added value molecules: Oleuropein." *Studies in natural products chemistry* 64 (2020): 131-180.
61. Hassen, Imed, Hervé Casabianca, and Karim Hosni. "Biological activities of the natural antioxidant oleuropein: Exceeding the expectation—A mini-review." *Journal of Functional Foods* 18 (2015): 926-940.

62. Carrasco-Pancorbo, A., et al. "Evaluation of the antioxidant capacity of individual phenolic compounds in virgin olive oil." *Journal of agricultural and food chemistry* 53.23 (2005): 8918-8925.
63. Visioli, Francesco, Andrea Poli, and Claudio Gall. "Antioxidant and other biological activities of phenols from olives and olive oil." *Medicinal research reviews* 22.1 (2002): 65-75.
64. Moreno-Sanz, Paula, et al. "Genetic resources of *Olea europaea* L. in the Garda Trentino olive groves revealed by ancient trees genotyping and parentage analysis of drupe embryos." *Genes* 11.10 (2020): 1171.
65. Cantini, Claudio, et al. "Assessment of the Tuscan olive germplasm by microsatellite markers reveals genetic identities and different discrimination capacity among and within cultivars." *Journal of the American Society for Horticultural Science* 133.4 (2008): 598-604.
66. Borghini, Francesca, et al. "Phenolic profiles in olive leaves from different cultivars in Tuscany and their use as a marker of varietal and geographical origin on a small scale." *Molecules* 29.15 (2024): 3617.
67. Alloway, Brian J. "Heavy metals and metalloids as micronutrients for plants and animals." *Heavy metals in soils: trace metals and metalloids in soils and their bioavailability*. Dordrecht: Springer Netherlands, 2012. 195-209.
68. DalCorso, Giovanni, et al. "Nutrient metal elements in plants." *Metallomics* 6.10 (2014): 1770-1788.
69. Bradl, Heike B. "Adsorption of heavy metal ions on soils and soils constituents." *Journal of colloid and interface science* 277.1 (2004): 1-18.
70. Wiczorek, Jerzy, Agnieszka Baran, and Anicenta Bubak. "Mobility, bioaccumulation in plants, and risk assessment of metals in soils." *Science of The Total Environment* 882 (2023): 163574.
71. Batarseh, Mufeed I., et al. "Treated municipal wastewater irrigation impact on olive trees (*Olea Europaea* L.) at Al-Tafilah, Jordan." *Water, Air, & Soil Pollution* 217.1 (2011): 185-196.
72. Prabagar, Subramaniam, et al. "Accumulation of heavy metals in grape fruit, leaves, soil and water: A study of influential factors and evaluating ecological risks in Jaffna, Sri Lanka." *Environmental and Sustainability Indicators* 12 (2021): 100147.
73. Alessandri, Stefano, Francesca Ieri, and Annalisa Romani. "Minor polar compounds in extra virgin olive oil: Correlation between HPLC-DAD-MS and the Folin-Ciocalteu spectrophotometric method." *Journal of agricultural and food chemistry* 62.4 (2014): 826-835.
74. Tominaga, Yukio. "Comparative study of class data analysis with PCA-LDA, SIMCA, PLS, ANNs, and k-NN." *Chemometrics and Intelligent Laboratory Systems* 49.1 (1999): 105-115.

## CHAPTER 3: *Delivery systems for sustainable agriculture*

Biofumigation was originally proposed as an alternative to toxic fumigants for the treatment of agricultural soils, owing to the biocidal effect of isothiocyanates (ITCs) released by some plant species like Brassicaceae. However, biofumigation also presents limitations; thus, an advanced and viable alternative could be the use of controlled-release systems such as gelled polymer networks. In the present work, we explore the use of biocompatible hydrogels based on sodium carboxymethylcellulose (CMC), conveniently loaded with a Brassicaceae extract for this purpose. The extract was characterized by means of HPLC-MS, showing its high glucosinolate content, especially glucoraphanin, a secondary metabolite produced by several species of this family, alongside sinapine, which contributes additional antimicrobial properties. The physicochemical properties of the synthesized gels were investigated by means of differential scanning calorimetry (DSC), rheometry, and scanning electron microscopy (SEM), both in the presence and absence of the loaded extract. Loading and release kinetics (in water) were studied by means of HPLC-DAD, and the Weibull model was employed to interpret the results. It was found that the CMC hydrogels can effectively confine the Brassicaceae extract's active principles, slowly releasing them in an aqueous environment following Fickian diffusion mechanisms. The system possesses excellent properties for real applications due to its high encapsulation efficiency, superior mechanical properties, robust internal structure with thick gel walls, and favorable surface-to-volume ratio resulting from the high viscosity of CMC solutions. These features, combined with the likely formation of Fe<sup>3+</sup>/glucosinolate complexes, enable effective retention and controlled release of bioactive compounds. These systems are promising tools for combating harmful microorganisms due to the biocidal properties of glucosinolates, but their potential goes beyond their use in agriculture, as they could be applied as antifouling or antimicrobial agents in cultural heritage cleaning or other fields. This chapter is about a study that was realized within the framework of the project "PROFOOD-IV—Prodotti e processi innovativi della filiera di IV gamma" and partially funded by the Centre for Colloid and Surface Science (CSGI).

The results reported in this chapter are published in the following article:

Baglioni, M., Clemente, I., Nardin, R., Bisozzi, F., Costantini, S., Fattori, G., Tamasi, G., & Rossi, C. (2025). Hydrogel Beads Loaded with Glucosinolate-Rich Brassicaceae Extract as a Controlled-Release Alternative to Biofumigation. *Molecules*, 30(18), 3660.

### 3.1 Introduction

The increasing global demand for higher crop yields has led to the widespread use of chemical treatments in agriculture. In this context, synthetic pesticides represent a particular concern due to their adverse effects on human health and the environment.<sup>1-6</sup> Thus, the challenge of balancing the control of effective soilborne pathogens with sustainability and safety has become a major focus in modern agrifood. These chemicals were introduced as less harmful alternatives to metam sodium, a highly effective fumigant whose use was severely limited by the 1987 Montreal Protocol due to its toxicity and its role in ozone layer depletion.<sup>7-11</sup>

A well-known and viable alternative to chemical fumigants is biofumigation.<sup>12-17</sup> In this method, fresh plants (mostly *Brassicaceae*) are cultivated, mown, and mixed into agricultural soils due to their biocidal properties against soilborne pathogens. *Brassicaceae* are characterized by high glucosinolate content, secondary metabolites produced by plants for defensive purposes. Glucosinolates can be hydrolyzed to isothiocyanates (ITCs) by the enzyme myrosinase.

In plant cells, glucosinolates and myrosinase are located in different compartments, so enzymatic hydrolysis can only be induced by mechanical tissue damage (grinding, mowing, etc.).<sup>18</sup> Myrosinase-catalyzed hydrolysis of glucosinolates initially involves the cleavage of the thioglucoside bond, thus forming D-glucose and thiohydroximate-O-sulfonate. The latter is unstable and spontaneously forms a wide range of products, such as thiocyanates, nitriles, and, as mentioned, ITCs. These are responsible for the defensive mechanisms of plants against soilborne phytopathogens, fungi, and insects.

The same principle is, in fact, used in biofumigation for the treatment of agricultural soils, owing to the biocidal effect of ITCs and the other chemicals derived from glucosinolates. The effectiveness of ITCs in inhibiting the growth of several microorganisms, such as the fungi *Rhizoctonia solani*, *Sclerotinia minor*, *Sclerotinia sclerotiorum*, *Alternaria brassicicola*, and *Fusarium oxysporum*, as well as other plant pathogens, has been extensively reported in the literature.<sup>19-22</sup> ITCs owe their biocidal properties to the strong electrophilicity of the isothiocyanate group's carbon, which is highly reactive with thiols, amines, and alcohols,<sup>21</sup> thus readily interacting with SH groups in proteins, causing mutations *in vivo* that can interfere with the regular biochemical processes of cells.<sup>23</sup>

However, biofumigation also has some limitations: (i) it is a time-consuming practice; (ii) the amount of glucosinolate/myrosinase delivered to the soil is hardly controllable<sup>24</sup>; and (iii) it is a relatively ineffective agricultural practice.<sup>25</sup> Some improvements have been developed over time, such as the

introduction of powdered *Brassicaceae* “flours” or dry pellets<sup>24</sup>, but research into alternative approaches for soil treatment has progressed, finding more reliable, more effective, and safer solutions.

A notable contribution to the search for more effective and high-performing alternatives to biofumigation is controlled-release (CR) systems for the delivery of several chemicals to agricultural soil. Several different strategies have been proposed to develop CR systems for different classes of active chemicals<sup>26-33</sup>, but one of the main and most effective is hydrogels based on biodegradable polymers.<sup>34-37</sup>

Several polymers (e.g., chitosan, alginate, pectin, or modified celluloses) have been proposed to synthesize gelled networks that can be used as carriers for active chemicals, such as pesticides (e.g., diuron, carbofuran, atrazine, isoproturon, imidacloprid, cyromazine, chloridazon, and metribuzin<sup>38</sup>); fertilizers (e.g., nitrogen, phosphorus, and potassium NPK<sup>29</sup>); plant growth inhibitors or retardants (e.g., paclobutrazol, flurprimidol, and uniconazole<sup>26</sup>); and other active substances.<sup>30</sup> However, it is evident that the state of the art in the field is mainly limited to systems for the CR of synthetic pesticides. Even if this represents an improvement over the uncontrolled use of free pesticides, fertilizers, and other chemicals, a further step toward sustainability needs to be taken. Borrowing the basic ideas and concepts behind biofumigation and aiming at a zerowaste circular economy concept, byproducts from agrifood supply chains can represent a source of extremely interesting bioactive compounds. Several (nano)carrier systems have been proposed for CR, where either the vector matrix or the bioactive compounds (or both) were derived from byproducts of agrifood production.<sup>39-44</sup> Food waste from *Brassicaceae* crops is a rich source of glucosinolates, which can be exploited for eco-friendly antimicrobial soil treatment as a viable alternative to synthetic fumigants. By encapsulating bioactive plant-derived compounds into hydrogel matrices, it is possible to develop innovative soil treatment methods that combine the benefits of biofumigation with CR principles. Hydrogel beads loaded with ITC-based microemulsions have recently been proposed as an enhanced and innovative alternative to biofumigation.<sup>45</sup>

This study proposes an approach that represents a step forward from that idea. Hydrogels based on carboxymethylcellulose (CMC) were synthesized and loaded with a commercial *Brassica oleracea* var. *Italica* (broccoli) extract for the advanced biofumigation of agricultural soils. The extract is rich in glucoraphanin (GRF), as shown through the HPLC-MS analyses reported in the present work. Glucoraphanin is a glucosinolate precursor to sulforaphane, a well-known ITC with antimicrobial and pesticidal properties, making it an ideal candidate for soil treatment applications. The choice to load

CMC hydrogels with a *Brassicaceae* extract rich in glucosinolates, particularly glucoraphanin was based on the premise that myrosinase is produced by soil microbiota and is therefore naturally present in agricultural soils.<sup>16</sup> Therefore, for the purposes of this study, glucoraphanin (and other glucosinolates) can be effectively considered the precursors of the actual biofumigant agents. On the other hand, the choice of CMC was based on the vast literature on its use as cheap, easily synthesized, and reliable hydrogel carriers for drug delivery in several applicative contexts. Several other biocompatible and biodegradable polymers were initially considered, including chitosan and pectin, but we eventually focused on the most promising system. The synthesized hydrogels were characterized by means of attenuated total reflectance Fourier transform infrared spectroscopy (ATR-FTIR), differential scanning calorimetry (DSC, for the determination of the free water index), scanning electron microscopy (SEM), and rheological analysis to determine their structural and physicochemical properties in the presence or absence of the encapsulated extract. Furthermore, the loading and release kinetics of the active compound in aqueous media were studied to assess their potential as a sustainable alternative for soil treatment. By combining hydrogel technology with plant-derived biocidal compounds, this study aims to contribute to the development of effective and environmentally responsible strategies for agricultural soil management, reducing reliance on synthetic pesticides and advancing sustainable agricultural practices.

## 3.2 Experimental Section

### 3.2.1 Chemicals

$\text{FeCl}_3 \cdot 6\text{H}_2\text{O}$  (purity  $\geq 99\%$ ) were purchased from Sigma Aldrich/Merck (Darmstadt, Germany) and used without further purification. Sodium carboxymethylcellulose polymer was purchased from Reoper GmbH (Hamburg, Germany). The *Brassica oleracea* extract was purchased from Shanghai Qionghui Industrial Co. (Shanghai, China). Glucoraphanin potassium salt (purity  $\geq 98\%$ ; Extrasynthese, Lyon, France) and sinapine chloride (purity  $\geq 98\%$ ; Extrasynthese, Lyon, France) were used as analytical standards for the extract's characterization performed via HPLC-MS. MilliQ Ultrapure (Merck Millipore, Darmstadt, Germany) water was used.

### 3.2.2 Hydrogel Synthesis

Crosslinked hydrogel beads were prepared similarly to what was described elsewhere<sup>46</sup>, starting with 1% *m/v* aqueous CMC solutions. These polymer solutions were added dropwise into saline solutions

of 0.3 M FeCl<sub>3</sub> at room temperature. These concentrations were preliminarily optimized to obtain gel beads that were mechanically resistant to handling. The promptly formed hydrogel beads (5–8 mm diameter) were then magnetically stirred for 15 min, removed from the crosslinking solutions, washed with distilled water (to remove any unreacted metal ions from the gels' surface), and stored in polyethylene containers at their equilibrium swelling degree in a slight excess of water. The 15 min stirring time in the crosslinking solution was assessed using preliminary tests to find the optimal compromise between suitable encapsulation efficiency and the hydrogel beads' mechanical properties. The preparation of the hydrogel beads loaded with the *Brassica oleracea* extract was carried out similarly by alternatively mixing 1%, 2.5%, or 5% *m/m* of the extract powder with the polymer solution right before bead formation. Samples were named as CMC-0, CMC-1, CMC-2.5, and CMC-5, indicating the polymeric nature of the hydrogel network and the extract concentration.

### 3.2.3 *Brassica Oleracea* Extract Characterization

The commercial *Brassica oleracea* extract was first characterized using an HPLC instrument (Thermo Scientific UltiMate 3000, Waltham, MA, USA), operated using the Xcalibur software (Version 4.3, Thermo-Scientific, Waltham, MA, USA) and coupled to a mass spectrometer (Thermo-Scientific LTQ XL, Waltham, MA, USA) equipped with a linear ion trap analyzer, with ESI (electrospray ionization) as the ionization technique. For chromatographic separation, a C18 Polar Phenomenex Kinetex column (150 × 2.1 mm, 2.6 μm, 100 Å) was used in combination with a Phenomenex C18 Polar (2 × 2.1 mm) pre-column, thermostated at 35 ± 1 °C. The solvents used as the mobile phase were A (H<sub>2</sub>O/formic acid 0.1%, *v/v*) and B (acetonitrile/formic acid 0.1%, *v/v*), and the following gradient was set up: 0–3 min 0% B (isocratic), 3–20 min 25% B (linear), 20–25 min 50% B (linear), 25–30 min 50% B (isocratic), 30–31 min 0% B (linear), 31–40 min 0% B (isocratic).

Each sample was analyzed in triplicate by injecting 3 μL at a flow rate of 0.4 mL/min. In more detail, an aqueous solution (1% *m/v*) of the extract was filtered using a Whatman PTFE syringe filter with a pore size of 0.2 μm and then analyzed. The mass spectra obtained by injecting the eluted analytes into the mass spectrometer were used to identify the main compounds present in the extract. The parameters used for ESI were spray voltage, 3000 V; sheath gas pressure, 35 AU; auxiliary gas pressure, 30 AU; capillary temperature, 350 °C. The analytes in the extract were identified by comparing the MS<sup>n</sup> spectra, acquired via negative ionization [M – H]<sup>–</sup>, with those reported in the literature. The quantitative determination of glucosinolate content in the extracts was performed using HPLC coupled with UV spectroscopy (HPLC-DAD) using an RS-3000 Diode Array Detector (Thermo-Scientific) at 230 nm. The gradient used for this chromatographic run was 0–3 min 0% B

(isocratic), 3–5 min 70%B (linear), 5–8 min 70% B (isocratic), 8–10 min 0% B (linear), 10–15 min 0% B (isocratic). The glucoraphanin and glucosinolates in the extract (quantified as glucoraphanin equivalents) were quantified using external calibration. The calibration curves ( $R^2 > 0.9986$  for both linear fittings) for glucoraphanin and sinapine were obtained by injecting standard solutions within the linear concentration range of 0.001–0.1 mM. The LOD and LOQ values were 0.0003 and 0.001 mM, respectively.

### 3.2.4 Equilibrium Water Content (EWC)

The EWC of the hydrogel beads was measured gravimetrically by completely drying each sample and weighing it before and after. All samples were left to equilibrate beforehand by releasing excess water. The EWC was then calculated using Equation (1).<sup>46</sup>

$$EWC = \frac{W_{wet} - W_{dry}}{W_{wet}} \times 100 \quad (1)$$

where  $W_{wet}$  is the weight of the swollen hydrogel and  $W_{dry}$  is the weight of the completely dry hydrogel (i.e., the sole polymeric network).

### 3.2.5 Differential Scanning Calorimetry (DSC) and Free Water Index (FWI)

DSC measurements were performed to calculate the free water index (FWI) of the gel systems and were carried out on a DSC Q1000 (TA Instruments, New Castle, DE, USA), using sealed aluminum pans under an inert nitrogen atmosphere (nitrogen flow:  $50.0 \pm 0.5 \text{ cm}^3/\text{min}$ ). The samples were equilibrated at  $-60 \text{ }^\circ\text{C}$  for 8 min, then heated from  $-60 \text{ }^\circ\text{C}$  up to  $25 \text{ }^\circ\text{C}$  at  $1 \text{ }^\circ\text{C}/\text{min}$ . The calculation of the FWI from the enthalpy of the fusion values (obtained from the integration of the DSC curve peak around  $0 \text{ }^\circ\text{C}$ ) was performed according to Equation (2)<sup>47</sup>:

$$FWI = \frac{\Delta H_{fus(exp)}}{EWC \cdot \Delta H_{fus(theo)}} \quad (2)$$

where  $\Delta H_{fus}(exp)$  (J/g) is the experimental value of the enthalpy variation relative to the melting of frozen free water and  $\Delta H_{fus}(theo)$  (333.1 J/g) is the theoretical value of the enthalpy of fusion for bulk water.

### 3.2.6 Scanning Electron Microscopy (SEM)

Scanning electron micrographs of pristine and loaded CMC gel was taken using a Quanta 400 SEM apparatus (FEI Company, Hillsboro, OR, USA) operating at a voltage of 20 kV. The hydrogel samples were freeze-dried to allow their investigation in high-vacuum conditions. Subsequently, they were placed onto stubs using double-sided conductive tape and sputter-coated with gold to make them conductive.

### 3.2.7 Rheometry on Polymer Solutions and Hydrogels

Rheological analyses were performed using a Discovery HR-2 rheometer (TA Instruments, New Castle, DE, USA) on CMC system for all extract concentrations explored (0%, 1%, 2.5%, and 5%).

First, the viscosity of the CMC polymeric solution (before the crosslinking gelation process) was determined as a function of the shear rate (1/s), using a rotational rheometer with cone–plate geometry.

Then, the determination of the  $G'$  and  $G''$  moduli was carried out on already formed hydrogels in the form of discs instead of beads. To obtain this gel shape (more suitable for rheometry), each system was crosslinked by pouring it into a Petri dish containing the crosslinker solution. Additional solution was added dropwise using a Pasteur pipette to reach an excess of cations, as in the hydrogel synthesis process described in Section 3.2.2. After 15 min, the crosslinker solutions were removed, and the hydrogels were left to rest for one day and stored, as in the previously analyzed systems. Then, they were washed and analyzed using the plate–plate geometry to avoid inconsistencies in force distribution.

### 3.2.8 Encapsulation Efficiency (EE%)

The loading kinetics and the encapsulation efficiency (EE%) were determined focusing on glucoraphanin, the most abundant glucosinolate found in the commercial *Brassica oleracea* extract. The EE% was calculated using the following equation:

$$EE\% = \frac{GRF_{sol} - GRF_{lost}}{GRF_{sol}} \times 100 \quad (3)$$

where  $GRF_{sol}$  is the amount of glucoraphanin initially mixed in the polymer solution (its value is simply obtained by multiplying the mass of polymer solution that underwent crosslinking by the extract concentration in the same solution (1%, 2.5%, or 5%) and the glucoraphanin fraction of the *Brassica oleracea* extract (22.10%), as obtained by HPLC-DAD measurements); and  $GRF_{lost}$  is the total amount of glucoraphanin lost in the crosslinker and rinsing solutions, determined via HPLC-DAD analyses, as reported in Section 3.2.3.

In this case, the EE% was not 100% because some of the glucoraphanin originally present in the polymeric solution used to synthesize the hydrogel beads was lost in the crosslinking saline solution during the gelation process. To determine the amount of glucoraphanin lost during this step and during the subsequent rinsing steps, both the crosslinker solution and the water used to rinse the hydrogels were collected and analyzed by means of HPLC-DAD, as described in Section 3.2.3, using an external calibration in the linear concentration range of 0.1–20 ppm.

### *3.2.9 Release Kinetics in Water and Release Efficiency (RE%)*

To study the release kinetics in water and the release efficiency (RE%), a known amount of the loaded hydrogels was immersed in water (hydrogel/water 1:10, v/v) and kept under magnetic stirring to favor the release of glucosinolates. Also in this case, the analysis focused on the release profile of glucoraphanin as a representative of the glucosinolates loaded into the hydrogel. Several 100  $\mu$ L samples were taken over three hours of observation, each time replacing the sampled volume with fresh water to maintain a constant volume. The samples were then diluted 1:100 and analyzed by means of HPLC-DAD, as described in Section 3.2.3, using an external calibration in the linear concentration range of 0.1–20 ppm. All measurements were performed in triplicate.

### 3.3 Results

#### 3.3.1 *Brassica Oleracea* Extract Characterization

First, the *Brassica oleracea* extract was characterized by means of HPLC-MS and HPLC-DAD analyses, as described in Section 3.2.3, to identify and quantify the main chemicals present. The chromatogram obtained from the chromatographic analysis is shown in **Figure 1A**, where peaks corresponding to the most abundant compounds present in the extract are clearly visible. The detected analytes were fragmented using tandem mass spectrometry ( $MS^n$ ), with He as the collision gas inside the ion trap, in negative ion mode, according to the method described in Section 3.2.3. The use of fragmentation patterns enabled the identification of the compounds listed in **Table 1**.

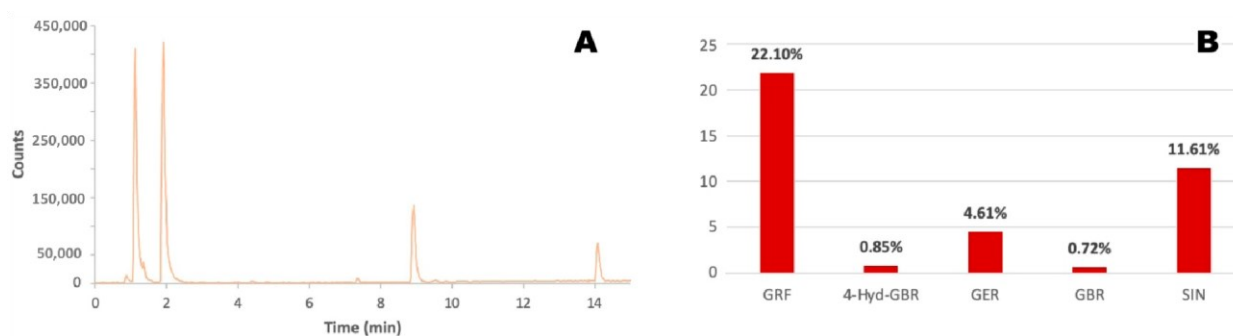


**Figure 1.** (A) Chromatogram obtained from the HPLC-DAD analysis for the characterization of the *Brassica oleracea* extract. (B) Relative amounts of the most abundant compounds identified in the *Brassica oleracea* extract. GRF: glucoraphanin,  $22.10 \pm 0.99\%$ ; 4-Hyd-GBR: 4-hydroxyglucobrassicin,  $0.85 \pm 0.04\%$ ; GER: glucoerucin,  $4.61 \pm 0.21\%$ ; GBR: glucobrassicin,  $0.72 \pm 0.03\%$ ; SIN: sinapine,  $11.61 \pm 0.52\%$ .

**Table 1.** Retention times and fragment ions for the identification of the components in the *Brassica oleracea* extract.

Analyte	Retention Time (min)	[M – H] <sup>–</sup>	Fragment Ions
Glucoraphanin	1.91	436	292, 275, 259, 194, 130
4-Hydroxyglucobrassicin	4.4	463	383, 285, 275, 267, 259, 240
Glucoerucin	8.93	420	340, 291, 275, 259, 242, 227, 224, 195, 178
Glucobrassicin	9.55	447	275, 259, 251, 205
Sinapine	14.09	354	294, 279, 264, 223, 208

Several diagnostic ions for glucosinolates have been reported in the literature, e.g., those related to the loss of the  $\text{HSO}_3^-$  ion ( $m/z$  96 or 97) and the neutral loss of the glucose moiety ( $m/z$  162)<sup>49</sup>. Glucoraphanin was clearly visible in the chromatogram at a retention time of 1.91 min, and the deprotonated molecule  $[\text{M} - \text{H}]^-$  was identified through comparison with literature data<sup>49</sup>. Besides glucoraphanin, other glucosinolates were present in the extract in significant amounts, such as 4-hydroxyglucobrassicin (an indolic glucosinolate derived from glucobrassicin), glucoerucin, and glucobrassicin, identified through their characteristic MS2 fragments,<sup>49</sup> as reported in **Table 1**.

The elution peak visible at 14.09 min in the chromatogram in **Figure 1A** was attributed to sinapine, an alkaloid derived from sinapic acid and commonly found in seeds of certain *Brassicaceae* plants<sup>49</sup>. Other minor compounds were also detected in the extract, but they were not identified.

The identified glucosinolates and sinapine were then quantified by means of HPLC-DAD analyses, and the results are reported in **Figure 1B**, showing a total glucosinolate content of  $28.28 \pm 1.27\%$ . It is worth noting that the relatively high content ( $11.61 \pm 0.52\%$ ) of sinapine can also contribute to the antimicrobial activity of the extract due to the demonstrated antimicrobial properties of this alkaloid.<sup>50</sup>

### 3.3.2 Physico-Chemical Characterization of CMC Hydrogel

The hydrogels based on CMC polymers were then synthesized, exploring several different extract concentrations, i.e., 0%, 1%, 2.5%, and 5% (with respect to the initial polymeric solution). The

equilibrium water content (EWC), calculated as described in Section 3.2.4, was found to be  $93 \pm 1\%$  for all gels, both unloaded and loaded with the extract.

The FWI of the developed systems was then obtained through DSC analysis (see Section 3.2.5), and the results determined for all samples are reported in **Table 2**.

**Table 2.** FWI measured in CMC-based hydrogels in the 0–5% concentration range.

Sample	$\Delta H_{\text{exp}}$ (J/g)	FWI (%)
CMC	$265 \pm 13$	$86 \pm 4$
CMC-1	$217 \pm 11$	$70 \pm 4$
CMC-2.5	$179 \pm 9$	$58 \pm 3$
CMC-5	$165 \pm 8$	$53 \pm 3$

As shown in **Table 2**, a decrease in the FWI was observed in the hydrogel with increasing extract concentration. This effect was particularly pronounced in systems with higher concentrations (2.5% and 5%), where the FWI difference was more significant. This behavior was likely due to a complex and synergistic effect that took into account the chemical nature of the polymer; its interactions with and  $\text{Fe}^{3+}$  cations; and its interactions with the variety of compounds included in the extract. It is indeed known that glucosinolates (particularly glucoraphanin and glucobrassicin) are prone to complexation with iron ions<sup>51-53</sup>. More specifically,  $\text{Fe}^{2+}$  ions are responsible for inducing non-enzymatic and thermal degradation of glucosinolates, while no such effects are observed for  $\text{Fe}^{3+}$ , which can still form stable complexes. Thus, it can be inferred that the glucosinolate/ $\text{Fe}^{3+}$  interactions were ultimately responsible for some water structuring in the proximity of the formed complexes, and this was observed as a consistent reduction in the FWI for the CMC/ $\text{Fe}^{3+}$  hydrogel systems.

**Figure 2** shows the frequency sweep graphs reporting the storage ( $G'$ ) and loss ( $G''$ ) moduli measured for the hydrogel.

The CMC-based systems displayed predominantly elastic behavior, typical of solid-like viscoelastic materials, with  $G'$  exceeding  $G''$  throughout the entire frequency range examined. The high mechanical properties observed, reflected in the absolute values of both moduli, were likely attributable to the crosslinking effect of  $\text{Fe}^{3+}$  ions, which are known to form stiff and mechanically resistant gels<sup>54</sup>.

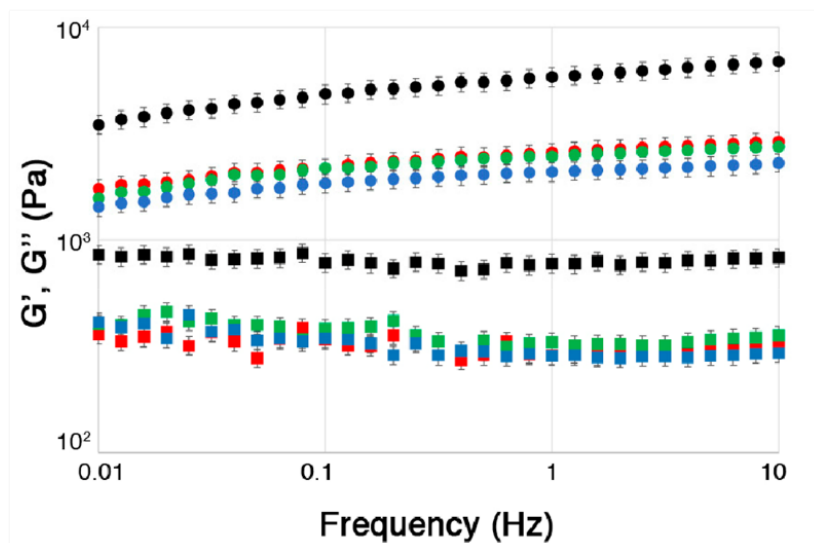


**Figure 2.** Frequency sweep graphs showing  $G'$  (circles) and  $G''$  (squares) moduli for the hydrogel.

Black: unloaded gels, initial extract concentration = 0%; red: initial extract concentration = 1%; green: initial extract concentration = 2.5%; blue: initial extract concentration = 5%. The measurements were carried out by selecting an amplitude in the linear viscoelastic region, identified through amplitude sweep analyses. The unloaded hydrogel displayed significantly higher moduli than the extract-loaded formulations, which all exhibited similar mechanical properties indicative of a generally weaker structure. These results support the hypothesis that the observed FWI decrease in these systems is attributable to the formation of glucosinolate/ $\text{Fe}^{3+}$  hydrated complexes, rather than to enhanced hydration of the carboxymethyl cellulose chains, as previously proposed in the discussion of the DSC data. SEM micrographs of both loaded and unloaded CMC-based hydrogels were subsequently acquired to investigate the micromorphology of these systems.

**Figure 3A** displays the surface of an unloaded CMC-0 hydrogel bead. The system demonstrates good structural integrity following the freeze-drying process, with limited surface deformation despite the dehydration stress. This resistance to structural changes is consistent with the rheological analyses, which confirmed the high mechanical strength of the carboxymethyl cellulose-based system. A cross-sectional view of the hydrogel bead (**Figure 3B**) provides insight into its internal architecture. The gel is characterized by a porous structure featuring an inhomogeneous network of thick gel walls separated by large pores. This apparently robust microstructure correlates well with the strong mechanical properties observed for the hydrogel, as previously discussed.

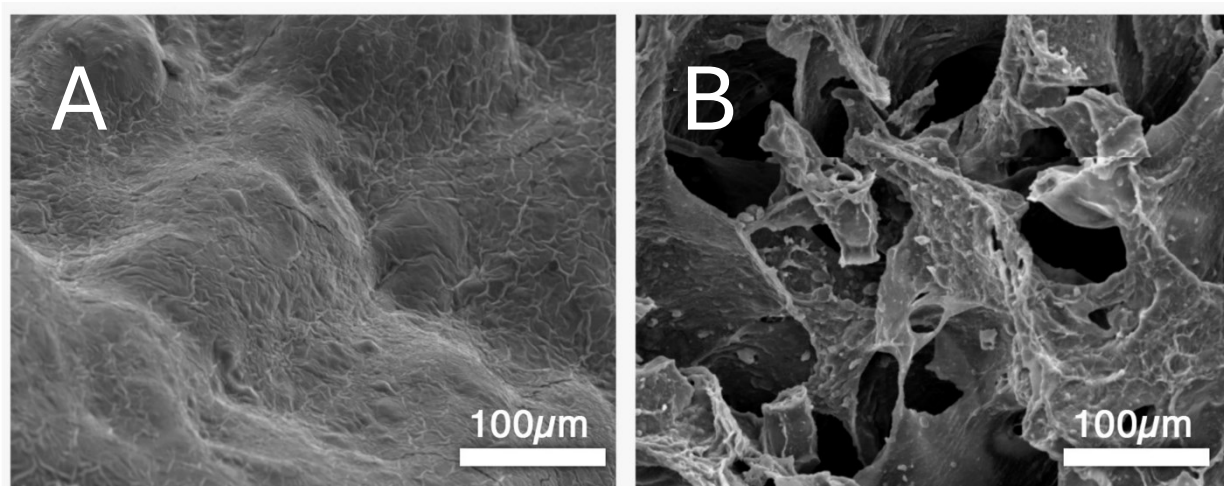


**Figure 3.** SEM micrographs taken on the freeze-dried hydrogels. (A) Surface of a CMC-0 hydrogel bead; (B) Cross-section of a CMC-5 hydrogel bead—some extract clumps are visible on the gel walls.

The encapsulation efficiency (EE%) was then measured, as described in Section 3.2.8., as it is a crucial parameter for the characterization of CR systems. In this case, it represents the amount of the active principle retained inside the hydrogels with respect to the amount initially mixed with the polymer solution. Knowing this parameter is necessary for calculating the subsequent release efficiency (RE%) of the hydrogel beads and provides insight into the nature of the interactions between the polymer network and the extract's compounds. As mentioned above, in the present case, glucoraphanin was quantified and taken as a marker to measure the loading and release profiles, being the main glucosinolate present in the *Brassica oleracea* extract.

The EE% values for the CMC-based hydrogels at different initial extract concentrations (1%, 2.5%, and 5%) are presented in **Figure 4**. Analysis of the data indicates an increasing trend in EE% with higher extract concentrations in the initial polymer solution. However, it should be noted that the magnitude of experimental errors in some instances requires cautious interpretation of the observed differences in average values.

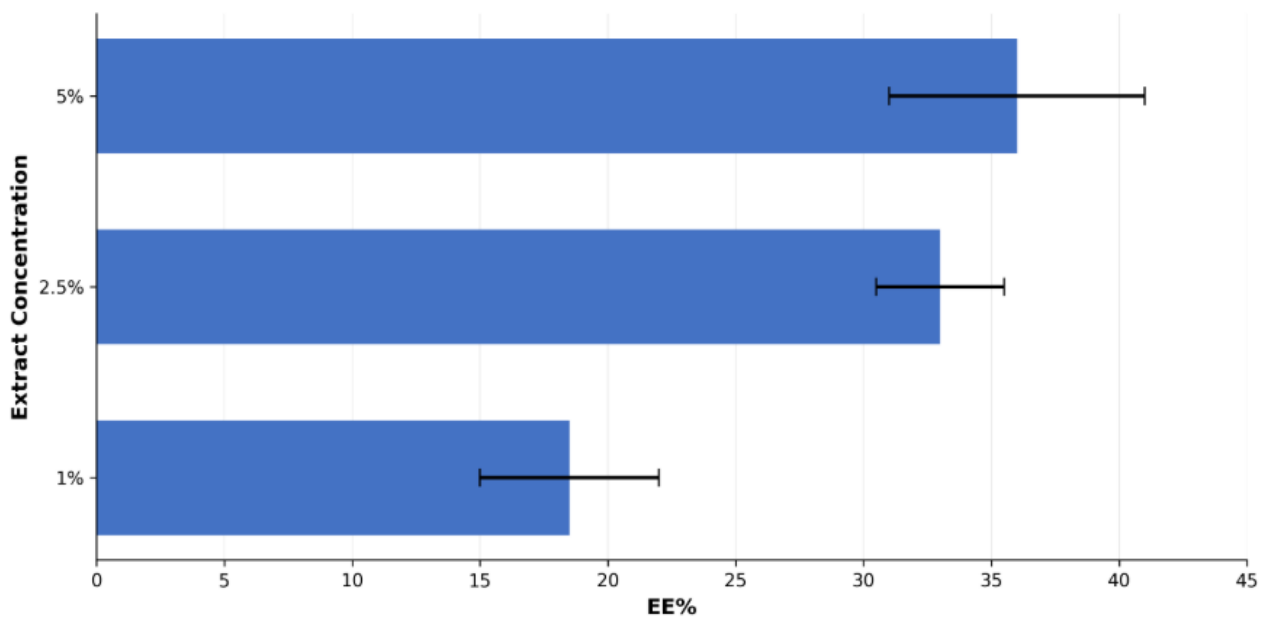


**Figure 4.** EE% for CMC hydrogels loaded with different extract concentrations.

The high encapsulation efficiency of the CMC-based hydrogels can be explained by multiple contributing factors. First, the probable formation of glucosinolate/ $\text{Fe}^{3+}$  complexes likely restricts glucoraphanin migration from within the gel matrix. Second, the robust inner structure of the hydrogel, featuring thick gel walls as revealed by SEM imaging, appears to effectively confine the bioactive compound. An additional key factor is the average size of the hydrogel beads, which is directly influenced by the solution viscosity. As shown in **Figure 5**, the CMC solutions exhibit substantial viscosity across varying extract concentrations, displaying typical shear-thinning behavior with viscosity values decreasing from approximately  $10^2$  Pa·s at low shear rates to below 1 Pa·s at high shear rates

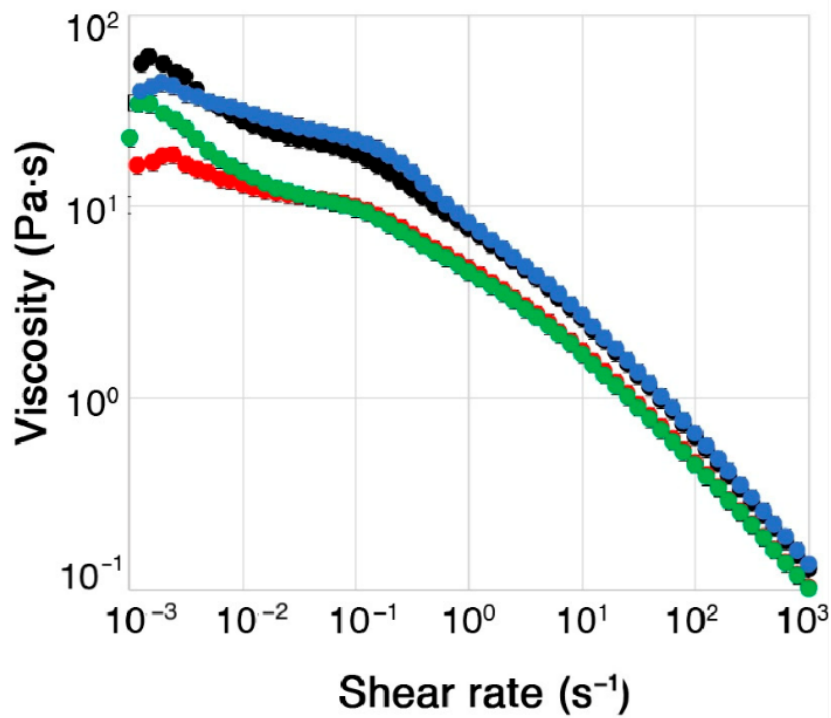


**Figure 5.** Viscosity of CMC polymeric solutions (with different extract concentrations) before crosslinking. Black: unloaded gels, initial extract concentration = 0%; red: initial extract concentration = 1%; green: initial extract concentration = 2.5%; blue: initial extract concentration = 5%. Error bars are not clearly visible, as they are smaller than the markers.

The CMC polymer solutions exhibited a shear-thinning trend in their viscosity, which is typical of non-Newtonian fluids, even in the presence of increasing extract concentrations. The high viscosity of the CMC solutions (approximately  $10^2$  Pa·s at low shear rates) resulted in the solution dripping more slowly from the funnel during the crosslinking process, thus forming larger hydrogel beads on average, with a slightly elongated shape (see **Figure 6**).

Since the EE% depends on the amount of glucoraphanin lost in the crosslinker solution and the rinsing water as a result of glucosinolate migration from the gel to the outer environment (driven by a concentration gradient), it is reasonable to hypothesize that it is also related to the surface-to-volume (S/V) ratio of the hydrogel beads. The sizes of the CMC hydrogel beads were measured using a digital caliper. The measurements revealed that the bead sizes did not significantly change with the extract concentration. The CMC beads were approximated as prolate ellipsoids, with an S/V ratio of  $1.13 \pm 0.04$  mm<sup>-1</sup>. This lower S/V ratio means that, for an equal volume of hydrogel, the interface between the gel beads and the outer aqueous environment was relatively small, which could be more efficient for retaining glucoraphanin inside the gel matrix and thus contributing to the high EE% observed.



**Figure 6.** CMC-5 hydrogel beads show dark color due to the presence of  $\text{Fe}^{3+}$  ions in the polymer network.

The second feature observed in the EE% of the investigated systems was related to the fact that the encapsulation efficiency increased with the extract concentration. It is worth noting that the absolute amount of glucoraphanin lost in the crosslinker saline solution was higher for higher extract concentrations; thus, one could have expected a constant EE% over the whole range of concentrations explored. However, this was not the case because, even though the increase in the initial internal glucoraphanin concentration inside the forming gel bead would enlarge the concentration gradient that drives active compound migration, the interfacial area was the same as for lower concentrations, meaning that the process has a self-limiting asymptotic trend. For this reason, the amount of glucoraphanin retained inside the hydrogel (i.e., the EE%) increased with increasing extract concentration.

The release efficiency (RE%) is another key parameter for characterizing hydrogels to be used as CR media, as it indicates their ability to release the active compound, a crucial step in the treatment of agricultural soils. Before studying the behavior of the loaded hydrogel beads in simulated or actual soils, their release profiles were investigated in water to compute a model system. In fact, since glucoraphanin is a water-soluble compound, it can be hypothesized that its release in soil also occurs primarily through soil moisture.

By knowing the initial amount of glucoraphanin confined in the investigated systems

(by exploiting the EE% values previously measured, as discussed above) and measuring the glucoraphanin (taken again as the reference glucosinolate, representative of all active compounds in

the extract) released by the hydrogel beads immersed in a known amount of water via HPLC-DAD, it was possible to plot the release profiles, as shown in **Figure 7**.

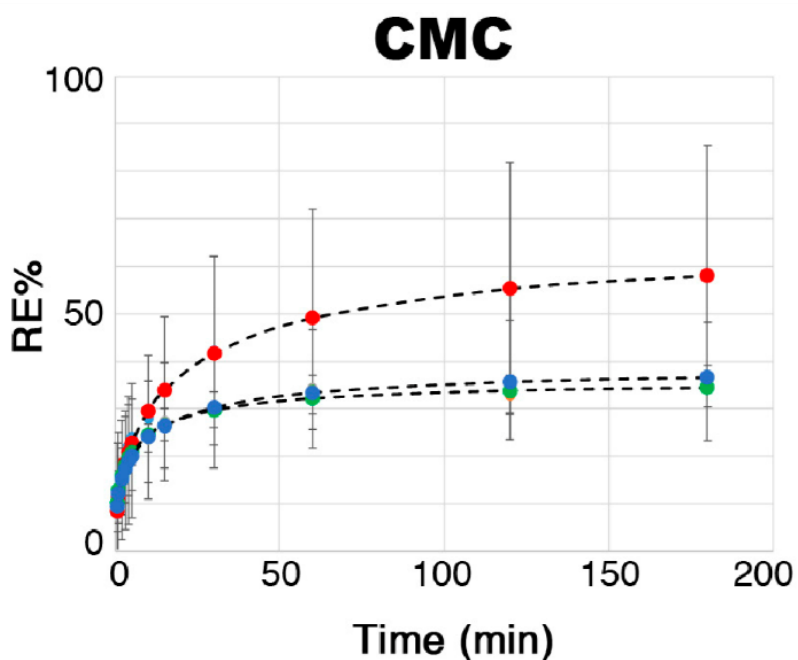


**Figure 7.** Release kinetics profiles of glucoraphanin for all loaded systems investigated. Red: initial extract concentration = 1%; green: initial extract concentration = 2.5%; blue: initial extract concentration = 5%. Dashed black lines represent the best-fitting curve for each system, computed using the Weibull model.

The CMC-based hydrogels exhibited asymptotic glucoraphanin release behavior in water. Notably, RE% decreased with increasing extract concentration, showing an inverse relationship to the EE% trend where 5% extract loading yielded the highest values. This inverse correlation was anticipated, as higher EE% indicates superior glucoraphanin retention within the hydrogel matrix, consequently reducing its release rate. Across all formulations, the RE% plateaued at approximately 40% of the initial active compound content. However, despite CMC-1 achieving the highest RE%, the absolute quantity of glucoraphanin released from CMC-5 was 5–6 times greater after 3 h in water (**Table 3**, last column), owing to its substantially higher initial loading.

**Table 3.** Weibull model fitting parameters for the release profiles in water for all investigated hydrogels.

<b>System</b>	<b>K</b>	<b>A</b>	<b>b</b>	<b>Max Glucoraphanin Released <sup>a</sup></b>
CMC 1%	62%	0.16	0.48	0.6 ± 0.1
CMC 2.5%	39%	0.46	0.41	1.4 ± 1.0
CMC 5%	35%	0.38	0.42	3.2 ± 1.0

<sup>a</sup> The concentration (ppm) of glucoraphanin, measured in the solution in which the hydrogels were immersed, after 3 h of release.

Many suitable models can be used to fit the release kinetics of porous matrices, such as hydrogels or mesoporous particles, e.g., those proposed by Higuchi et al.<sup>55</sup> or Peppas and coworkers<sup>56-58</sup>. Such models represent short-time approximations of kinetic curves related to diffusion processes, which can conveniently account for approx. 60% of the whole curve<sup>59</sup>. In this case, similarly to what has been done before on similar systems<sup>45</sup>, the Weibull model was used. This is a modified version of first-order kinetics models, and it is described by Equation (4):

$$C_t = C_\infty(1 - e^{-at^b}) \quad (4)$$

where  $C_t$  is the experimental concentration measured in the water in which the hydrogels were immersed as a function of time;  $C_\infty$  is the maximum concentration reached at infinite time (an asymptotic value);  $t$  is the time the hydrogels were immersed in water;  $a$  is a dimensionless empirical constant; and  $b$  is another dimensionless constant, which has been shown to have a linear correlation with the Peppas exponent,  $n$ , as reported in the following Equation (5):

$$\frac{C_t}{C_\infty} = Kt^n \quad (5)$$

It has been demonstrated that if  $b < 0.75$ , the process is governed by Fickian diffusion; if  $0.75 < b < 1$ , a combination of Fickian diffusion and Case II diffusion takes place, while for  $b > 1$ , a complex diffusion mechanism occurs.<sup>60</sup> In the present case, Equation (4) was normalized by the total concentration of glucoraphanin initially present in each hydrogel system ( $C_{TOT}$ ), and this gave Equation (6), which was then used to fit the experimental data and to obtain the ER%:

$$\frac{C_t}{C_{tot}} = \frac{C_\infty}{C_{tot}} (1 - e^{-at^b}) = \text{ER}\% = K (1 - e^{-at^b}) \quad (6)$$

**Table 3** shows the values obtained for the fitting parameters ( $K$ ,  $a$ ,  $b$ ) for all investigated systems. The best-fitting curves are shown together with the experimental data in **Figure 7**. The Weibull model provided an excellent fit for all six systems. Since the values of the dimensionless constant  $b$  were all below 0.75, the release of glucoraphanin in water followed Fickian diffusion kinetics.

The release process in water, although it only roughly approximates the real case, provides evidence that glucosinolate delivery is slow and gradual. This would increase control over the fumigation potential in agricultural soils. Finally, it is worth noting that, in a real soil treatment, hydrogel beads would act well beyond 3 h, until complete disruption of the gel network and subsequent release of the active compounds, ensuring a durable effect over time.

### 3.4 Conclusions

The potential of Fe<sup>3+</sup>/carboxymethyl cellulose (CMC)-based hydrogel beads as vehicles for the controlled release of glucosinolates in agricultural soils was explored, with the aim of developing improved and innovative treatments inspired by biofumigation. A commercial *Brassica oleracea* extract was first characterised through HPLC-MS-DAD analyses, revealing that the total glucosinolate content was around 28% *m/m*, with glucoraphanin being the most abundant, whilst 12% *m/m* of sinapine was also detected, which can contribute to the biocidal properties of the product. The extract was then loaded (exploring a 1–5% concentration range, representing the initial extract concentration in the pre-crosslinking polymeric solution) into CMC hydrogel beads, which were physico-chemically characterised through DSC, rheometry, and SEM, whilst the encapsulation efficiency (EE%) and release efficiency (RE%) in water were investigated through HPLC-DAD analyses. The CMC hydrogels exhibited an equilibrium water content (EWC) of 93% and a high free water index (FWI), which decreased with increasing extract concentration. This drop in FWI was attributed to the likely formation of hydrated Fe<sup>3+</sup>/glucosinolate complexes. Rheological measurements supported this hypothesis, showing that the CMC hydrogels possessed high mechanical properties, with G' exceeding G'' across the entire frequency range explored, indicative of predominantly elastic, solid-like viscoelastic behaviour. The CMC-based hydrogels demonstrated high EE%, which increased with extract concentration. This could be attributed to a combination of factors, including the inner structure and the surface-to-volume (S/V) ratio of the beads. SEM micrographs revealed a thick and more robust gel walls, which could confine the active compounds inside the beads. Additionally, the high viscosity of the CMC polymer solution resulted in large hydrogel beads with a low S/V ratio ( $1.13 \pm 0.04 \text{ mm}^{-1}$ ), accounting for an important glucoraphanin retention within the gel matrix and reduced migration to the surrounding aqueous environment. The

release profiles, fitted using the Weibull model function, showed a gradual and slow release that tended to reach an asymptotic value after almost 3 h of hydrogel immersion in water. This sustained release behaviour would enable a prolonged and controlled effect in agricultural soils. Overall, the CMC-based hydrogels possess excellent properties for real *in-field* applications. Their high EE%, robust mechanical properties, and effective retention of extract active molecules suggest they could deliver a gradual and prolonged effect during soil treatment. Additionally, the potential enhanced contributions of Fe (III) to the biocidal properties of the gel beads make this system particularly promising for further testing. Further experiments will include the investigation of release profiles in artificial model soils and -most importantly- in real agricultural soils, even though the organic compounds naturally present in soils complicate the analysis due to possible interference with the analytes' quantification. This work clearly demonstrated the potential of cheap, simple, and eco-friendly CMC-based hydrogels as carriers for active compounds, possibly extracted from plants or by-products of agrifood production, as an advanced tool for agricultural soil treatment. The versatility of these materials enables their use in other applicative fields, such as the cleaning of biodegraded artistic surfaces in the context of cultural heritage conservation, among others.

## References

1. Rani, Lata, et al. "An extensive review on the consequences of chemical pesticides on human health and environment." *Journal of cleaner production* 283 (2021): 124657.
2. Kalyabina, Valeriya P., et al. "Pesticides: formulants, distribution pathways and effects on human health—a review." *Toxicology reports* 8 (2021): 1179-1192.
3. Toppari, Jorma, et al. "Male reproductive health and environmental xenoestrogens." *Environmental health perspectives* 104.suppl 4 (1996): 741-803.
4. Damalas, Christos A., and Ilias G. Eleftherohorinos. "Pesticide exposure, safety issues, and risk assessment indicators." *International journal of environmental research and public health* 8.5 (2011): 1402-1419.
5. Tudi, Muyesaier, et al. "Agriculture development, pesticide application and its impact on the environment." *International journal of environmental research and public health* 18.3 (2021): 1112.

6. Horrigan, Leo, Robert S. Lawrence, and Polly Walker. "How sustainable agriculture can address the environmental and human health harms of industrial agriculture." *Environmental health perspectives* 110.5 (2002): 445-456.
7. Devkota, Pratap, Jason K. Norsworthy, and Ronald Rainey. "Comparison of allyl isothiocyanate and metam sodium with methyl bromide for weed control in polyethylene-mulched bell pepper." *Weed Technology* 27.3 (2013): 468-474.
8. Pruet, Stephen B., L. Peyton Myers, and Deborah E. Keil. "Toxicology of metam sodium." *Journal of toxicology and environmental health part B: critical reviews* 4.2 (2001): 207-222.
9. Sederholm, Maya R., et al. "Effects of metam sodium fumigation on the abundance, activity, and diversity of soil bacterial communities." *Applied soil ecology* 124 (2018): 27-33.
10. Zheng, Wei, et al. "Conversion of metam sodium and emission of fumigant from soil columns." *Atmospheric Environment* 40.36 (2006): 7046-7056.
11. European Food Safety Authority (EFSA), et al. "Peer review of the pesticide risk assessment of the active substance ferric pyrophosphate." *EFSA Journal* 18.1 (2020): e05986.
12. Kirkegaard, J. A., and M. Sarwar. "Biofumigation potential of brassicas." *Plant and soil* 201.1 (1998): 71-89.
13. Sarwar, M., et al. "Biofumigation potential of brassicas." *Plant and Soil* 201.1 (1998): 103-112.
14. Hanschen, Franziska S., and Traud Winkelmann. "Biofumigation for fighting replant disease-a review." *Agronomy* 10.3 (2020): 425.
15. Gimsing, A. L., and J. A. Kirkegaard. "Glucosinolate and isothiocyanate concentration in soil following incorporation of Brassica biofumigants." *Soil Biology and Biochemistry* 38.8 (2006): 2255-2264.
16. Gimsing, Anne Louise, and John A. Kirkegaard. "Glucosinolates and biofumigation: fate of glucosinolates and their hydrolysis products in soil." *Phytochemistry Reviews* 8.1 (2009): 299-310.
17. Matthiessen, John N., and John A. Kirkegaard. "Biofumigation and enhanced biodegradation: opportunity and challenge in soilborne pest and disease management." *Critical reviews in plant sciences* 25.3 (2006): 235-265.
18. Pardini, Alessio, et al. "Kinetics of glucosinolate hydrolysis by myrosinase in Brassicaceae tissues: A high-performance liquid chromatography approach." *Food Chemistry* 355 (2021): 129634.

19. Brown, Paul D., et al. "Allelochemicals produced during glucosinolate degradation in soil." *Journal of Chemical Ecology* 17.10 (1991): 2021-2034.
20. Antonious, George Fouad. "The impact of organic, inorganic fertilizers, and biochar on phytochemicals content of three Brassicaceae vegetables." *Applied Sciences* 13.15 (2023): 8801.
21. Plaszkó, Tamás, et al. "Effects of glucosinolate-derived isothiocyanates on fungi: A comprehensive review on direct effects, mechanisms, structure-activity relationship data and possible agricultural applications." *Journal of Fungi* 7.7 (2021): 539.
22. Mari, Marta, et al. "Control of brown rot on stonefruit by synthetic and glucosinolate-derived isothiocyanates." *Postharvest Biology and Technology* 47.1 (2008): 61-67.
23. Dufour, Virginie, Martin Stahl, and Christine Baysse. "The antibacterial properties of isothiocyanates." *Microbiology* 161.2 (2015): 229-243.
24. Lazzeri, L., O. Leoni, and L. M. Manici. "Biocidal plant dried pellets for biofumigation." *Industrial crops and products* 20.1 (2004): 59-65.
25. Morris, E. Kathryn, Rachel Fletcher, and Stavros D. Veresoglou. "Effective methods of biofumigation: a meta-analysis." *Plant and Soil* 446.1 (2020): 379-392.
26. Mun, Alexandra, et al. "Alginate hydrogel beads embedded with drug-bearing polycaprolactone microspheres for sustained release of paclobutrazol." *Scientific Reports* 11.1 (2021): 10877.
27. Singh, Amrita, et al. "Advances in controlled release pesticide formulations: Prospects to safer integrated pest management and sustainable agriculture." *Journal of hazardous materials* 385 (2020): 121525.
28. Singh, Gurwinder, et al. "Nanoporous materials for pesticide formulation and delivery in the agricultural sector." *Journal of Controlled Release* 343 (2022): 187-206.
29. Michalik, Regina, and Ilona Wandzik. "A mini-review on chitosan-based hydrogels with potential for sustainable agricultural applications." *Polymers* 12.10 (2020): 2425.
30. Kashyap, Prem Lal, Xu Xiang, and Patricia Heiden. "Chitosan nanoparticle based delivery systems for sustainable agriculture." *International journal of biological macromolecules* 77 (2015): 36-51.
31. Gallagher, Louise, et al. "Preparation and antimicrobial properties of alginate and serum albumin/glutaraldehyde hydrogels impregnated with silver (I) ions." *Chemistry* 3.2 (2021): 672-686.

32. Vejan, Pravin, et al. "Encapsulation of plant growth promoting Rhizobacteria—prospects and potential in agricultural sector: a review." *Journal of Plant Nutrition* 42.19 (2019): 2600-2623.
33. Cadena, Marimar Bravo, et al. "Enhancing cinnamon essential oil activity by nanoparticle encapsulation to control seed pathogens." *Industrial Crops and Products* 124 (2018): 755-764.
34. Matricardi, P.; Di Meo, C.; Coviello, T.; Hennink, W. E.; Alhaique, F. Interpenetrating Polymer Networks Polysaccharide Hydrogels for Drug Delivery and Tissue Engineering. *Adv. Drug Deliv. Rev.* 65, 1172–1187 (2013).
35. Mikula, K., et al. "Preparation of hydrogel composites using Ca<sup>2+</sup> and Cu<sup>2+</sup> ions as crosslinking agents." *SN Applied Sciences* 1.6 (2019): 643.
36. Traffano-Schiffo, Maria Victoria, et al. "Alginate beads containing lactase: stability and microstructure." *Biomacromolecules* 18.6 (2017): 1785-1792.
37. Kim, Min Sup, et al. "Ionically crosslinked alginate–carboxymethyl cellulose beads for the delivery of protein therapeutics." *Applied Surface Science* 262 (2012): 28-33.
38. Neri-Badang, Maria Cleofe, and Soma Chakraborty. "Carbohydrate polymers as controlled release devices for pesticides." *Journal of carbohydrate chemistry* 38.1 (2019): 67-85.
39. Kyriakoudi, Anastasia, et al. "Innovative delivery systems loaded with plant bioactive ingredients: Formulation approaches and applications." *Plants* 10.6 (2021): 1238.
40. Manca, Maria Letizia, et al. "From waste to health: Sustainable exploitation of grape pomace seed extract to manufacture antioxidant, regenerative and prebiotic nanovesicles within circular economy." *Scientific reports* 10.1 (2020): 14184.
41. Basta, Altaf H., and Vivian F. Lotfy. "The synergistic route for enhancing rice by-product derived nanoparticles in sustained release of bioactive compound." *Cellulose* 30.18 (2023): 11473-11491.
42. Clemente, Ilaria, et al. "Lipids from algal biomass provide new (nonlamellar) nanovectors with high carrier potentiality for natural antioxidants." *European Journal of Pharmaceutics and Biopharmaceutics* 158 (2021): 410-416.
43. Clemente, Ilaria, et al. "Structuring and de-structuring of nanovectors from algal lipids. Part 1: physico-chemical characterization." *Colloids and Surfaces B: Biointerfaces* 220 (2022): 112939.
44. Bonechi, Claudia, et al. "Cationic liposomes as carriers of natural compounds from plant extract." *Biophysical Chemistry* 318 (2025): 107381.

45. Baglioni, Michele, et al. "Isothiocyanate-Based Microemulsions Loaded into Biocompatible Hydrogels as Innovative Biofumigants for Agricultural Soils." *Molecules* 29.16 (2024): 3935.
46. Clemente, Ilaria, et al. "Green hydrogels loaded with extracts from Solanaceae for the controlled disinfection of agricultural soils." *Polymers* 15.22 (2023): 4455.
47. Łabowska, Magdalena B., et al. "Influence of cross-linking conditions on drying kinetics of alginate hydrogel." *Gels* 9.1 (2023): 63.
48. Domingues, Joana AL, et al. "Innovative hydrogels based on semi-interpenetrating p (HEMA)/PVP networks for the cleaning of water-sensitive cultural heritage artifacts." *Langmuir* 29.8 (2013): 2746-2755.
49. Rochfort, Simone J., et al. "Class targeted metabolomics: ESI ion trap screening methods for glucosinolates based on MS<sub>n</sub> fragmentation." *Phytochemistry* 69.8 (2008): 1671-1679.
50. Mouterde, L. M. M.; Peru, A. A. M.; Mention, M. M.; Brunissen, F.; Allais, F. Sustainable Straightforward Synthesis and Evaluation of the Antioxidant and Antimicrobial Activity of Sinapine and Analogues. *J. Agric. Food Chem.* 68, 6998–7004 (2020).
51. Hanschen, Franziska S., et al. "Reactivity and stability of glucosinolates and their breakdown products in foods." *Angewandte Chemie International Edition* 53.43 (2014): 11430-11450.
52. Santos, Carlos Edward B., C. Yu Hillary, and Marissa G. Noel. "IDENTIFICATION OF MAJOR GLUCOSINOLATES IN BROCCOLI (Brassica oleracea var. italica) BY LIQUID CHROMATOGRAPHY–MASS SPECTROMETRY (LC-MS) AND DETERMINATION OF ANTICANCER PROPERTIES OF BROCCOLI EXTRACTS." (2013).
53. Bellostas, Natalia, et al. "Fe<sup>2+</sup>-catalyzed formation of nitriles and thionamides from intact glucosinolates." *Journal of Natural Products* 71.1 (2008): 76-80.
54. Roquero, Daniel Massana, et al. "Iron (III)-cross-linked alginate hydrogels: A critical review." *Materials Advances* 3.4 (2022): 1849-1873.
55. Higuchi, Takeru. "Rate of release of medicaments from ointment bases containing drugs in suspension." *Journal of pharmaceutical sciences* 50.10 (1961): 874-875.
56. Korsmeyer, Richard W., et al. "Mechanisms of solute release from porous hydrophilic polymers." *International journal of pharmaceutics* 15.1 (1983): 25-35.

57. Peppas, Nikolaos A., and Jennifer J. Sahlin. "A simple equation for the description of solute release. III. Coupling of diffusion and relaxation." *International journal of pharmaceutics* 57.2 (1989): 169-172.
58. Korsmeyer, Richard W., and Nikolaos A. Peppas. "Effect of the morphology of hydrophilic polymeric matrices on the diffusion and release of water soluble drugs." *Journal of membrane Science* 9.3 (1981): 211-227.
59. Caccavo, Diego. "An overview on the mathematical modeling of hydrogels' behavior for drug delivery systems." *International journal of pharmaceutics* 560 (2019): 175-190.
60. Papadopoulou, Vasiliki, et al. "On the use of the Weibull function for the discernment of drug release mechanisms." *International journal of pharmaceutics* 309.1-2 (2006): 44-50.

## *CHAPTER 4: alfalfa (Medicago sativa L.) as a potential ingredient for food fortification*

A balanced diet is fundamental for maintaining human health and preventing disease. In recent years, nutritional research has expanded beyond the traditional focus on macronutrients (carbohydrates, lipids, and proteins) to include the characterization of micronutrients and secondary metabolites, particularly polyphenols. These bioactive compounds function as antioxidant agents and have been associated with reduced risk of chronic diseases and physiological disorders. Since the natural concentration of these molecules in foods is considerably lower than that of macronutrients, considerable efforts have been directed toward enhancing the health benefits of commonly consumed foods through a process known as “food fortification”

This study focuses on the characterization of alfalfa (*Medicago sativa* L.) as a potential ingredient for food fortification. The research presented here was funded by the Italian Ministry of Enterprises and Made in Italy (MIMIT) through the 2022 "Accordi per l'Innovazione" program (DM 31/12/2021) in collaboration with GITOMA s.r.l. The results reported represent preliminary findings from the initial sampling campaigns conducted during 2023, 2024, and 2025. Research on these matrices is ongoing, with future work aimed at comprehensive metabolomic profiling and *in vivo* bioavailability studies

### *4.1 Introduction*

*Medicago sativa* L., commonly known as alfalfa or lucerne, is a perennial leguminous forage crop that has been cultivated for over 2,000 years, primarily as animal feed due to its high protein content, excellent digestibility, and remarkable adaptability to diverse climatic conditions.<sup>1</sup> Native to southwestern Asia, alfalfa has become one of the most widely grown forage crops globally, with cultivation spanning temperate and subtropical regions across North America, Europe, Asia, and Australia.<sup>2</sup> While its traditional role in animal nutrition is well established, growing interest in plant-based foods and functional ingredients has prompted researchers to explore alfalfa's potential for direct human consumption, particularly as a source of bioactive compounds with health-promoting properties.<sup>3</sup>

The nutritional composition of alfalfa is remarkably diverse. Beyond its high protein content (15-25% dry weight), alfalfa contains significant amounts of dietary fiber, vitamins (particularly vitamin K, vitamin C, and B-complex vitamins), minerals (calcium, potassium, iron, magnesium), and an array

of bioactive phytochemicals including phenolic acids, flavonoids, saponins, and carotenoids.<sup>4</sup> This rich phytochemical profile has attracted considerable attention from the functional food industry, as epidemiological and experimental studies increasingly demonstrate the health benefits associated with plant polyphenol consumption, including reduced risk of cardiovascular diseases, certain cancers, neurodegenerative disorders, and metabolic syndrome.<sup>5</sup>

#### *4.1.1 Phenolic compounds in Alfalfa: free and bound fractions*

Plant phenolic compounds exist in two distinct forms: free (soluble) phenolics, which are easily extractable with aqueous or organic solvents, and bound (insoluble) phenolics, which are covalently linked to cell wall structural components such as cellulose, hemicellulose, and lignin.<sup>6</sup> The bound fraction is typically released only through acid or alkaline hydrolysis, or enzymatically during digestion by colonic microbiota.<sup>7</sup> While free phenolics have received extensive research attention due to their ready extractability and rapid absorption in the upper gastrointestinal tract, on the other side bound phenolics represent a substantial portion of total dietary polyphenols, in some plant materials accounting for 50-90% of total phenolic content.<sup>8</sup>

In legumes specifically, including alfalfa, bound phenolic acids are predominantly hydroxycinnamic acid derivatives, with ferulic acid, p-coumaric acid, and caffeic acid being the most abundant.<sup>9-10</sup> Ferulic acid is particularly significant due to its structural role in cross-linking cell wall polysaccharides through ester and ether bonds, contributing to cell wall rigidity and providing a physical barrier against pathogen invasion.<sup>11</sup> These bound phenolics, once considered nutritionally unavailable, are now recognized as important contributors to antioxidant capacity and health benefits, as they reach the colon intact where microbial esterases can release them, potentially providing sustained antioxidant protection in the lower gastrointestinal tract.<sup>12</sup>

#### *4.1.2 Antioxidant properties and health benefits*

The antioxidant capacity of plant-derived phenolic compounds stems from their ability to scavenge free radicals, chelate pro-oxidant metals, and modulate cellular antioxidant defense systems.<sup>13</sup> Chronic oxidative stress, resulting from an imbalance between free radical production and antioxidant defenses, is implicated in the pathogenesis of numerous chronic diseases including atherosclerosis, cancer, diabetes, and neurodegeneration.<sup>14</sup> Dietary antioxidants, particularly polyphenols, can mitigate oxidative damage and reduce disease risk.<sup>15</sup>

Ferulic acid, the predominant bound phenolic in alfalfa, exhibits potent antioxidant activity and has demonstrated cardioprotective, neuroprotective, anti-inflammatory, and anticancer properties in numerous *in vitro* and *in vivo* studies.<sup>11,16</sup> It functions not only as a direct free radical scavenger but also upregulates endogenous antioxidant enzymes including superoxide dismutase, catalase, and glutathione peroxidase.<sup>17</sup> P-coumaric acid similarly demonstrates anti-inflammatory effects by inhibiting pro-inflammatory cytokine production and has shown promising anticancer activity in preclinical studies<sup>18</sup> while caffeic acid contributes significantly to overall antioxidant capacity and exhibits antimicrobial properties.<sup>19</sup>

The unique advantage of bound phenolics lies in their sustained release profile. While free phenolics are rapidly absorbed in the small intestine and undergo extensive first-pass metabolism, resulting in relatively brief bioavailability, bound phenolics resist digestion in the upper gastrointestinal tract and reach the colon where they are gradually released by microbial esterases.<sup>20</sup> This controlled release may provide prolonged antioxidant protection and beneficial modulation of gut microbiota composition, potentially contributing to the well-documented health benefits of high-fiber, phenolic-rich diets.<sup>21</sup>

### *4.1.3 Factors influencing phytochemical content in plants*

The accumulation of phenolic compounds in plants is influenced by a complex interplay of genetic, developmental, and environmental factors. Genotype represents the primary determinant, establishing the baseline biosynthetic capacity for secondary metabolite production.<sup>22</sup> However, environmental stresses including UV radiation, drought, temperature extremes, soil nutrient deficiencies, and pathogen attack can substantially modulate phenolic biosynthesis through stress-responsive signaling pathways.<sup>23-24</sup>

Soil properties such as texture, pH, organic matter content, mineral composition, water retention capacity, nutrient availability, and microbial community composition influence both plant growth and secondary metabolism, ultimately impacting phytochemical profiles.<sup>25</sup> Similarly, harvest timing influences phytochemical content as plants undergo developmental changes throughout the growing season, with younger tissues often exhibiting different metabolite profiles than mature tissues.<sup>26</sup>

Inter-annual variation in climatic conditions represents an additional source of phytochemical variability. Temperature, precipitation patterns, solar radiation, and growing degree days vary from year to year, potentially affecting both plant growth and stress responses.<sup>27</sup> Understanding this natural

variability is essential for developing standardized functional food ingredients with predictable bioactive compound content.

#### *4.1.4 Post-harvest processing*

While considerable research has focused on agronomic factors influencing phytochemical content, post-harvest processing often exerts an even greater impact on final product quality.<sup>28</sup> Drying is typically necessary to reduce moisture content for storage stability and prevent microbial spoilage, but the drying method profoundly affects bioactive compound retention. Traditional air-drying or oven-drying at elevated temperatures can cause substantial losses of heat-sensitive compounds through thermal degradation, enzymatic oxidation, and volatilization.<sup>29</sup>

Freeze-drying (lyophilization) represents the gold standard for preserving bioactive compounds due to its low-temperature vacuum process that minimizes thermal degradation and enzymatic activity, and despite being more expensive than conventional drying methods, it typically yields superior retention of phenolics, vitamins, and antioxidant capacity, making it the preferred method for high-value functional ingredients.<sup>30</sup>

#### *4.1.5 Heavy metals and food safety*

Any plant material intended for human consumption must be evaluated not only for nutritional and functional properties but also for safety, particularly regarding heavy metal content. Plants can accumulate heavy metals from soil, water, and atmospheric deposition, and excessive dietary intake of metals such as arsenic, mercury, lead, and cadmium poses serious health risks including neurotoxicity, carcinogenicity, and organ damage.<sup>31</sup> For alfalfa specifically, as a deep-rooted perennial legume with high biomass production, understanding its metal accumulation patterns across different soil types is essential for ensuring food safety when considering human consumption applications.

Importantly, not all metals are toxic; several are essential micronutrients required for proper physiological function. Iron, copper, manganese, zinc, chromium, and cobalt play critical roles in enzymatic catalysis, oxygen transport, immune function, and metabolic regulation,<sup>32</sup> the presence of these essential minerals at appropriate concentrations enhances the nutritional value of plant-based foods.

#### *4.1.6 Alfalfa as a functional food ingredient*

The convergence of alfalfa's nutritional richness, bioactive phytochemical content, and agricultural sustainability positions it as a promising candidate for functional food applications. Functional foods are defined as foods that provide health benefits beyond basic nutrition, typically through the presence of bioactive compounds that may reduce disease risk or promote optimal health.<sup>33</sup> The functional food market has experienced substantial growth driven by consumer demand for health-promoting foods and preventive nutrition.<sup>34</sup>

The use of alfalfa leaf meal or extract as a functional ingredient in staple foods such as bread, pasta, and baked goods remains relatively unexplored, despite its potential to enhance nutritional value, antioxidant capacity, and health-promoting properties of these widely consumed products.<sup>35</sup> Fortification of cereal-based products with alfalfa could provide consumers with increased intake of dietary fiber, protein, essential minerals, and phenolic antioxidants without requiring substantial dietary modifications.

The feasibility of such fortification depends on several factors: the bioactive compound content must be sufficiently high to provide meaningful health benefits at realistic incorporation levels; heavy metal and other contaminant levels must comply with food safety regulations; sensory properties (color, flavor, texture) must remain acceptable to consumers; and processing stability must ensure that bioactive compounds survive food manufacturing processes.<sup>36</sup> Addressing these considerations requires comprehensive characterization of alfalfa's phytochemical profile, safety assessment, and understanding of how agronomic and processing factors influence final product quality.

#### *4.1.7 Analytical approaches*

Comprehensive evaluation of alfalfa as a functional ingredient requires multiple analytical techniques. Spectrophotometric assays provide high-throughput screening of total phenolic content (Folin-Ciocalteu method), total flavonoid content (aluminum chloride colorimetric method), and antioxidant capacity using various mechanistic approaches (DPPH radical scavenging, ABTS radical cation decolorization).<sup>37-40</sup> While these methods provide valuable information on overall bioactive content and antioxidant potential, they do not identify specific compounds.

High-performance liquid chromatography with diode array detection (HPLC-DAD) enables separation, identification, and quantification of individual phenolic compounds based on their

chromatographic retention times and UV-visible absorption spectra.<sup>41</sup> This targeted approach is essential for quality control, standardization, and understanding which specific compounds contribute to biological activities.

Inductively coupled plasma mass spectrometry (ICP-MS) represents the gold standard for multi-element analysis, enabling simultaneous quantification of both essential minerals and potentially toxic heavy metals at trace concentrations with high precision and accuracy, making this technique indispensable for food safety assessment and nutritional profiling.<sup>42</sup>

#### *4.1.8 Study objectives*

Given alfalfa's promising potential as a functional food ingredient yet limited systematic investigation of factors influencing its phytochemical quality, this study aims to comprehensively evaluate how agronomic factors (harvest period, soil type, plant part), inter-annual variation, and post-harvest processing methods (freeze-drying vs. air-drying) affect its bioactive compound profile and nutritional value. Through quantification of total phenolic and flavonoid content, antioxidant capacity (TEAC-ABTS and TEAC-DPPH) in both free and bound fractions, identification of major bound phenolic acids (caffeic, p-coumaric, and ferulic acids) via HPLC-DAD, and mineral composition analysis by ICP-MS, this three-year investigation (2023, 2024, 2025) seeks to optimize alfalfa production and processing strategies while ensuring compliance with European food safety regulations (Regulation 2023/915), ultimately establishing a scientific foundation for developing alfalfa-fortified functional foods that can enhance dietary antioxidant intake and contribute to improved public health.

### *4.2 Experimental section*

#### *4.2.1 Chemicals*

All the reagents were purchased from Merck (Milan, Italy): 3,4,5- trihydroxybenzoic acid (gallic acid), sodium carbonate ( $\text{Na}_2\text{CO}_3$ ), Folin-Ciocalteu reagent (FCR), (2R,3S)-2-(3,4-dihydroxyphenyl)-3,4-dihydro-2H-chromene-3,5,7-triol ((+)-catechin hydrate), sodium nitrite ( $\text{NaNO}_2$ ), aluminum trichloride hexahydrate ( $\text{AlCl}_3(\text{H}_2\text{O})_6$ ), sodium hydroxide ( $\text{NaOH}$ ), 2,2'-Azinobis(3-ethylbenzothiazoline-6-sulfonic acid) (ABTS), potassium persulphate ( $\text{K}_2\text{S}_2\text{O}_8$ ), (2R)-6hydroxy-2,5,7,8-tetramethyl-3,4-dihydrochromene-2-carboxylic acid

(Trolox), methanol (MeOH, analytical grade), 1,1-diphenyl-2-(2,4,6-trinitrophenyl)hydrazine (DPPH), acetone (CH<sub>3</sub>COCH<sub>3</sub>, analytical grade), chloridric acid (HCl, analytical grade), ethyl acetate (EtOAc, analytical grade), ethanol (EtOH, analytical grade), nitric acid (HNO<sub>3</sub> 70%, for trace analysis), hydrogen peroxide (H<sub>2</sub>O<sub>2</sub>, for trace analysis), multielement standard (16 Elements, 50 mg/L each: Sc, Y, La, Ce, Pr, Nd, Sm, Eu, Gd, Tb, Dy, Ho, Er, Tm, Yb and Lu in 2% nitric acid) for REEs, multielement standard (32 Elements, 100 mg/L each: Ag, Al, As, B, Ba, Bi, Ca, Cd, Co, Cr, Cu, Fe, K, Li, Mg, Mn, Mo, Na, Ni, Pb, Sb, Se, Si, Sr, Ti, Tl, V, Zn, Rb, Cs, Te and P in 5% nitric acid + Tr. hydrofluoric acid), internal standard (Ge, In) solutions were obtained by dilution of a stock solution of each metal (1000 ppb).

The ultra-pure water was obtained through Direct-Pure, RephiLe Bioscience system.

#### 4.2.2 Samples description and pre-treatment

The *Medicago sativa* L. samples were harvested near Parma (Italy) during three months (July, August, and September) across three consecutive years (2023, 2024, and 2025) from three different soil types: loamy (L), sandy (S), and clayey (C). The majority of samples consisted of whole plants that were freeze-dried (lyophilized). Additionally, a few samples were either air-dried in the dark or sun-dried, and some samples included only the apical parts with flowers. In **Table 1** is reported a detailed description of the samples.

**Table 1.** Description of *Medicago sativa* samples.

Samples	Harvest period	Soil	Plant part	Drying method
J1	July 2023	Loamy	Upper part	Freeze-drying
J2	July 2023	Loamy	Whole plant	Freeze-drying
J3	July 2023	Sandy	Upper part	Freeze-drying
J4	July 2023	Sandy	Whole plant	Freeze-drying
J5	July 2023	Sandy	Whole plant	Sun-drying
A1	August 2023	Loamy	Whole plant	Freeze-drying
A2	August 2023	Sandy	Whole plant	Sun-drying
A3	August 2023	Clayey	Whole plant	Freeze-drying
S1	September 2023	Loamy	Whole plant	Freeze-drying
S2	September 2023	Sandy	Whole plant	Freeze-drying
S3	September 2023	Clayey	Whole plant	Freeze-drying

A4	August 2024	Loamy	Whole plant	Freeze-drying
A5	August 2024	Clayey	Whole plant	Freeze-drying
S4	September 2024	Loamy	Whole plant	Freeze-drying
S5	September 2024	Sandy	Whole plant	Freeze-drying
S6	September 2024	Clayey	Whole plant	Freeze-drying
J6	July 2025	Loamy	Whole plant	Freeze-drying
J7	July 2025	Sandy	Whole plant	Freeze-drying
J8	July 2025	Clayey	Whole plant	Freeze-drying
J9	July 2025	Loamy	Whole plant	Air-drying
A6	August 2025	Loamy	Whole plant	Freeze-drying
A7	August 2025	Sandy	Whole plant	Freeze-drying
A8	August 2025	Clayey	Whole plant	Freeze-drying
S7	September 2025	Loamy	Whole plant	Freeze-drying
S8	September 2025	Sandy	Whole plant	Freeze-drying
S9	September 202	Clayey	Whole plant	Freeze-drying

The samples were freeze-dried (48 h, 300  $\mu$ bar,  $-45 \pm 2$  °C, 5Pascal), milled (Pulverisette 11, Fritsch) and sieved with granulometry  $< 250$   $\mu$ m. Soil samples were left air-drying under a flow hood in the same bag used for the collection (up to two weeks) and then grounded using an agate mortar. The resulting powder was sieved (125  $\mu$ m) and stored in pre-cleaned PE containers until further processes.

### *4.2.3 Extraction of antioxidants compounds*

Both free and bound phenolic fractions were extracted from the samples using a sequential extraction protocol. 200 mg of samples were analytically weighted and extracted with a solution of MeOH/H<sub>2</sub>O (80/20%, v/v). For the free fraction were performed three cycles of extraction assisted by ultrasonic bath (Bandelin, Sonorex) for 10 min at room temperature. After the extraction the samples were centrifuged for 5 min at 4000 rpm and the supernatants were collected. At the end of the three cycles the supernatants were combined for a total volume of 15 mL and the extracts were stored at  $-20 \pm 1$  °C until the further analyses. On the residues the extraction of the bound fraction through basic hydrolysis was performed. The solid residue was treated by adding 10 mL of NaOH 2 M and maintained in an ultrasonic bath for 30 min at 40 °C. Then 3.3 mL of HCl 6 M were added to the mixture (final pH 2). The two cycles of extraction with EtOAc ultrasound assisted (10 min at room temperature) were performed. After the extraction the samples were centrifuged for 5 min at 4000 rpm and the supernatants were collected. At the end of the two cycles the supernatants were combined

for a total volume of 10 mL. The extracts were dried under N<sub>2</sub> flux, stored at - 20 ± 1 °C, and resuspended in 5 mL of MeOH/H<sub>2</sub>O (80/20%, v/v) before the analysis.

#### 4.2.4 Spectrophotometric assays

Total polyphenols content (TPC) assay was carried out as previously reported,<sup>37</sup> with some modifications. Briefly, an appropriate volume of standard (gallic acid) or samples was added in cuvettes to 100 µL of FCR and 300 µL of Na<sub>2</sub>CO<sub>3</sub> 20% (w/v), the final volume of 2000 µL was reached with H<sub>2</sub>O. The calibration curve was constructed with gallic acid in the linear range of concentrations 0.5 – 10 mg/L ( $y = 0.0982 x$ ,  $R^2 = 0.9998$ ). The absorbances were recorded against water, at  $\lambda = 765$  nm after 30 min of incubation in the dark. The results were expressed as mg GAE/g DW (dry weight) of sample.

Total flavonoids content (TFC) assay was carried out as previously reported,<sup>38</sup> with some modifications. Briefly, an appropriate volume of standard (catechin) or samples was added in cuvettes to 60 µL of NaNO<sub>2</sub> 5% (w/v), 120 µL of AlCl<sub>3</sub> 10% (w/v) and 400 µL of NaOH 1M, the final volume of 2000 µL was reached with H<sub>2</sub>O.

The calibration curve was constructed with catechin in the linear range of concentrations 2.5 – 40 mg/L ( $y = 0.0352 x$ ,  $R^2 = 0.9997$ ). The absorbances were recorded against water, at  $\lambda = 510$  nm. The results were expressed as mg CE/g DW of sample. Trolox equivalent antioxidant capacity against ABTS/DPPH (TEAC-ABTS and TEAC-DPPH) assays were conducted as previously reported, with some modification.<sup>39-40</sup> The formation of the cationic radical (ABTS<sup>•+</sup>) was carried out through the addition of K<sub>2</sub>S<sub>2</sub>O<sub>8</sub> (2.45 mM) in a solution of ABTS (7mM) in water and let react overnight in the fridge. The ABTS<sup>•+</sup> and DPPH<sup>•</sup> solutions were dilute, EtOH and MeOH respectively, before use. In cuvettes were added 1000 µL of ABTS<sup>•+</sup>/DPPH<sup>•</sup> an appropriate volume of standard (Trolox) or samples, and the final volume of 1100 µL was reached with EtOH/MeOH. The calibration curves were constructed with Trolox in the linear range of concentrations 5 – 20 µM ( $y = 3.954 x$ ,  $R^2 = 0.9986$  for ABTS<sup>•+</sup> and  $y = 4.1584 x$ ,  $R^2 = 0.9992$  for DPPH<sup>•</sup>). The absorbances were recorded against EtOH or MeOH, at  $\lambda = 734$  nm or  $\lambda = 512$  nm, for ABTS<sup>•+</sup> and DPPH<sup>•</sup> respectively, after 30 min of incubation in the dark. The percentage of the decay in absorbance at the different wavelength (Abs %) was determined through the Equation 1:

$$Abs \% = \left[ 1 - \frac{Abs_{Std}}{Abs_{Spl}} \right] \times 10 \quad (\text{Eq. 1})$$

where the  $Abs_{Std/Spl}$  was the absorbance of standard or sample and the  $Abs_{Blk}$  was the absorbance of the blank (1000  $\mu\text{L}$  ABTS<sup>•+</sup>/ DPPH<sup>•</sup> + 100  $\mu\text{L}$  EtOH/MeOH). The results were expressed as  $\mu\text{mol TE/g DW}$  of sample.

#### 4.2.5 HPLC-DAD Metabolites Analysis

Samples were analyzed using a Dionex UltiMate 3000 HPLC-DAD equipped with a Kinetex 2.6  $\mu\text{m}$  C18 100Å Phenomenex (150  $\times$  2.1 mm). DAD operated in 3D field mode (min. wavelength: 190 nm, max. wavelength: 500 nm, bunch width: 1 nm) and quantification of the metabolites was done by integrating the peak at a wavelength of 275 nm. ACN/H<sub>2</sub>O acidified with formic acid (0.1% v/v) gradient run was used to separate the compounds of interest in the extracts as reported in **Table 2**.

**Table 2.** Gradient run used in the separation of metabolites via HPLC-DAD. The asterisk (\*) indicates a linear gradient.

Time (min)	% CAN
0.0	5.0
2.0	5.0
14.0	25.0 *
15.0	90.0 *
20.5	90.0
21.0	5.0 *
25.0	5.0

The separation was performed at a flow rate of 0.4 mL/min with the column temperature maintained at 30 °C. Example of chromatographic separation of bonded fraction is reported in **Figure 1**. Quantification of phenolic acids was performed using external calibration curves prepared with reference standards in the range of 2-30 ppm. The limits of detection (LOD) and quantification (LOQ) were calculated according to the signal-to-noise method ( $3.3\sigma/S$  and  $10\sigma/S$ , respectively), where  $\sigma$  represents the standard deviation of blank measurements and  $S$  the slope of the calibration curve. The calculated values were 0.10 and 0.31 ppm for caffeic acid, 0.07 and 0.23 ppm for p-coumaric acid, and 0.06 and 0.19 ppm for ferulic acid. All calibration curves showed excellent linearity ( $R^2 > 0.99$ ).

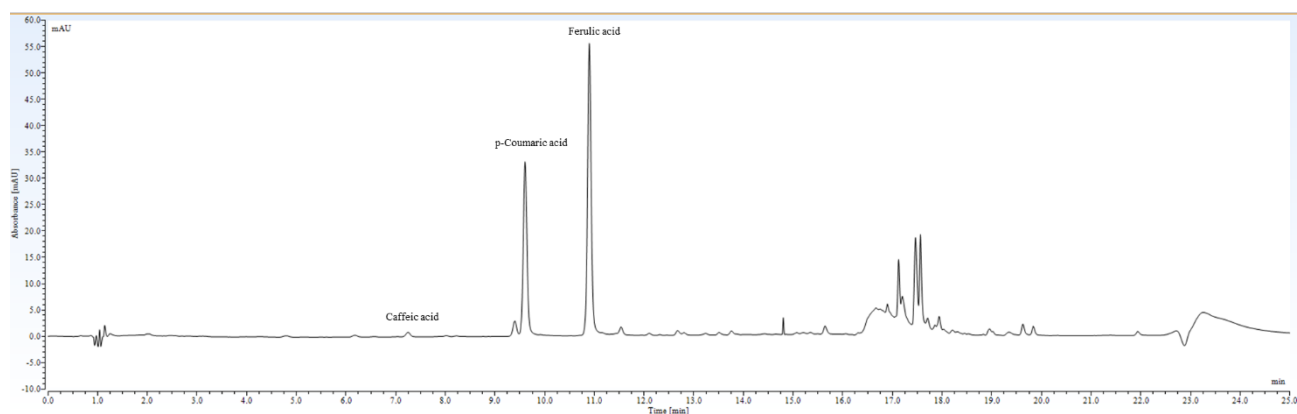


**Figure 1.** Example of chromatographic separation of phytochemicals found in bound phenolic fractions.

#### 4.2.6 Determination of inorganic compounds through ICP-MS

For the determination of the inorganic compounds in samples of *Medicago sativa* and in the soils was used the Inductively Coupled Plasma-Mass Spectroscopy (ICP-MS).<sup>42</sup>

The mineralisation of the samples was performed through a microwave digester (Microwave Labstation Ethos Easy, Milestone), the alfalfa and soil samples were analytically weighted (200 mg for alfalfa and 100 mg for soil), transfer in a Teflon tubes and 4 mL of HNO<sub>3</sub> 70% and 1 mL of H<sub>2</sub>O<sub>2</sub> (both for trace analysis) were added. The mineralisation program is summarised in **Table 3**.

**Table 3.** Program of the microwave digester for the mineralisation of the samples.

<b>Time (min)</b>	<b>Power (W)</b>	<b>Temperature (°C)</b>
10	1800	160
15	1800	210
10	1800	210

The tubes were let dried and the mineralised samples were diluted in 50 mL volumetric flask with diluted HNO<sub>3</sub> and stored at room temperature until the further analysis. Samples were analysed using an Agilent 8900 ICP-MS QQQ (Agilent Technologies, Santa Clara, CA, USA) equipped with Ni-Cu interface cones and a quartz shielded torch with a 2.5mm injector. Samples were introduced using an Agilent SPS 4 Autosampler connected to a MicroMist glass concentric nebulizer, a quartz Scott spray chamber cooled by a Peltier thermoelectric module (2°C) to reduce water vapours in each sample. Two Internal standards were used, the first one a solution of 200 ppb of Indium (In), to monitor the nebulizer and spray chamber efficiency and was introduced online with an ISTD G3280-60590 kit from Agilent. The second one (Ge) was used for the quantification of the elemental content in the samples and was introduced directly in the sample at a concentration of 20 ppb. Each element was analysed with 3 replicates with 10 sweeps/replicates.

## 4.3 Results

### 4.3.1 Inorganic composition of *Medicago sativa*

Tables 4 and 5 report minerals content in alfalfa and soils, respectively.

**Table 4.** Mineral content in *Medicago sativa* of Cr, Co, Ni, As, Hg, Na, Mn, Fe, Cu, Sr ( $\mu\text{g/g DW}$ ), Mg and K ( $\text{mg/g DW}$ ).

Sample	Cr	Co	Ni	As	Hg	Na	Mn	Fe	Cu	Sr	Mg	K
J1	0.13 $\pm$ 0.01	2.5 $\pm$ 1.3	28.4 $\pm$ 0.8	0.44 $\pm$ 0.16	0.026 $\pm$ 0.004	134 $\pm$ 4	4.3 $\pm$ 1.1	0.44 $\pm$ 0.01	0.43 $\pm$ 0.18	2.24 $\pm$ 0.08	2.48 $\pm$ 0.07	32.8 $\pm$ 0.9
J2	0.20 $\pm$ 0.02	1.2 $\pm$ 0.7	30.2 $\pm$ 0.9	0.63 $\pm$ 0.23	0.048 $\pm$ 0.006	158 $\pm$ 5	5.2 $\pm$ 1.3	0.48 $\pm$ 0.01	0.56 $\pm$ 0.23	1.83 $\pm$ 0.07	2.52 $\pm$ 0.07	32.4 $\pm$ 0.9
J3	0.16 $\pm$ 0.01	1.5 $\pm$ 0.8	23.9 $\pm$ 0.7	0.77 $\pm$ 0.29	0.031 $\pm$ 0.004	256 $\pm$ 8	4.9 $\pm$ 1.3	0.41 $\pm$ 0.01	0.45 $\pm$ 0.19	2.48 $\pm$ 0.09	3.69 $\pm$ 0.10	23.7 $\pm$ 0.6
J4	0.21 $\pm$ 0.02	0.9 $\pm$ 0.5	25.3 $\pm$ 0.8	0.65 $\pm$ 0.24	0.109 $\pm$ 0.014	254 $\pm$ 8	1.6 $\pm$ 0.4	0.53 $\pm$ 0.01	0.87 $\pm$ 0.36	2.58 $\pm$ 0.09	3.88 $\pm$ 0.11	22.7 $\pm$ 0.6
J5	0.64 $\pm$ 0.06	0.9 $\pm$ 0.5	28.7 $\pm$ 0.9	0.43 $\pm$ 0.26	0.146 $\pm$ 0.019	134 $\pm$ 4	2.8 $\pm$ 0.7	1.46 $\pm$ 0.03	0.31 $\pm$ 0.13	3.33 $\pm$ 0.12	3.22 $\pm$ 0.09	29.0 $\pm$ 0.8
A1	0.45 $\pm$ 0.04	1.1 $\pm$ 0.6	32.5 $\pm$ 1.0	0.42 $\pm$ 0.16	0.081 $\pm$ 0.011	107 $\pm$ 3	3.0 $\pm$ 0.8	1.00 $\pm$ 0.02	0.41 $\pm$ 0.17	3.24 $\pm$ 0.12	2.64 $\pm$ 0.07	27.8 $\pm$ 0.7
A2	0.45 $\pm$ 0.04	1.2 $\pm$ 0.6	20.7 $\pm$ 0.6	0.31 $\pm$ 0.12	0.113 $\pm$ 0.015	165 $\pm$ 5	2.4 $\pm$ 0.6	1.17 $\pm$ 0.03	0.29 $\pm$ 0.12	3.30 $\pm$ 0.12	3.23 $\pm$ 0.09	18.7 $\pm$ 0.5
A3	0.12 $\pm$ 0.01	2.4 $\pm$ 1.3	15.8 $\pm$ 0.5	0.53 $\pm$ 0.20	0.036 $\pm$ 0.005	231 $\pm$ 7	5.2 $\pm$ 1.4	0.44 $\pm$ 0.01	0.57 $\pm$ 0.23	1.35 $\pm$ 0.05	3.23 $\pm$ 0.09	22.7 $\pm$ 0.6
S1	0.78 $\pm$ 0.07	0.4 $\pm$ 0.2	28.4 $\pm$ 0.8	0.50 $\pm$ 0.19	0.174 $\pm$ 0.023	170 $\pm$ 5	2.3 $\pm$ 0.6	1.10 $\pm$ 0.03	0.32 $\pm$ 0.13	2.14 $\pm$ 0.08	3.25 $\pm$ 0.09	20.9 $\pm$ 0.6
S2	1.61 $\pm$ 0.14	0.8 $\pm$ 0.4	48.8 $\pm$ 1.4	0.73 $\pm$ 0.27	0.383 $\pm$ 0.051	146 $\pm$ 5	1.2 $\pm$ 0.3	4.66 $\pm$ 0.11	0.29 $\pm$ 0.12	5.38 $\pm$ 0.19	2.89 $\pm$ 0.08	21.3 $\pm$ 0.6
S3	0.62 $\pm$ 0.05	0.8 $\pm$ 0.4	34.2 $\pm$ 1.0	0.44 $\pm$ 0.16	0.101 $\pm$ 0.013	95 $\pm$ 3	2.4 $\pm$ 0.6	1.14 $\pm$ 0.03	0.52 $\pm$ 0.21	2.99 $\pm$ 0.11	1.71 $\pm$ 0.05	17.8 $\pm$ 0.5

**Table 5.** Mineral content in soil sample of Cr, Co, Ni, As, Hg, Na, Mn, Fe, Cu, Sr ( $\mu\text{g/g DW}$ ), Mg, K ( $\text{mg/g DW}$ ).

Sample	Cr	Co	Ni	As	Hg	Na	Mn	Fe	Cu	Sr	Mg	K
L	8.32 $\pm$ 0.19	1.29 $\pm$ 0.28	83 $\pm$ 1	1.48 $\pm$ 0.48	1.56 $\pm$ 0.08	43 $\pm$ 2	1.4 $\pm$ 0.6	8.98 $\pm$ 0.05	0.93 $\pm$ 0.15	7.3 $\pm$ 0.1	1.37 $\pm$ 0.02	1.20 $\pm$ 0.03
S	51 $\pm$ 2	0.92 $\pm$ 0.51	728 $\pm$ 15	1.40 $\pm$ 0.95	17.0 $\pm$ 0.6	303 $\pm$ 48	1.3 $\pm$ 0.2	155 $\pm$ 4	0.88 $\pm$ 0.41	127 $\pm$ 3	19.9 $\pm$ 0.3	5.19 $\pm$ 0.63
C	65 $\pm$ 3	1.00 $\pm$ 0.41	1014 $\pm$ 35	1.18 $\pm$ 0.30	12.3 $\pm$ 0.5	400 $\pm$ 35	2.0 $\pm$ 0.7	98 $\pm$ 4	1.18 $\pm$ 0.79	92 $\pm$ 3	17.8 $\pm$ 0.7	10.4 $\pm$ 0.6

Through their diet, organisms daily assimilate the nutrients necessary for proper functioning. Food may also contain a certain amount of heavy metals, of which excessive intake should be avoided. Heavy metal intoxication can lead to the malfunctioning of the central nervous system and damage to blood components and organs.<sup>43</sup> On 25 April 2023, the European Commission issued Regulation 2023/915 concerning maximum levels of certain contaminants in foodstuffs, including heavy metals. The permissible maximum concentrations of certain heavy metals in final food products are as follows: arsenic 0.30–0.15 mg/kg for various types of cereals; mercury 0.1 mg/kg for dietary supplements. Different thresholds have been established for infant foods and mercury in fish species. In the mineralised *Medicago sativa* L. samples analysed in this study, the total concentrations of these two metalloids were determined (Table 4), yielding values in compliance with European regulations. This supports their potential use as flours (or extracts) for fortifying baked goods, with a maximum addition of 5% to cereal flour. All the values obtained for the flours are well below the thresholds set by the European Commission, and they would be even lower if aqueous/hydroalcoholic extracts were analysed. Consequently, the analysed samples can be considered safe for human health.

Among the metals analysed in the *Medicago sativa* L. samples are some that are essential for humans: Na, Mg, K, Fe, Mn, Cr, Co, and Cu.<sup>44-45</sup> The presence of metals in the samples is influenced by various factors, such as soil type, conductivity, cation exchange capacity, pH, and seasonal variations.<sup>46-47</sup> Table 4 shows the metal concentrations across all samples. The concentrations of all metals were found to be well below the regulatory limits established by European Commission Regulation 2023/915. Considering the consistency of the cultivation conditions across the years, the samples can be considered safe for human consumption.

### 4.3.2 Spectrophotometric Assays (2023)

**Tables 6-9** report the spectrophotometric assay results for the 2023 alfalfa samples, including total phenolic content (TPC), total flavonoid content (TFC), and antioxidant capacity determined by TEAC-ABTS and TEAC-DPPH methods.

**Table 6.** Total phenolic content (TPC, mg GAE/g DW) obtained for alfalfa samples in the free, bound, and total fractions (free + bound), reported as mean  $\pm$  standard deviation (n = 3).

TPC (mg GAE/g DW)			
Sample	Free fraction	Bound fraction	Total fraction
<b>J1</b>	15.29 $\pm$ 0.29	3.06 $\pm$ 0.03	18.43 $\pm$ 0.29
<b>J2</b>	15.57 $\pm$ 0.43	3.07 $\pm$ 0.06	18.71 $\pm$ 0.43
<b>J3</b>	11.07 $\pm$ 0.20	3.43 $\pm$ 0.06	14.43 $\pm$ 0.29
<b>J4</b>	10.79 $\pm$ 0.06	3.84 $\pm$ 0.09	14.57 $\pm$ 0.14
<b>J5</b>	7.03 $\pm$ 0.14	3.36 $\pm$ 0.06	10.39 $\pm$ 0.20
<b>A1</b>	11.99 $\pm$ 0.70	3.66 $\pm$ 0.01	15.57 $\pm$ 0.71
<b>A2</b>	7.11 $\pm$ 0.31	3.43 $\pm$ 0.01	10.53 $\pm$ 0.33
<b>A3</b>	10.17 $\pm$ 0.19	3.43 $\pm$ 0.04	13.57 $\pm$ 0.23
<b>S1</b>	8.16 $\pm$ 0.30	4.06 $\pm$ 0.11	12.21 $\pm$ 0.41
<b>S2</b>	8.49 $\pm$ 0.13	4.41 $\pm$ 0.04	12.90 $\pm$ 0.19
<b>S3</b>	8.87 $\pm$ 0.21	4.24 $\pm$ 0.01	13.11 $\pm$ 0.24

**Table 7.** Total flavonoid content (TFC, mg CE/g DW) obtained for alfalfa samples in the free, bound, and total fractions (free + bound), reported as mean  $\pm$  standard deviation (n = 3).

<b>TFC (mg CE/g DW)</b>			
<b>Sample</b>	<b>Bound fraction</b>	<b>Free fraction</b>	<b>Total fraction</b>
<b>J1</b>	3.54 $\pm$ 0.14	1.79 $\pm$ 0.07	5.31 $\pm$ 0.23
<b>J2</b>	3.53 $\pm$ 0.16	1.69 $\pm$ 0.03	5.21 $\pm$ 0.19
<b>J3</b>	4.00 $\pm$ 0.17	2.03 $\pm$ 0.01	6.03 $\pm$ 0.19
<b>J4</b>	4.57 $\pm$ 0.09	1.47 $\pm$ 0.01	6.04 $\pm$ 0.10
<b>J5</b>	3.70 $\pm$ 0.07	1.09 $\pm$ 0.00	4.79 $\pm$ 0.07
<b>A1</b>	4.74 $\pm$ 0.10	2.33 $\pm$ 0.06	7.07 $\pm$ 0.16
<b>A2</b>	2.57 $\pm$ 0.10	1.09 $\pm$ 0.06	3.66 $\pm$ 0.17
<b>A3</b>	3.96 $\pm$ 0.19	1.27 $\pm$ 0.03	5.23 $\pm$ 0.20
<b>S1</b>	3.34 $\pm$ 0.03	4.06 $\pm$ 0.00	4.94 $\pm$ 0.03
<b>S2</b>	3.47 $\pm$ 0.20	4.41 $\pm$ 0.13	5.50 $\pm$ 0.33
<b>S3</b>	3.11 $\pm$ 0.09	4.24 $\pm$ 0.04	4.63 $\pm$ 0.13

**Table 8.** Results for the determination of antioxidant activity of hydrophilic extracts by TEAC-ABTS assay ( $\mu$ mol TE/g DW) in the free, bound, and total fractions (free + bound), reported as mean  $\pm$  standard deviation (n = 3).

<b>TEAC-ABTS (<math>\mu</math>mol TE/g DW)</b>			
<b>Sample</b>	<b>Bound fraction</b>	<b>Free fraction</b>	<b>Total fraction</b>
<b>J1</b>	74.7 $\pm$ 6.1	22.0 $\pm$ 0.1	96.7 $\pm$ 6.3
<b>J2</b>	69.7 $\pm$ 2.0	19.9 $\pm$ 0.3	89.6 $\pm$ 2.3
<b>J3</b>	37.1 $\pm$ 1.6	20.7 $\pm$ 0.1	57.9 $\pm$ 1.6
<b>J4</b>	38.3 $\pm$ 0.6	23.0 $\pm$ 0.3	61.3 $\pm$ 1.0
<b>J5</b>	29.7 $\pm$ 3.0	23.1 $\pm$ 0.3	52.9 $\pm$ 3.1
<b>A1</b>	39.0 $\pm$ 0.6	22.6 $\pm$ 1.0	61.6 $\pm$ 1.6
<b>A2</b>	27.4 $\pm$ 0.4	20.9 $\pm$ 0.3	48.1 $\pm$ 0.9
<b>A3</b>	32.6 $\pm$ 4.0	23.1 $\pm$ 0.3	55.6 $\pm$ 4.3
<b>S1</b>	35.6 $\pm$ 0.1	22.3 $\pm$ 0.1	57.9 $\pm$ 0.3
<b>S2</b>	33.0 $\pm$ 1.4	26.3 $\pm$ 0.3	59.3 $\pm$ 1.7
<b>S3</b>	41.1 $\pm$ 2.4	25.0 $\pm$ 0.4	66.1 $\pm$ 2.9

**Table 9.** Results for the determination of antioxidant activity of hydrophilic extracts by TEAC-DPPH assay ( $\mu\text{mol TE/g DW}$ ) in the free, bound, and total fractions (free + bound), reported as mean  $\pm$  standard deviation ( $n = 3$ ).

TEAC-DPPH ( $\mu\text{mol TE/g DW}$ )			
Sample	Free fraction	Bound fraction	Total fraction
J1	20.1 $\pm$ 3.0	6.4 $\pm$ 0.2	26.6 $\pm$ 3.3
J2	23.1 $\pm$ 0.6	6.4 $\pm$ 0.1	29.6 $\pm$ 0.7
J3	19.0 $\pm$ 2.4	7.4 $\pm$ 0.0	26.4 $\pm$ 2.4
J4	15.3 $\pm$ 0.3	8.1 $\pm$ 0.2	23.4 $\pm$ 0.4
J5	14.9 $\pm$ 1.3	7.6 $\pm$ 0.3	22.4 $\pm$ 1.6
A1	18.4 $\pm$ 1.0	7.9 $\pm$ 0.2	26.3 $\pm$ 1.1
A2	14.3 $\pm$ 0.7	7.6 $\pm$ 0.4	21.7 $\pm$ 1.1
A3	22.7 $\pm$ 1.1	8.0 $\pm$ 0.1	30.7 $\pm$ 1.3
S1	17.0 $\pm$ 0.3	8.7 $\pm$ 0.1	25.7 $\pm$ 0.4
S2	16.3 $\pm$ 0.4	9.0 $\pm$ 0.1	25.3 $\pm$ 0.6
S3	19.1 $\pm$ 0.1	9.1 $\pm$ 0.0	28.3 $\pm$ 0.1

T-test analysis of the 2023 alfalfa harvest revealed that the drying method exerts a profound influence on phytochemical preservation, whereas plant part selection has no meaningful effect. Sun-drying caused substantial losses of bioactive compounds compared to freeze-drying, with significant reductions in total phenolic content ( $p < 0.05$ ), total flavonoids ( $p < 0.05$ ), and antioxidant capacity ( $p < 0.05$ ). These reductions result from enzymatic oxidation mediated by polyphenol oxidase, thermal degradation from solar heating, and photo-oxidative damage induced by prolonged UV exposure.<sup>29</sup> In contrast, freeze-drying effectively preserves phytochemicals by halting enzymatic activity through rapid freezing, removing water via sublimation under sub-zero conditions, and excluding oxygen throughout the process, thereby maintaining nearly complete phytochemical integrity.<sup>30</sup> Plant part selection (upper portion vs. whole plant) showed no significant differences, with total phenolic and flavonoid contents varying by less than 2% ( $p > 0.05$ ) and only sporadic, inconsistent effects observed in antioxidant assays.

Further ANOVA analysis from 2023 confirmed that harvest month (July, August, September) and soil type (loamy, sandy, clayey) did not significantly affect total phenolics, or antioxidant capacity (all  $p > 0.05$ ).

The results of spectrophotometric assays for the determination of antioxidant profile in the samples of *Medicago sativa* are reported in **Figure 2**.

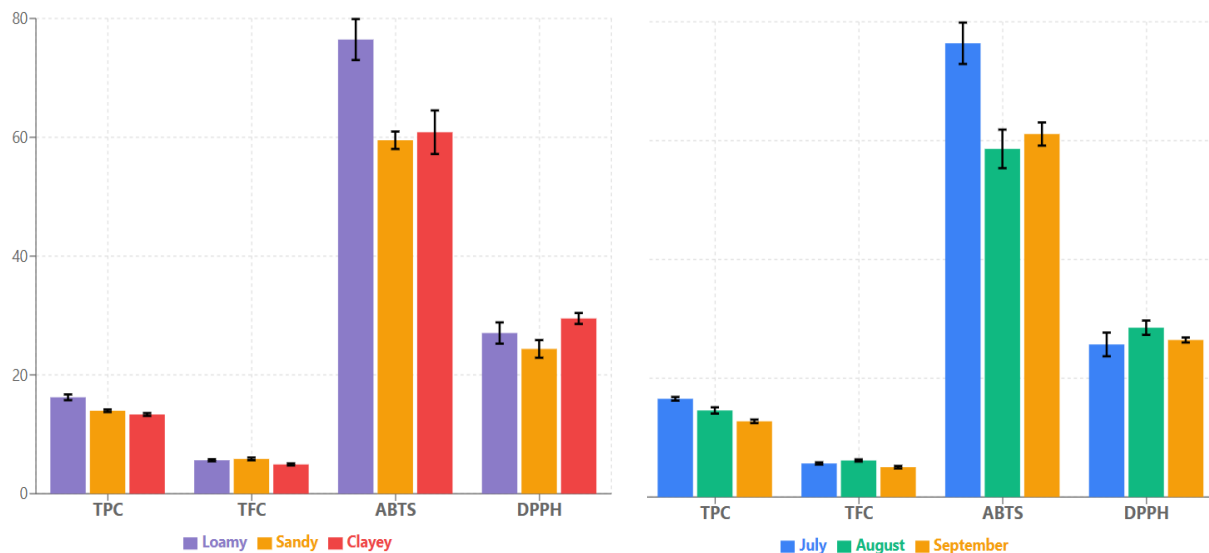


**Figure 2.** Bar graph displaying TPC (mg GAE/g DW), TFC (mg CE/g DW), TEAC-ABTS ( $\mu\text{mol TE/g DW}$ ), and TEAC-DPPH ( $\mu\text{mol TE/g DW}$ ) values of alfalfa samples grouped by soil type and harvest month.

### 4.3.3 Spectrophotometric Assays (2024)

**Tables 10-13** report the spectrophotometric assay results for the 2024 alfalfa samples, including total phenolic content (TPC), total flavonoid content (TFC), and antioxidant capacity determined by TEAC-ABTS and TEAC-DPPH methods.

**Table 10.** Total phenolic content (TPC, mg GAE/g DW) obtained for alfalfa samples in the free, bound, and total fractions (free + bound), reported as mean  $\pm$  standard deviation ( $n = 3$ ).

TPC (mg GAE/g DW)			
Sample	Free fraction	Bound fraction	Total fraction
A4	8.15 $\pm$ 0.04	4.38 $\pm$ 0.03	12.53 $\pm$ 0.07
A5	8.95 $\pm$ 0.31	2.94 $\pm$ 0.15	11.89 $\pm$ 0.46
S4	8.85 $\pm$ 0.13	3.15 $\pm$ 0.07	12.00 $\pm$ 0.20
S5	7.65 $\pm$ 1.21	2.38 $\pm$ 0.03	10.03 $\pm$ 1.24
S6	9.01 $\pm$ 0.07	3.80 $\pm$ 0.12	12.81 $\pm$ 0.19

**Table 11.** Total flavonoid content (TFC, mg CE/g DW) obtained for alfalfa samples in the free, bound, and total fractions (free + bound), reported as mean  $\pm$  standard deviation (n = 3).

<b>TFC (mg CE/g DW)</b>			
<b>Sample</b>	<b>Free fraction</b>	<b>Bound fraction</b>	<b>Total fraction</b>
<b>A4</b>	4.92 $\pm$ 0.12	2.29 $\pm$ 0.39	7.21 $\pm$ 0.51
<b>A5</b>	3.65 $\pm$ 0.12	2.01 $\pm$ 0.42	5.66 $\pm$ 0.54
<b>S4</b>	4.87 $\pm$ 0.05	2.15 $\pm$ 0.04	7.02 $\pm$ 0.09
<b>S5</b>	2.10 $\pm$ 0.01	0.65 $\pm$ 0.17	2.75 $\pm$ 0.18
<b>S6</b>	4.38 $\pm$ 0.09	2.62 $\pm$ 0.01	7.00 $\pm$ 0.10

**Table 12.** Results for the determination of antioxidant activity of hydrophilic extracts by TEAC-ABTS assay ( $\mu\text{mol TE/g DW}$ ) in the free, bound, and total fractions (free + bound), reported as mean  $\pm$  standard deviation (n = 3).

<b>TEAC-ABTS (<math>\mu\text{mol TE/g DW}</math>)</b>			
<b>Sample</b>	<b>Free fraction</b>	<b>Bound fraction</b>	<b>Total fraction</b>
<b>A4</b>	47.91 $\pm$ 1.28	10.65 $\pm$ 4.82	58.56 $\pm$ 6.10
<b>A5</b>	56.65 $\pm$ 0.98	11.47 $\pm$ 0.19	68.12 $\pm$ 1.17
<b>S4</b>	52.05 $\pm$ 1.43	12.39 $\pm$ 0.38	64.44 $\pm$ 1.81
<b>S5</b>	57.85 $\pm$ 5.26	14.66 $\pm$ 1.88	72.50 $\pm$ 7.14
<b>S6</b>	58.13 $\pm$ 3.54	12.60 $\pm$ 0.59	70.73 $\pm$ 4.13

**Table 13.** Results for the determination of antioxidant activity of hydrophilic extracts by TEAC-DPPH assay ( $\mu\text{mol TE/g DW}$ ) in the free, bound, and total fractions (free + bound), reported as mean  $\pm$  standard deviation (n = 3).

<b>TEAC-DPPH (<math>\mu\text{mol TE/g DW}</math>)</b>			
<b>Campione</b>	<b>Frazione Libera</b>	<b>Frazione Legata</b>	<b>Totale</b>
<b>A4</b>	11.95 $\pm$ 0.02	3.98 $\pm$ 0.21	15.93 $\pm$ 0.23
<b>A5</b>	12.64 $\pm$ 0.07	3.89 $\pm$ 0.01	16.53 $\pm$ 0.08
<b>S4</b>	11.67 $\pm$ 0.01	3.95 $\pm$ 0.11	15.62 $\pm$ 0.12
<b>S5</b>	8.34 $\pm$ 1.80	4.31 $\pm$ 0.08	12.65 $\pm$ 1.88
<b>S6</b>	11.93 $\pm$ 0.06	3.79 $\pm$ 0.49	15.72 $\pm$ 0.55

The 2024 analysis examined 5 alfalfa samples distributed across three soil types (Clayey, Loamy, Sandy) and two harvest months (August, September). Loamy soil showed the highest values for TFC

TPC and DPPH suggesting that this soil type could favor the accumulation of phenolic compounds and flavonoids.

The comparison between August and September revealed that August harvest produces higher values for all four analyzed parameters. This trend suggests that earlier harvest in August could increase both the content of bioactive secondary metabolites and the antioxidant activity of alfalfa.

It is necessary to emphasize that the 2024 analysis is limited by a reduced number of samples ( $n=5$ ), with insufficient replicates per soil type (1-2 per group). This limitation prevents the application of rigorous statistical tests such as ANOVA, which would require at least 3-5 replicates per group to ensure adequate statistical power. July data are completely absent, which precludes evaluation of the early harvest effect observed in other years of the dataset. Therefore, results should be interpreted as preliminary trends rather than definitive conclusions.

The results of spectrophotometric assays for the determination of antioxidant profile in the samples of *Medicago sativa* are reported in **Figure 3**.

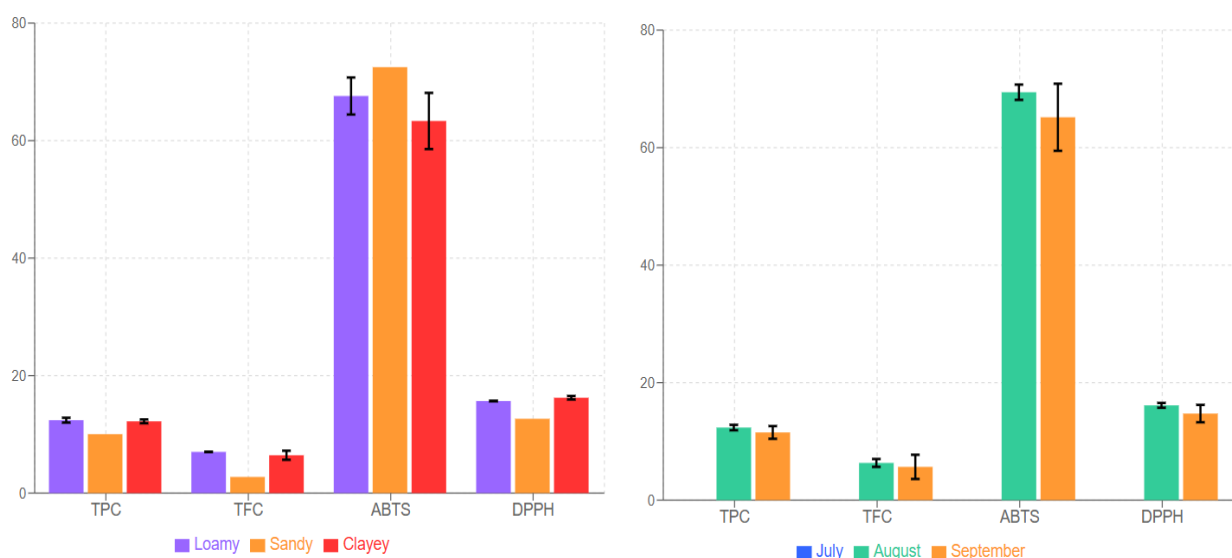


**Figure 3.** Bar graph displaying TPC (mg GAE/g DW), TFC (mg CE/g DW), TEA-ABTS ( $\mu\text{mol TE/g DW}$ ), and TEAC-DPPH ( $\mu\text{mol TE/g DW}$ ) values of alfalfa samples grouped by soil type and harvest month.

#### 4.3.4 Spectrophotometric Assays (2025)

**Tables 14-17** report the spectrophotometric assay results for the 2025 alfalfa samples, including total phenolic content (TPC), total flavonoid content (TFC), and antioxidant capacity determined by TEAC-ABTS and TEAC-DPPH methods.

**Table 14.** Total phenolic content (TPC, mg GAE/g DW) obtained for alfalfa samples in the free, bound, and total fractions (free + bound), reported as mean  $\pm$  standard deviation (n = 3).

<b>TPC (mg GAE/g DW)</b>			
<b>Sample</b>	<b>Free fraction</b>	<b>Bound fraction</b>	<b>Total fraction</b>
<b>J6</b>	10.71 $\pm$ 0.12	3.40 $\pm$ 0.06	14.11 $\pm$ 0.18
<b>J7</b>	13.35 $\pm$ 0.25	2.79 $\pm$ 0.07	16.14 $\pm$ 0.32
<b>J8</b>	10.55 $\pm$ 0.32	1.60 $\pm$ 0.11	12.15 $\pm$ 0.43
<b>J9</b>	10.38 $\pm$ 0.11	2.13 $\pm$ 0.13	12.51 $\pm$ 0.24
<b>A6</b>	10.25 $\pm$ 0.09	2.26 $\pm$ 0.10	12.51 $\pm$ 0.19
<b>A7</b>	11.42 $\pm$ 0.24	3.41 $\pm$ 0.43	14.83 $\pm$ 0.67
<b>A8</b>	8.81 $\pm$ 0.23	3.32 $\pm$ 0.05	12.13 $\pm$ 0.28
<b>S7</b>	11.50 $\pm$ 0.19	3.63 $\pm$ 0.08	15.13 $\pm$ 0.27
<b>S8</b>	8.82 $\pm$ 0.56	2.90 $\pm$ 0.11	11.72 $\pm$ 0.67
<b>S9</b>	8.62 $\pm$ 0.12	3.57 $\pm$ 0.05	12.19 $\pm$ 0.17

**Table 15.** Total flavonoid content (TFC, mg CE/g DW) obtained for alfalfa samples in the free, bound, and total fractions (free + bound), reported as mean  $\pm$  standard deviation (n = 3).

<b>TFC (mg CE/g DW)</b>			
<b>Sample</b>	<b>Free fraction</b>	<b>Bound fraction</b>	<b>Total fraction</b>
<b>J6</b>	4.86 $\pm$ 0.25	2.05 $\pm$ 0.06	6.91 $\pm$ 0.31
<b>J7</b>	7.11 $\pm$ 0.61	2.01 $\pm$ 0.02	9.12 $\pm$ 0.63
<b>J8</b>	3.49 $\pm$ 0.09	0.57 $\pm$ 0.10	4.06 $\pm$ 0.19
<b>J9</b>	4.45 $\pm$ 0.03	1.27 $\pm$ 0.23	5.72 $\pm$ 0.27
<b>A6</b>	4.88 $\pm$ 0.41	0.84 $\pm$ 0.03	5.72 $\pm$ 0.44
<b>A7</b>	5.48 $\pm$ 0.31	1.68 $\pm$ 0.59	7.16 $\pm$ 0.90
<b>A8</b>	4.67 $\pm$ 0.67	1.60 $\pm$ 0.06	6.27 $\pm$ 0.73
<b>S7</b>	5.38 $\pm$ 0.16	1.77 $\pm$ 0.25	7.15 $\pm$ 0.41
<b>S8</b>	3.71 $\pm$ 0.32	1.54 $\pm$ 0.15	5.25 $\pm$ 0.47
<b>S9</b>	4.44 $\pm$ 0.31	1.88 $\pm$ 0.13	6.32 $\pm$ 0.44

**Table 16.** Results for the determination of antioxidant activity of hydrophilic extracts by TEAC-ABTS assay ( $\mu\text{mol TE/g DW}$ ) in the free, bound, and total fractions (free + bound), reported as mean  $\pm$  standard deviation ( $n = 3$ ).

<b>TEAC-ABTS (<math>\mu\text{mol TE/g DW}</math>)</b>			
<b>Sample</b>	<b>Free fraction</b>	<b>Bound fraction</b>	<b>Total fraction</b>
<b>J6</b>	52.02 $\pm$ 3.89	13.36 $\pm$ 1.04	65.38 $\pm$ 4.93
<b>J7</b>	71.87 $\pm$ 4.70	12.78 $\pm$ 1.74	84.65 $\pm$ 6.44
<b>J8</b>	49.99 $\pm$ 2.31	7.11 $\pm$ 0.34	57.10 $\pm$ 2.65
<b>J9</b>	61.28 $\pm$ 12.57	9.13 $\pm$ 1.49	70.41 $\pm$ 14.05
<b>A6</b>	41.99 $\pm$ 3.08	10.41 $\pm$ 0.21	52.40 $\pm$ 3.29
<b>A7</b>	47.76 $\pm$ 3.80	12.41 $\pm$ 0.77	60.17 $\pm$ 4.57
<b>A8</b>	35.16 $\pm$ 2.67	12.49 $\pm$ 0.39	47.65 $\pm$ 3.06
<b>S7</b>	43.90 $\pm$ 1.93	13.51 $\pm$ 0.87	57.41 $\pm$ 2.80
<b>S8</b>	33.37 $\pm$ 1.57	10.79 $\pm$ 0.39	44.16 $\pm$ 1.96
<b>S9</b>	31.20 $\pm$ 1.82	12.34 $\pm$ 0.63	43.54 $\pm$ 2.45

**Table 17.** Results for the determination of antioxidant activity of hydrophilic extracts by TEAC-DPPH assay ( $\mu\text{mol TE/g DW}$ ) in the free, bound, and total fractions (free + bound), reported as mean  $\pm$  standard deviation ( $n = 3$ ).

<b>TEAC-DPPH (<math>\mu\text{mol TE/g DW}</math>)</b>			
<b>Sample</b>	<b>Free fraction</b>	<b>Bound fraction</b>	<b>Total fraction</b>
<b>J6</b>	18.75 $\pm$ 0.91	5.64 $\pm$ 0.18	24.39 $\pm$ 1.09
<b>J7</b>	28.88 $\pm$ 1.11	4.30 $\pm$ 0.60	33.18 $\pm$ 1.71
<b>J8</b>	14.48 $\pm$ 0.03	2.36 $\pm$ 0.12	16.84 $\pm$ 0.15
<b>J9</b>	10.33 $\pm$ 0.01	4.04 $\pm$ 0.07	14.37 $\pm$ 0.08
<b>A6</b>	13.07 $\pm$ 0.64	2.96 $\pm$ 0.04	16.03 $\pm$ 0.68
<b>A7</b>	15.21 $\pm$ 0.04	3.47 $\pm$ 0.11	18.68 $\pm$ 0.15
<b>A8</b>	8.27 $\pm$ 0.41	3.02 $\pm$ 0.11	11.29 $\pm$ 0.52
<b>S7</b>	15.05 $\pm$ 0.09	3.20 $\pm$ 0.28	18.25 $\pm$ 0.37
<b>S8</b>	8.95 $\pm$ 0.46	2.61 $\pm$ 0.09	11.56 $\pm$ 0.55
<b>S9</b>	7.83 $\pm$ 0.24	2.43 $\pm$ 0.23	10.26 $\pm$ 0.47

The 2025 analysis examined 9 alfalfa samples distributed across three soil types (Clayey, Loamy, Sandy) and three harvest months (July, August, September), with 3 replicates per soil type and per month. This balanced design allows for more robust statistical analysis compared to 2024.

To evaluate the impact of drying methodology on the preservation of bioactive compounds in alfalfa, independent samples t-tests were performed comparing sample J6 (freeze-dried) and sample J9 (air-dried), both harvested in July 2025 from loamy soil.

Statistical analysis revealed that freeze-drying significantly preserved higher levels of total phenolic content compared to air-dried ( $p < 0.05$ ). Similar trends were observed for total flavonoid content, where both free and bound fractions showed statistically significant differences favoring the freeze-dried sample.

Regarding antioxidant capacity, the ABTS assay showed no significant differences in total values between the two drying methods, while DPPH assay revealed dramatically higher antioxidant capacity in the freeze-dried sample across both free and bound fractions, with all differences being significant ( $p < 0.05$ ).

These findings clearly demonstrate that freeze-drying is superior to air-drying for preserving the phytochemical composition and antioxidant properties of alfalfa.

Sandy soil consistently showed the highest mean values across all parameters, oamy soil ranked second with intermediate values, while Clayey soil showed the lowest values for all measured parameters. However, ANOVA analysis revealed that these differences were not statistically significant ( $p > 0.05$  for all parameters), likely due to high within-group variability, particularly in Sandy soil samples. The lack of statistical significance despite observable trends suggests that larger sample sizes or reduced experimental variability would be needed to confirm soil type effects definitively.

A clear decreasing trend was observed from July to September for all parameters but ANOVA analysis revealed that these differences were not statistically significant ( $p > 0.05$  for all parameters). This finding supports the recommendation for early harvest to maximize antioxidant activity, particularly for DPPH radical scavenging capacity. The results of spectrophotometric assays for the determination of antioxidant profile in the samples of *Medicago sativa* are reported in **Figure 4**.

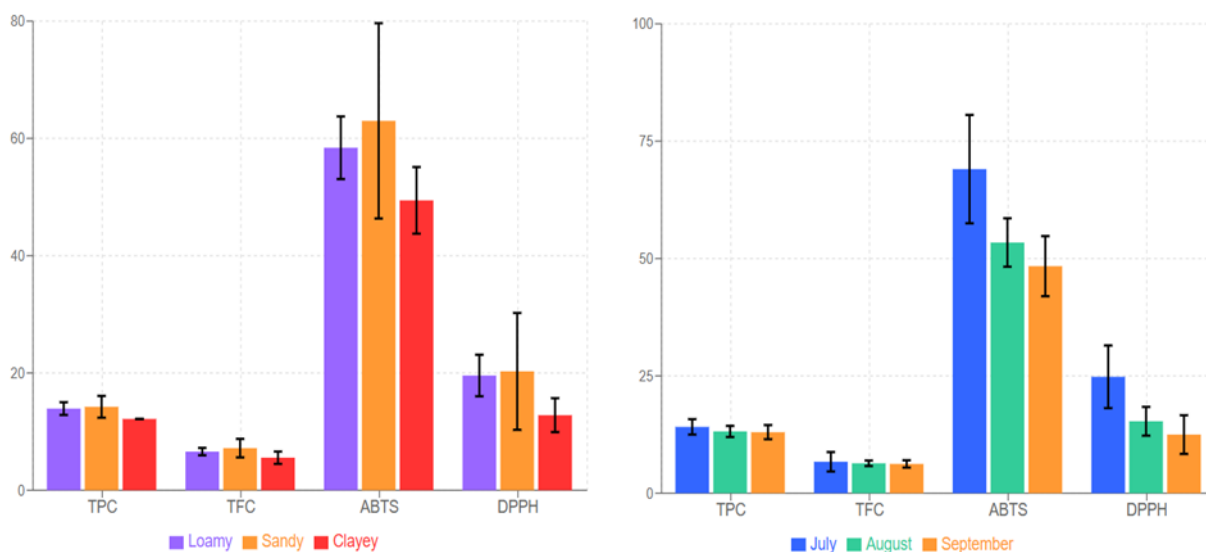


**Figure 4.** Bar graph displaying TPC (mg GAE/g DW), TFC (mg CE/g DW), TEA-ABTS ( $\mu\text{mol TE/g DW}$ ), and TEAC-DPPH ( $\mu\text{mol TE/g DW}$ ) values of alfalfa samples grouped by soil type and harvest month.

#### 4.3.5 Pooled Three-Year Analysis and Inter-Annual Comparison.

Given the limited number of biological replicates collected in each individual year, data from three consecutive growing seasons were pooled to create a more robust dataset that would provide greater statistical power for detecting treatment effects. For this analysis, only freeze-dried samples were considered ( $n=23$ ) to eliminate the confounding effect of drying method on bioactive compound retention. One-way ANOVA performed on the pooled dataset revealed that harvest period (July, August, September) had a significant effect on total phenolic content (TPC;  $p=0.008$ ) and TEAC-ABTS antioxidant capacity ( $p=0.042$ ), with July samples consistently showing the highest values for both parameters. Conversely, soil type (clayey, sandy, mixed) showed no significant effect on any of the measured bioactive compounds or antioxidant activities ( $p>0.05$  for all variables), suggesting that harvest timing is a more critical factor than edaphic conditions in determining the nutraceutical value of alfalfa. These findings indicate that optimizing harvest schedules, particularly targeting early summer collection, could be more important than soil selection for maximizing the functional properties of *Medicago sativa* L. as a source of bioactive compounds.

To assess temporal variations in bioactive compound content, one-way ANOVA was performed comparing freeze-dried alfalfa samples collected in 2023 ( $n=9$ ) with those from 2024-2025 ( $n=14$ ). Sun-dried and oven-dried samples were excluded from the analysis to ensure methodological consistency.

The analysis revealed significant inter-annual differences for two of the four assays. Total phenolic content (TPC) showed a statistically significant decrease from 2023 to 2024-2025 ( $p < 0.05$ ), indicating reduced phenolic accumulation in the later harvest period. Most notably, DPPH antioxidant capacity exhibited a highly significant decline ( $p < 0.05$ ), representing approximately a 37% reduction in radical scavenging activity.

In contrast, total flavonoid content (TFC) and ABTS antioxidant capacity showed no statistically significant differences between years ( $p > 0.05$ ), suggesting relative stability of these parameters across the two growing seasons.

These findings indicate that environmental factors varying between years such as temperature, precipitation patterns, or soil nutrient availability significantly influenced phenolic biosynthesis and antioxidant capacity in alfalfa, while flavonoid production remained more consistent. The marked reduction in DPPH activity suggests that climatic or agronomic conditions in 2024-2025 were less favorable for the accumulation of certain antioxidant compounds, highlighting the importance of year-to-year monitoring in assessing the nutritional quality of forage crops.

#### *4.3.6 Quantification of Phenolic Acids by HPLC-DAD (2024-2025)*

The HPLC-DAD quantification focused on phenolic acids present in the bound fraction of alfalfa extracts. This fraction was selected for analysis due to its simpler chromatographic profile, which facilitated accurate identification and quantification of target compounds (caffeic, p-coumaric, and ferulic acids). The free phenolic fraction, while potentially rich in bioactive compounds, presented highly complex chromatograms with multiple unresolved peaks requiring advanced analytical techniques such as untargeted LC-MS/MS for comprehensive characterization. Table 18 shows the concentrations of caffeic acid, p-coumaric acid, and ferulic acid quantified in the bound fraction of alfalfa samples collected during the 2024-2025 growing season.

**Table 18.** Results for the determination of Caffeic acid, p-Coumaric acid and Ferulic-acid by HPLC-DAD ( $\mu\text{g/g DW}$ ) in bound fraction, reported as mean  $\pm$  standard deviation ( $n = 3$ ).

<b>Sample</b>	<b>Caffeic acid</b>	<b>p-Coumaric acid</b>	<b>Ferulic-acid</b>
<b>A4</b>	329.90 $\pm$ 3.31	1163.97 $\pm$ 10.36	2438.41 $\pm$ 11.13
<b>A5</b>	312.84 $\pm$ 5.03	706.56 $\pm$ 22.07	1237.75 $\pm$ 62.77
<b>S4</b>	317.19 $\pm$ 1.99	790.55 $\pm$ 19.94	1485.26 $\pm$ 51.92
<b>S5</b>	314.08 $\pm$ 0.22	627.20 $\pm$ 35.76	1044.44 $\pm$ 63.45
<b>S6</b>	320.93 $\pm$ 3.79	932.06 $\pm$ 37.03	1958.11 $\pm$ 93.89
<b>J6</b>	326.94 $\pm$ 4.03	1048.84 $\pm$ 7.83	1858.98 $\pm$ 25.98
<b>J7</b>	371.99 $\pm$ 6.18	792.36 $\pm$ 48.88	1115.15 $\pm$ 77.67
<b>J8</b>	324.80 $\pm$ 1.56	755.93 $\pm$ 9.12	1133.29 $\pm$ 10.26
<b>J9</b>	314.05 $\pm$ 3.64	653.82 $\pm$ 3.11	962.08 $\pm$ 6.19
<b>A6</b>	338.06 $\pm$ 1.92	739.80 $\pm$ 24.56	1283.44 $\pm$ 65.02
<b>A7</b>	370.08 $\pm$ 3.23	996.28 $\pm$ 80.89	1718.23 $\pm$ 167.74
<b>A8</b>	336.12 $\pm$ 2.09	1059.98 $\pm$ 14.01	1837.08 $\pm$ 43.50
<b>S7</b>	411.66 $\pm$ 16.54	944.69 $\pm$ 36.07	1799.03 $\pm$ 88.40
<b>S8</b>	319.22 $\pm$ 5.43	773.93 $\pm$ 10.15	1495.75 $\pm$ 38.74
<b>S9</b>	354.77 $\pm$ 3.31	1109.94 $\pm$ 15.68	2005.70 $\pm$ 46.50

The analysis of alfalfa samples collected during the 2024-2025 harvest seasons revealed substantial levels of bound phenolic acids. The bound fraction contained primarily three hydroxycinnamic acids: caffeic acid, p-coumaric acid, and ferulic acid.

These values align remarkably well with published literature. The hierarchical order observed in our samples: ferulic acid > p-coumaric acid > caffeic acid reflects the typical distribution of hydroxycinnamic acids in cell wall-bound fractions of plant materials. This pattern is consistent with previous findings<sup>10</sup>, which reported that ferulic acid (2198.2  $\mu\text{g/g DM}$ ) and p-coumaric acid (983.7  $\mu\text{g/g DM}$ ) were the most abundant compounds in the bound phenolic extract of alfalfa leaves, with total bound phenolics (3638.0  $\mu\text{g/g DM}$ ) substantially exceeding soluble forms (912.3  $\mu\text{g/g DM}$ ). The predominance of ferulic acid consistently observed across our samples corroborates this established pattern in alfalfa phenolic composition. Ferulic acid's prominence is attributed to its structural role in cross-linking cell wall polysaccharides, particularly in grasses and legumes.<sup>11</sup>

Our one-way ANOVA analysis focused exclusively on the 2025 harvest season (n=13 samples, excluding J9 due to different drying method) to assess the impact of harvest period (July, August, September) and soil type (Loamy, Sandy, Clayey) on phenolic acid accumulation. The statistical analysis revealed no significant differences in bound phenolic acid content across the three harvest months. While a numerical trend toward increasing ferulic acid content from July to September was observed, this did not reach statistical significance. This relative stability across harvest periods aligns with findings suggesting that structural phenolics are less responsive to short-term environmental fluctuations compared to soluble forms.<sup>48</sup> Soil type also showed no significant influence on bound phenolic acid accumulation. Mean values across soil types varied minimally, with coefficients of variation below 10% for all compounds, suggesting that bound phenolic acid biosynthesis represents a constitutive rather than inducible component of alfalfa's secondary metabolism.

While agronomic factors showed minimal impact, the drying method emerged as a critical determinant of phenolic acid preservation. Sample J9, subjected to air-drying rather than freeze-drying, exhibited dramatic reductions compared to its freeze-dried counterpart J6 from the same harvest period and soil type. These losses likely result from enzymatic oxidation by polyphenol oxidase and peroxidase, which remain active during slow air-drying, as well as thermal degradation of phenolic compounds.<sup>49</sup> This finding has profound practical implications: freeze-drying or rapid dehydration methods are essential for preserving the nutraceutical value of alfalfa intended for human consumption or functional food applications.

The bound phenolic acids quantified in our study possess well-documented bioactivities. Ferulic acid exhibits strong antioxidant properties and has been implicated in cardiovascular protection, anti-inflammatory effects, and neuroprotection<sup>50</sup> and p-coumaric acid demonstrates anti-inflammatory and anticancer activities.<sup>18</sup> Bound phenolic acids represent a sustained-release reservoir, during digestion, colonic microbiota can liberate these compounds from their cell wall matrix through enzymatic hydrolysis, potentially providing prolonged antioxidant protection in the lower gastrointestinal tract.<sup>20</sup> This controlled release may offer advantages over free phenolics, which are rapidly absorbed and metabolized in the upper GI tract.<sup>20</sup>

**Figure 5** presents the concentrations of caffeic, p-coumaric, and ferulic acids across different soil types and harvest periods. While ANOVA revealed no significant differences ( $p > 0.05$ ), descriptive trends suggest potential agronomic influences worth investigating with larger sample sizes

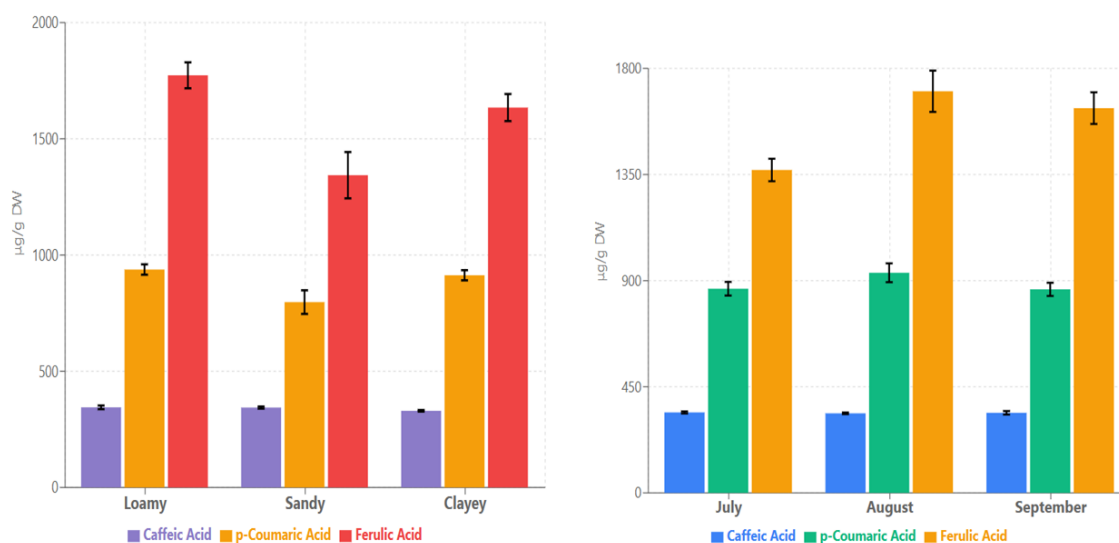


**Figure 5.** Concentrations of caffeic acid, p-coumaric acid, and ferulic acid in alfalfa samples collected from different soil types (left panel: Loamy, Sandy, Clayey) and harvest periods (right panel: July, August, September). Error bars indicate standard error of the mean.

#### 4.4 Conclusions

This study evaluated the phytochemical composition, antioxidant capacity, and safety profile of *Medicago sativa* L. across different harvest periods, soil types, and processing methods to assess its suitability as a functional food ingredient.

The most critical finding was the overwhelming impact of processing method on bioactive compound retention. Air-dried samples exhibited significant losses in bound phenolic acids and antioxidant capacity compared to freeze-dried counterparts from identical harvest conditions. These losses, attributable to enzymatic oxidation and thermal degradation, demonstrate that post-harvest processing supersedes all agronomic variables in determining final product quality. Freeze-drying is therefore essential for applications requiring maximum nutraceutical value.

Harvest period and soil type showed no significant effect when data from individual years were analyzed separately. However, it is important to acknowledge that the limited number of biological replicates within each year may have constrained the statistical power to detect moderate differences. To overcome this limitation, data from three consecutive growing seasons were pooled, considering only freeze-dried samples ( $n=23$ ) to eliminate the confounding effect of drying method. This three-year pooled analysis revealed that harvest period (July, August, September) had a statistically significant effect on total phenolic content ( $p=0.008$ ) and TEAC-ABTS antioxidant capacity ( $p=0.042$ ), with July samples consistently showing the highest values for both parameters. Conversely, soil type (clayey, sandy, mixed) remained non-significant even with the expanded dataset ( $p>0.05$  for all variables), suggesting that harvest timing is indeed a more critical factor than edaphic conditions in determining the nutraceutical value of alfalfa. While descriptive statistics from

individual years revealed some numerical trends across harvest periods and soil types that were not statistically significant due to high within-group variability and limited sample size, the pooled analysis confirms that at least for harvest period, these trends represent genuine agronomic effects rather than natural biological variation. Future studies employing a larger number of biological replicates within individual years would be valuable to confirm these findings and potentially detect more subtle soil effects. Whole plant versus apical portions showed equivalent bioactive content, offering harvesting flexibility.

HPLC-DAD quantification revealed ferulic acid and p-coumaric acid as the major bound hydroxycinnamic acids. These compounds possess documented antioxidant, anti-inflammatory, and cardioprotective properties, and their bound form enables sustained release through colonic microbial hydrolysis during digestion.

ICP-MS analysis confirmed compliance with European Commission Regulation 2023/915, with all heavy metals well below maximum permissible levels. Essential minerals (Mg, K, Fe, Mn, Cr, Co, Cu) were present at nutritionally significant concentrations, enhancing alfalfa's functional value.

These results establish that freeze-dried alfalfa constitutes a safe, bioactive-rich ingredient suitable for food fortification at up to 5% incorporation levels in cereal products. The negligible influence of cultivation variables on bound phenolic content, combined with regulatory-compliant heavy metal levels, supports its commercial viability. Future research should employ untargeted metabolomics to characterize the free phenolic fraction and conduct in vivo bioavailability studies of bound phenolic acids.

## References

1. Bouton, J. H. (2012). Breeding lucerne for persistence. *Crop and Pasture Science*, 63(2), 95-106.
2. Annicchiarico, P., Barrett, B., Brummer, E. C., Julier, B., & Marshall, A. H. (2015). Achievements and challenges in improving temperate perennial forage legumes. *Critical Reviews in Plant Sciences*, 34(1-3), 327-380.
3. Karimi, E., Oskoueian, E., Oskoueian, A., Omidvar, V., Hendra, R., & Nazeran, H. (2013). Insight into the functional and medicinal properties of *Medicago sativa* (Alfalfa) leaves extract. *Journal of Medicinal Plants Research*, 7(7), 290-297.
4. Bora, K. S., & Sharma, A. (2011). Phytochemical and pharmacological potential of *Medicago sativa*: a review. *Pharmaceutical Biology*, 49(2), 211-220.
5. Del Rio, D., Rodriguez-Mateos, A., Spencer, J. P., Tognolini, M., Borges, G., & Crozier, A. (2013). Dietary (poly)phenolics in human health: structures, bioavailability, and evidence of protective effects against chronic diseases. *Antioxidants & Redox Signaling*, 18(14), 1818-1892.

6. Acosta-Estrada, B. A., Gutiérrez-Urbe, J. A., & Serna-Saldívar, S. O. (2014). Bound phenolics in foods, a review. *Food Chemistry*, 152, 46-55.
7. Saura-Calixto, F. (2011). Dietary fiber as a carrier of dietary antioxidants: an essential physiological function. *Journal of Agricultural and Food Chemistry*, 59(1), 43-49.
8. Arranz, S., Saura-Calixto, F., Shaha, S., & Kroon, P. A. (2009). High contents of nonextractable polyphenols in fruits suggest that polyphenol contents of plant foods have been underestimated. *Journal of Agricultural and Food Chemistry*, 57(16), 7298-7303.
9. Sosulski, F., Krygier, K., & Hogge, L. (1982). Free, esterified, and insoluble-bound phenolic acids. 3. Composition of phenolic acids in cereal and potato flours. *Journal of Agricultural and Food Chemistry*, 30(2), 337-340.
10. Horvat, D., Šimić, G., Drezner, G., Lalić, A., Ledenčan, T., Tucak, M., ... & Viljevac Vuletić, M. (2022). Phenolic acid profiles and antioxidant activity of major cereal crops. *Antioxidants*, 11(9), 1-18.
11. Kumar, N., & Pruthi, V. (2014). Potential applications of ferulic acid from natural sources. *Biotechnology Reports*, 4, 86-93.
12. Hole, A. S., Rud, I., Grimmer, S., Sigl, S., Narvhus, J., & Sahlstrøm, S. (2012). Improved bioavailability of dietary phenolic acids in whole grain barley and oat groat following fermentation with probiotic *Lactobacillus acidophilus*, *Lactobacillus johnsonii*, and *Lactobacillus reuteri*. *Journal of Agricultural and Food Chemistry*, 60(25), 6369-6375.
13. Rice-Evans, C., Miller, N., & Paganga, G. (1997). Antioxidant properties of phenolic compounds. *Trends in Plant Science*, 2(4), 152-159.
14. Valko, M., Leibfritz, D., Moncol, J., Cronin, M. T., Mazur, M., & Telser, J. (2007). Free radicals and antioxidants in normal physiological functions and human disease. *The International Journal of Biochemistry & Cell Biology*, 39(1), 44-84.
15. Scalbert, A., Johnson, I. T., & Saltmarsh, M. (2005). Polyphenols: antioxidants and beyond. *The American Journal of Clinical Nutrition*, 81(1), 215S-217S.
16. Srinivasan, M., Sudheer, A. R., & Menon, V. P. (2007). Ferulic acid: therapeutic potential through its antioxidant property. *Journal of Clinical Biochemistry and Nutrition*, 40(2), 92-100.
17. Calabrese, V., Cornelius, C., Dinkova-Kostova, A. T., Calabrese, E. J., & Mattson, M. P. (2008). Cellular stress responses, the hormesis paradigm, and vitagenes: novel targets for therapeutic intervention in neurodegenerative disorders. *Antioxidants & Redox Signaling*, 13(11), 1763-1811.
18. Ferguson, L. R., Zhu, S. T., & Harris, P. J. (2004). Antioxidant and antigenotoxic effects of plant cell wall hydroxycinnamic acids in cultured HT-29 cells. *Molecular Nutrition & Food Research*, 49(6), 585-693.

19. Almeida, I. F., Fernandes, E., Lima, J. L., Costa, P. C., & Bahia, M. F. (2008). Walnut (*Juglans regia*) leaf extracts are strong scavengers of pro-oxidant reactive species. *Food Chemistry*, 129(4), 1782-1788.
20. Konishi, Y., Hitomi, Y., & Yoshioka, E. (2004). Intestinal absorption of p-coumaric and gallic acids in rats after oral administration. *Journal of Agricultural and Food Chemistry*, 52(9), 2527-2532.
21. Cardona, F., Andrés-Lacueva, C., Tulipani, S., Tinahones, F. J., & Queipo-Ortuño, M. I. (2013). Benefits of polyphenols on gut microbiota and implications in human health. *The Journal of Nutritional Biochemistry*, 24(8), 1415-1422.
22. Dixon, R. A., & Paiva, N. L. (1995). Stress-induced phenylpropanoid metabolism. *The Plant Cell*, 7(7), 1085-1097.
23. Beckman, C. H. (2000). Phenolic-storing cells: keys to programmed cell death and periderm formation in wilt disease resistance and in general defence responses in plants? *Physiological and Molecular Plant Pathology*, 57(3), 101-110.
24. Lattanzio, V., Lattanzio, V. M. T., & Cardinali, A. (2006). Role of phenolics in the resistance mechanisms of plants against fungal pathogens and insects. *Phytochemistry: Advances in Research*, 66(3), 23-67.
25. Heimler, D., Isolani, L., Vignolini, P., Tombelli, S., & Romani, A. (2007). Polyphenol content and antioxidative activity in some species of freshly consumed salads. *Journal of Agricultural and Food Chemistry*, 55(5), 1724-1729.
26. Javanmardi, J., Stushnoff, C., Locke, E., & Vivanco, J. M. (2003). Antioxidant activity and total phenolic content of Iranian *Ocimum* accessions. *Food Chemistry*, 83(4), 547-550.
27. Llorach, R., Martínez-Sánchez, A., Tomás-Barberán, F. A., Gil, M. I., & Ferreres, F. (2008). Characterisation of polyphenols and antioxidant properties of five lettuce varieties and escarole. *Food Chemistry*, 108(3), 1028-1038.
28. Korus, A. (2011). Effect of preliminary processing, method of drying and storage temperature on the level of antioxidants in kale (*Brassica oleracea* L. var. *acephala*) leaves. *LWT-Food Science and Technology*, 44(8), 1711-1716.
29. Chan, E. W. C., Lim, Y. Y., Wong, S. K., Lim, K. K., Tan, S. P., Lianto, F. S., & Yong, M. Y. (2009). Effects of different drying methods on the antioxidant properties of leaves and tea of ginger species. *Food Chemistry*, 113(1), 166-172.
30. Ratti, C. (2001). Hot air and freeze-drying of high-value foods: a review. *Journal of Food Engineering*, 49(4), 311-319.
31. Järup, L. (2003). Hazards of heavy metal contamination. *British Medical Bulletin*, 68(1), 167-182.

32. Soetan, K. O., Olaiya, C. O., & Oyewole, O. E. (2010). The importance of mineral elements for humans, domestic animals and plants: A review. *African Journal of Food Science*, 4(5), 200-222.
33. Roberfroid, M. B. (2002). Global view on functional foods: European perspectives. *British Journal of Nutrition*, 88(S2), S133-S138.
34. Bigliardi, B., & Galati, F. (2013). Innovation trends in the food industry: the case of functional foods. *Trends in Food Science & Technology*, 31(2), 118-129.
35. Doxastakis, G., Zafiriadis, I., Irakli, M., Marlani, H., & Tananaki, C. (2002). Lupin, soya and triticale addition to wheat flour doughs and their effect on rheological properties. *Food Chemistry*, 77(2), 219-227.
36. Dewettinck, K., Van Bockstaele, F., Kühne, B., Van de Walle, D., Courtens, T. M., & Gellynck, X. (2008). Nutritional value of bread: Influence of processing, food interaction and consumer perception. *Journal of Cereal Science*, 48(2), 243-257.
37. Ainsworth, E. A., & Gillespie, K. M. (2007). Estimation of total phenolic content and other oxidation substrates in plant tissues using Folin–Ciocalteu reagent. *Nature Protocols*, 2(4), 875-877.
38. Chang, C. C., Yang, M. H., Wen, H. M., & Chern, J. C. (2002). Estimation of total flavonoid content in propolis by two complementary colorimetric methods. *Journal of Food and Drug Analysis*, 10(3).
39. Brand-Williams, W., Cuvelier, M. E., & Berset, C. (1995). Use of a free radical method to evaluate antioxidant activity. *LWT - Food Science and Technology*, 28(1), 25-30.
40. Re, R., Pellegrini, N., Proteggente, A., Pannala, A., Yang, M., & Rice-Evans, C. (1999). Antioxidant activity applying an improved ABTS radical cation decolorization assay. *Free Radical Biology and Medicine*, 26(9-10), 1231-1237.
41. Robbins, R. J. (2003). Phenolic acids in foods: an overview of analytical methodology. *Journal of Agricultural and Food Chemistry*, 51(10), 2866-2887.
42. Ammann, A. A. (2007). Inductively coupled plasma mass spectrometry (ICP MS): a versatile tool. *Journal of Mass Spectrometry*, 42(4), 419-427.
43. Azeh Engwa, G., Udoka Ferdinand, P., Nweke Nwalo, F., & N. Unachukwu, M. (2019). Mechanism and Health Effects of Heavy Metal Toxicity in Humans. *IntechOpen*. doi: 10.5772/intechopen.8251.
44. Zoroddu, M. A. *et al.* (2019). The essential metals for humans: a brief overview. *J Inorg Biochem* 195, 120–129.
45. Jomova, K., Makova, M., Alomar, S. Y., Alwasel, S. H., Nepovimova, E., Kuca, K., ... & Valko, M. (2022). Essential metals in health and disease. *Chemico-biological interactions*, 367, 110173.

46. De Matos, A. T., Fontes, M. P. F., Da Costa, L. M., & Martínez, M. A. (2001). Mobility of heavy metals as related to soil chemical and mineralogical characteristics of Brazilian soils. *Environmental pollution*, *111*(3), 429-435.
47. Xing, X., Kang, D. G., & Ma, X. (2017). Differences in loam water retention and shrinkage behavior: Effects of various types and concentrations of salt ions. *Soil and Tillage Research*, *167*, 61-72.
48. Shahidi, F., & Hossain, A. (2023). Importance of insoluble-bound phenolics to the antioxidant potential is dictated by source material. *Antioxidants*, *12*(1), 203.
49. Henriquez, C., Córdova, A., Almonacid, S., & Saavedra, J. (2014). Kinetic modeling of phenolic compound degradation during drum-drying of apple peel by-products. *Journal of Food Engineering*, *143*, 146-153.
50. Heleno, S. A., Martins, A., Queiroz, M. J. R., & Ferreira, I. C. (2015). Bioactivity of phenolic acids: Metabolites versus parent compounds: A review. *Food chemistry*, *173*, 501-513.

## *CAPTER 5: Comprehensive Conclusion*

This doctoral research comprehensively investigated three interconnected approaches to valorizing agricultural resources and enhancing food quality through advanced analytical characterization and innovative delivery systems, each contributing unique insights to the modern agrifood science landscape.

The systematic evaluation of these distinct yet complementary studies reveal several overarching themes critical to sustainable food production and quality assurance.

The *Medicago sativa* study demonstrated that the drying method plays a crucial role, air-dried and sun-dried samples exhibited 38-48% losses in bound phenolic acids and over 40% reduction in antioxidant capacity compared to freeze-dried counterparts from identical harvest conditions. These substantial losses, attributable to enzymatic oxidation and thermal degradation during the drying process, demonstrate unequivocally that post-harvest processing supersedes all agronomic variables in determining final product quality. In contrast, the choice between whole plants and apical portions did not significantly affect the bioactive content, providing greater flexibility in harvesting strategies. The three-year pooled spectrophotometric analysis revealed that the harvest period (July, August, September) had a statistically significant effect on total phenolic content ( $p = 0.008$ ) and TEAC-ABTS antioxidant capacity ( $p = 0.042$ ), with July samples consistently exhibiting the highest values for both parameters. In contrast, soil type (clayey, sandy, mixed) showed no significant influence indicating that harvest timing plays a much more critical role than soil characteristics in determining the nutraceutical value of alfalfa.

HPLC-DAD quantification identified ferulic acid and *p*-coumaric acid as the predominant bound hydroxycinnamic acids. Owing to their well-documented antioxidant, anti-inflammatory, and cardioprotective properties, these phenolics are particularly valuable in their bound form, which allows a gradual and sustained release through colonic microbial hydrolysis during digestion. ICP-MS analysis confirmed compliance with European Commission Regulation 2023/915, with all heavy metals well below maximum permissible levels, while essential minerals (Mg, K, Fe, Mn, Cr, Co, Cu) were present at nutritionally significant concentrations, enhancing alfalfa's functional value. These results establish freeze-dried alfalfa as a promising resource for food fortification, suitable for incorporation at up to 5% levels in cereal products.

The second study on *Olea europaea* L. demonstrated the remarkable power of multi-analytical approaches in food authentication and quality assessment within Tuscany's diverse geological terrain. The research revealed that soil element concentrations vary significantly across the region, directly

affecting the elemental composition of crops and providing a valuable tool for product traceability, enhanced marketability, and protection against fraud. The combined use of ICP-MS for trace and ultra-trace metal(loid) analysis and HPLC-DAD for secondary metabolite quantification achieved up to 30% improvement in geographical and varietal discrimination accuracy compared to single-technique approaches. Among the investigated metabolites, oleacin emerged as the most interesting marker for assessing both varietal and geographical origin of drupes and leaves, providing a new strategy to protect consumer choice and producers of olive oil, particularly for high-value EVOO characterized by restrictive quality parameters and specific PDOs.

The combined PCA-LDA chemometric analysis proved to be the most reliable approach for both varietal and geographical assessment, demonstrating that multiple techniques not only improve classification accuracy but also provide additional consumer benefits through multi-level product testing. This is particularly important as metabolomic profiles can identify adulteration in the EVOO production chain, with specific polyphenol levels associated with particular *Olea europaea* L. genera, while metal(loid) monitoring ensures consumer safety by tracking potentially toxic elements throughout the production process.

The third investigation explored the innovative development of Fe<sup>3+</sup>/carboxymethyl cellulose (CMC)-based hydrogel beads as vehicles for controlled glucosinolate release in agricultural soils, representing a significant advancement in biofumigation-inspired treatments. The commercial *Brassica oleracea* extract characterization revealed a total glucosinolate content of approximately 28% m/m, with glucoraphanin as the most abundant component, alongside 12% m/m sinapine contributing to biocidal properties. Overall, the study demonstrated that Fe<sup>3+</sup>/CMC-based hydrogel beads can serve as efficient carriers for the controlled release of glucosinolates, combining high water-holding capacity, robust viscoelastic properties, and structural integrity. The resulting slow and sustained glucoraphanin release highlights their promise as a novel, eco-friendly approach to biofumigation and soil health management.

This comprehensive work provides valuable scientific evidence supporting the valorization of agricultural resources through advanced characterization and innovative processing technologies. The demonstrated potential of cheap, simple, and eco-friendly materials as carriers for active compounds, possibly extracted from plants or by-products of agrifood production, represents an advanced tool for agricultural soil treatment and beyond. The research contributes significantly to both food security and sustainable agriculture objectives within the broader framework of circular economy principles in the agrifood sector, while deepening our understanding of the correlation between plants' chemistry and their geographical location. Most importantly, this study showcases the potential of multi-analytical approaches combined with multivariate statistical models as the future of traceability and

quality assessment in the agrifood field, providing a synergistic and integrated approach that ensures product quality, authenticity, and safety throughout the entire production chain.

## *Acknowledgments*

This work was realized within the framework of the projects:

- “PROFOOD-IV—Prodotti e processi innovativi della filiera di IV gamma” (PON ARS01\_00755)
  
- Agritech National Research Center, European Union Next-GenerationEU (PIANO NAZIONALE DI RIPRESA E RESILIENZA (PNRR)—MISSIONE 4 COMPONENTE 2, INVESTIMENTO 1.4—D.D. 1032 17/06/2022, CN00000022)
  
- MIMIT 2022 "Accordi per l'Innovazione - DM 31/12/2021 (Secondo Bando) - Nuovo prodotto alimentare panificato, nutraceutico, salutistico, completo, equo ed etico che utilizza originali biomasse proteiche vegetali alternative alle proteine animali estratte da colture agricole alimentari ad alta sostenibilità climatica attualmente destinati alla zootecnia, realizzate con moderno sistema produttivo ad alta efficienza in termini di risorse, destinato anche al frugale, pratico e veloce consumo, Made in Italy

## *List of Publication*

1. Baglioni, M., Clemente, I., Nardin, R., Bisozzi, F., Costantini, S., **Fattori, G.**, Tamasi, G., Rossi C. "Hydrogel Beads Loaded with Glucosinolate-Rich Brassicaceae Extract as a Controlled-Release Alternative to Biofumigation." *Molecules* 30.18 (2025): 3660.
2. Tatini, Duccio, Bisozzi, F., Costantini, S., **Fattori, G.**, Boldrini, A., Baglioni, M., Bonechi, C., Donati, A., Tozzi, C., Riccaboni, A., Tamasi, G., Rossi, C. "Geographical Origin Authentication of Leaves and Drupes from *Olea europaea* via 1H NMR and Excitation–Emission Fluorescence Spectroscopy: A Data Fusion Approach." *Molecules* 30.15 (2025): 3208.
3. Baglioni, M., Clemente, I., Tamasi, G., Bisozzi, F., Costantini, S., **Fattori, G.**, Gentile, M., Rossi C. "Isothiocyanate-Based Microemulsions Loaded into Biocompatible Hydrogels as Innovative Biofumigants for Agricultural Soils." *Molecules* 29.16 (2024): 3935.
4. Nardin, R.; Tamasi, G.; Baglioni, M.; **Fattori, G.**; Boldrini, A.; Esposito, R.; Rossi, C. Combining Metal(loid) and Secondary Metabolite Levels in *Olea europaea* L. Samples for Geographical Identification. *Foods* **2024**, *13*, 4017.
5. Nardin, R., Tamasi, G., Baglioni, M., Bisozzi, F., Consumi, M., Costa, J., **Fattori, G.**, Tozzi, C., Riccaboni, A., Rossi, C. (2024). Determination of Elemental Content in Vineyard Soil, Leaves, and Grapes of Sangiovese Grapes from the Chianti Region Using ICP-MS for Geographical Identification. *ACS Food Science & Technology*, *4*(11), 2585-2599.

## *Scientific communications*

1. Duccio Tatini, Sara Costantini, Flavia Bisozzi, **Giacomo Fattori**, Claudia Bonechi, Michele Baglioni, Gabriella Tamasi, Claudio Rossi - Geographical traceability of olive products using <sup>1</sup>H-NMR spectroscopy – Spoke 9–WP1 Agritech, Siena 19/06/2024
2. Duccio Tatini, Sara Costantini, Flavia Bisozzi, **Giacomo Fattori**, Claudia Bonechi, Marco Andreassi, Michele Baglioni, Gabriella Tamasi, Claudio Rossi - Geographical origin characterization of agri-food products used in Sangiovese wine production through <sup>1</sup>H-NMR spectroscopy coupled with multivariate statistical analysis – Spoke 9–WP1 Agritech, Siena 19/06/2024
3. Raffaello Nardin, Gabriella Tamasi, Flavia Bisozzi, **Giacomo Fattori**, Marco Consumi, Michele Baglioni, Cristiana Tozzi, Angelo Riccaboni e Claudio Rossi - Multivariate analysis combining metabolites and metal levels in leaves, drupes and EVOO for the geographical traceability and quality assessment of agricultural goods - Spoke 9–WP1 Agritech, Siena 19/06/2024
4. Gemma Leone, Michele Baglioni, Raffaello Nardin, Gabriella Tamasi, Flavia Bisozzi, Sara Costantini, **Giacomo Fattori** and Claudio Rossi - Physico-chemical characterization of a chitosan-based nanocomposite film containing copper nanoparticles – PON PROFOOD-IV Workshop, Roma 19/09/2024
5. Gemma Leone, Michele Baglioni, Raffaello Nardin, Gabriella Tamasi, Flavia Bisozzi, Sara Costantini, **Giacomo Fattori** and Claudio Rossi - Physico-chemical characterization of a zein-based nanocomposite film containing silver nanoparticles - PON PROFOOD-IV Workshop, Roma 19/09/2024
6. Michele Baglioni, Raffaello Nardin, Gabriella Tamasi, Flavia Bisozzi, Sara Costantini, **Giacomo Fattori** and Claudio Rossi - Use of dilute HClO solutions as an innovative, cost-effective, and safe method for disinfection of fresh-cut (pre-packaged) produce – PON PROFOOD-IV Workshop, Roma 19/09/2024
7. Michele Baglioni, Gabriella Tamasi, Flavia Bisozzi, Sara Costantini, **Giacomo Fattori**, Duccio Tatini, Claudio Rossi - Microemulsions based on synthetic pesticides loaded into controlled-release hydrogels - PON PROFOOD-IV Workshop, Roma 19/09/2024
8. Michele Baglioni, Duccio Tatini, Gabriella Tamasi, Flavia Bisozzi, Sara Costantini, **Giacomo Fattori** e Claudio Rossi - Physical mixtures of isothiocyanates adsorbed on biocompatible polymers for the fumigation of agricultural soils - PON PROFOOD-IV Workshop, Roma 19/09/2024

9. Michele Baglioni, Duccio Tatini, Ilaria Clemente, Raffaello Nardin, Gabriella Tamasi, Flavia Bisozzi, Sara Costantini, **Giacomo Fattori** and Claudio Rossi - Hydrogels for the controlled release of glucosinolates extracted from Brassicaceae – a sustainable treatment for agricultural soils - PON PROFOOD-IV Workshop, Roma 19/09/2024
10. Michele Baglioni, Duccio Tatini, Ilaria Clemente, Gabriella Tamasi, Flavia Bisozzi, Sara Costantini, **Giacomo Fattori**, Claudio Rossi - Isothiocyanate-based microemulsions loaded into biocompatible hydrogels as innovative biofumigants for agricultural soils - PON PROFOOD-IV Workshop, Roma 19/09/2024
11. Sara Costantini, **Giacomo Fattori**, Claudia Bonechi, Gabriella Tamasi, Alessandro Donati and Claudio Rossi - Chlorogenic acid in zwitterionic liposomes: microfluidic optimization, synthesis and physicochemical characterization – Poster presentation at Meeting of CSGI, Bari 18/09/2025